PER-ARNT-SIM KINASE REGULATES NUTRIENT UTILIZATION AND GROWTH

by

Caleb Michael Cardon

A dissertation submitted to the faculty of
The University of Utah
in partial fulfillment of the requirements for the degree of

Doctor of Philosophy

Department of Biochemistry

The University of Utah

December 2011

The University of Utah Graduate School

STATEMENT OF DISSERTATION APPROVAL

The dissertation of   **Caleb Michael Cardon**

has been approved by the following supervisory committee members:

Jared P. Rutter	, Chair	**10/10/2011**	Date Approved
Janet Shaw	, Member	**10/10/2011**	Date Approved
Tim Formosa	, Member	**10/10/2011**	Date Approved
E. Dale Abel	, Member	**10/10/2011**	Date Approved
Dennis Winge	, Member	**10/10/2011**	Date Approved

and by   **Christopher Hill**   , Chair of

the Department of   **Biochemistry**

and by Charles A. Wight, Dean of The Graduate School.

ABSTRACT

There is a fundamental connection between growth and nutrient availability. An inbalance between energy intake and energy expenditure can lead to the common diseases of the developed world, including type 2 diabetes, obesity, heart disease and cancer, as well as less common diseases such as anorexia, malnutrition and sarcopenia. The tight link between growth and nutrient availability is extended beyond the whole body level down to a cellular level. There exist cell autonomous signaling mechanisms that allow the cell to detect the environmental conditions and decide to grow, through increase in cell size or cell division. Malfunctions in these signaling pathways are fundamental to many of the diseases related to energetic misregulation. Many of the proteins that are central to these signaling pathways have also become good therapeutic targets. Two well characterized proteins that are central to cellular energy balance are AMPK and TOR. In response to depleted cellular ATP levels AMPK is activated in order to up-regulate ATP generating pathways and downregulate ATP consuming pathways, including growth. However as nutrients become available TOR is rapidly activated in order to efficiently utilize the available nutrients for growth. As our understanding of the function of these two proteins has increased, AMPK and TOR have become effective therapeutic targets. PAS kinase is a newly characterized serine/threonine kinase that can respond to the extracellular

conditions in order to regulate nutrient partitioning and provide a progrowth signal. We show here that in budding yeast PAS kinase can respond to environmental cues to phosphorylate the metabolic enzyme Ugp1. P-Ugp1 then nucleates the formation of a unique signaling complex that includes Rom2 and Ssd1. Complex formation is able to activate the small GTPase Rho1, which functions as a progrowth signal. We also show that PASK-/- mice are resistant to the damaging effects of a high fat diet, specifically, obesity, insulin resistance and hepatic steatosis. This protection is likely due to the increased metabolic rate of PASK-/- mice. The hypermetabolic phenotype of the PASK-/- can be recapitulated in cultured cells, which indicates that the increased metabolic rate is due to a cell autonomous change in metabolism. Further characterization of PAS kinase may lead to novel therapeutic strategies to treat the metabolic syndrome.

TABLE OF CONTENTS

LIST OF TABLES

LIST OF FIGURES

LIST OF ABBREVIATIONS

ACC	acetyl-CoA carboxylase
AgRP	Agouti-related protein
AMPK	5'Adenosine monophosphate protein kinase
ARC	arcuate nucleus
ATG13	autophagy related
ATP	adenosine triphosphate
AVO	adheres voraciously
BIT61	binding partner of Tor2p
CART	cocaine and amphetamine-regulated transcript protein
CBK1	cell wall biosynthesis kinase
CPT1	carnitine palmitoyltransferase
DMN	dorsomedial nucleus
DNA	deoxyribonucleic acid
FAT	FRAP, ATM, TTRAP domain
GAP	GTPase activating protein
GCN4	general control nonderepressible
GEF	Guanine nucleotide exchange factor
GLN3	glutamine metabolism
GTP	guanosine triphosphate
HEAT	huntingtin, elongation factor 3, A subunit of type 2A protein phosphatase, Tor
HFD	High fat diet
IR	insulin receptor
IRS	insulin receptor substrate
LST8	lethal with Sec13
MC4R	melanocortin receptor 4
MEF	mouse embryonic fibroblast
MSH	melanocyte-stimulating hormone
mTOR	mammalian target of rapamycin
NPY	neuropeptide Y
PAS	Per-Arnt-Sim
PASK	PAS kinase
PGC1	PPAR-gamma coactivator
PIKK	phosphoinositide 3-kinase related kinases
POMC	pro-opiomelanocortin
PP2A	protein phosphatase-2A

PPAR	peroxisome proliferator-activated receptor
PVN	paraventricular nucleus
RHO1	Ras homolog
RNA	ribonucleic acid
ROM2	Rho1 multicopy suppressor
S6K	p70 ribosomal S6 kinase
SDS	sodium dodecyl sulfate
SREBP	sterol regulatory element binding protein
SSD1	suppresor of Sit4 deletion
TOR	target of rapamycin
tor2ts	temperature sensitive allele of TOR2
TORC1	TOR complex 1
TORC2	TOR complex 2
TSC11	temperature-sensitive suppressors of Csg2 mutants
UDP	uridine diphosphate
UGP1	UDP-glucose pyrophosphorylase
VMN	ventralmedial nucleus
YPK2	yeast protein kinase

ACKNOWLEDGEMENTS

with their time: Janet Shaw, Tim Formosa, E. Dale Abel, Dennis Winge, Janet Lindsley, and David Stillman.

I would also like to extend my gratitude to my family for their never-ending support, in what felt like a never-ending degree at times. This never would have happened without the support of my wife Marcelina and my children Gavin, Henry and Wyatt; thank you for the time and helpful words in difficult times.

CHAPTER 1

INTRODUCTION

Energy homeostasis and growth

The ability of organisms to recognize and respond to a diverse extracellular environment is critical for survival. Organisms must be able to adapt to environmental stress and reproduce in order to have any fitness advantage. An organism's fitness advantage is largely determined by its ability to maintain energy homeostasis. Energy homeostasis is the process by which organisms are able to acutely respond to changes in the nutritional environment in order to sustain energy demand. This flexibility allows organisms to rapidly increase catabolic processes in response to nutrient-replete conditions in order to efficiently utilize available nutrients for growth and reproduction. Conversely, this flexibility allows organisms to increase anabolic processes in nutrient-deplete conditions in order to efficiently use energy stores until conditions become more advantageous for reproduction and growth. In higher eukaryotes these appropriate metabolic adaptations are partially controlled via the central nervous system. The nervous system monitors whole body energy homeostasis primarily through the endocrine system, which includes but is not limited to the brain, liver, gut, and pancreas(*4*).

In addition to the central control of metabolism seen in many metazoa, multicellular organisms have cell autonomous mechanisms of metabolic regulation(*2, 3, 5*). Cell autonomous regulation of metabolism allows each cell to respond to fluctuations within its unique microenvironment to maximize the efficient utilization of nutrients. The cell contains many mechanisms that are able

to detect changes in either the availability of nutrients or the energy status of the cell. Once these mechanisms are activated they modulate cellular nutrient utilization through complex, integrated signaling networks. Under conditions of nutrient abundance these signaling networks lead to an increase in nutrient uptake and growth, through protein synthesis and cell division(*6*). In nutrient deplete conditions other signaling networks regulate cellular nutrient conservation and energy production(*7*). These networks up-regulate autophagy, mobilize energy stores and inhibit growth by decreasing protein synthesis and inhibiting cell cycle progression. These represent the two extremes of nutrient availability. However most organisms live in a more complex environment. Given the complexity of the nutritional milieu as well as other extracellular signals, such as growth factors or toxins, cellular growth decisions must integrate multiple inputs. Signal integration happens through overlap, or cross talk, between signaling pathways. Integration allows the cell to efficiently utilize available nutrients to grow or conserve nutrients in times of starvation in order to survive.

Our understanding of cellular signaling mechanisms involved in coupling nutrient utilization to growth has increased with the detailed characterization of PAS kinase. Specifically, we have been able to show that PAS kinase, a conserved serine/threonine kinase, can control growth in response to stress in budding yeast and is required for normal energy homeostasis in the mouse(*8*).

PAS kinase function in *S. cerevisiae*

The decision to grow or reproduce under conditions of nutrient limitation can be catastrophic for any organism. Each cell, within an organism, contains mechanisms that are designed to detect changes to nutrient availability and respond appropriately. These signaling mechanisms are designed to couple nutrient availability to growth to prevent cell death. Given the fundamental relationship between nutrients and growth, many signaling mechanisms that couple the two are highly conserved over evolution(*9*). This conservation has allowed us to use *S. cerevisiae* as a tool to dissect these complex signaling networks. Polarized cell growth in *S. cerevisiae* requires the coordinate up-regulation of cell wall/membrane synthesis, protein synthesis, polarized localization of protein and mRNA, and DNA replication(*6, 10-13*). If any of these processes proceed out of sync with the others it can be lethal to the cell. The TOR signaling network is one mechanism that is able to respond to nutrient-replete conditions to coordinate cell growth and division(*13, 14*). In order to regulate these diverse cellular processes the TOR signaling network overlaps with many other networks(*7*). The ability to coordinate polarized cell growth through the TOR signaling network is essential in *S. cerevisiae(15)*. However, when TOR signaling is compromised, PAS kinase activation is necessary and sufficient to sustain growth.

Here we show that the phosphorylation of Ugp1 via PAS kinase plays two roles. First, it increases cell wall biosynthesis at the expense of glycogen

storage(*12*). Phosphorylation of Ugp1 does not affect enzymatic activity. However it does regulate localization of the protein to the cell periphery. At the cell periphery the product of Ugp1's enzymatic reaction is used predominantly for production of cell wall glucans. Second, it nucleates the formation of a pro-growth signaling complex that includes Ssd1 and Rom2. The translocation of Ugp1, mediated via PAS kinase phosphorylation, may be required for the formation of competent signaling complexes. Localizing to the cell periphery would bring the complex into proximity with Rho1, which is known to localize to the cell periphery(*16*). It may be that all of these proteins (PAS kinase, Rom2, Ssd1, Ugp1, Rho1) require independent inputs to translocate to the cell periphery, allowing the complex to integrate multiple inputs. Phosphorylation of Ugp1 allows coordination of polarized cell growth with an increase in cell wall synthesis that is required to accommodate the dramatic increase in size that is concomitant with cell division. This is the first evidence that Ugp1, thought only to catalyze the formation of UDP-glucose, plays a role in coupling the nutritional environment to growth.

Target-Of-Rapamycin (TOR1/TOR2) function

The target-of-rapamycin (TOR) is a highly conserved lipid kinase of the phosphoinositide 3-kinase (PI3K)-related protein kinases (PIKK) family. TOR functions as a master regulator of cell and organismal size. TOR was first identified as the target of the immunosuppressant rapamycin(*17*). Since its discovery, TOR has been extensively studied

for its ability to control cell size in response to nutrient availability. The domain organization of TOR can been seen in Figure 1-1, which consists of N-terminal HEAT (huntingtin, elongation factor 3, A subunit of type 2A protein phosphatase, TOR) repeats that mediate protein-protein interactions and target TOR to the cell periphery(*3, 18*). The HEAT repeats are followed by a FAT domain (FRAP, ATM, TTRAP), which may also be involved in protein binding. The FKBP12-rapamycin binding site is localized between the FAT domain and the kinase domain of TOR and can disrupt some TOR-protein interactions. The C-terminus of TOR contains a FAT domain that is thought to be involved in redox-dependent degradation.

The *S. cerevisiae* genome contains two paralogs of *TOR*: *TOR1* and *TOR2*. The protein products of these two genes function in two distinct complexes termed TOR complex 1 (TORC1) and TOR complex 2 (TORC2) (Figure 1-2)(*13*). TORC1, which contains either Tor1 or Tor2 as well as Kog1 (raptor), Tco89 and Lst8, regulates protein synthesis and cell size in response to nutrient availability. TORC1 function is sensitive to the inhibitor rapamycin. TORC2, which contains Tor2 (but not Tor1), Avo1, Avo2, Avo3 (Tsc11 or rictor), Bit61 and Lst8, is essential for cell division and cell cycle- dependent polarization of the actin cytoskeleton. TORC2 function is not directly sensitive to rapamycin.
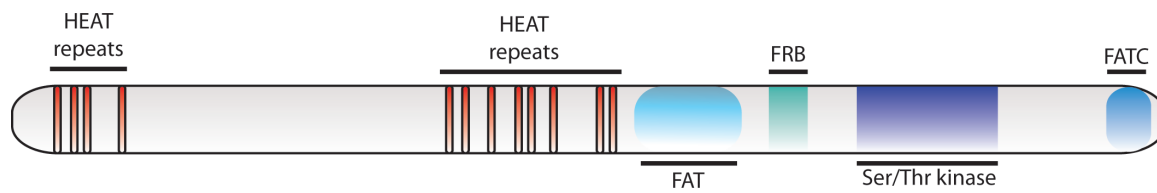
Figure 1-1). Domain organization of Tor. The domain organization is the same for Tor1 and Tor2. The HEAT repeats and FAT domains have been shown to mediate the majority of the many protein-protein interactions of TOR. This domain organization is highly conserved across eukaryotes. Adapted from reference (*3*)
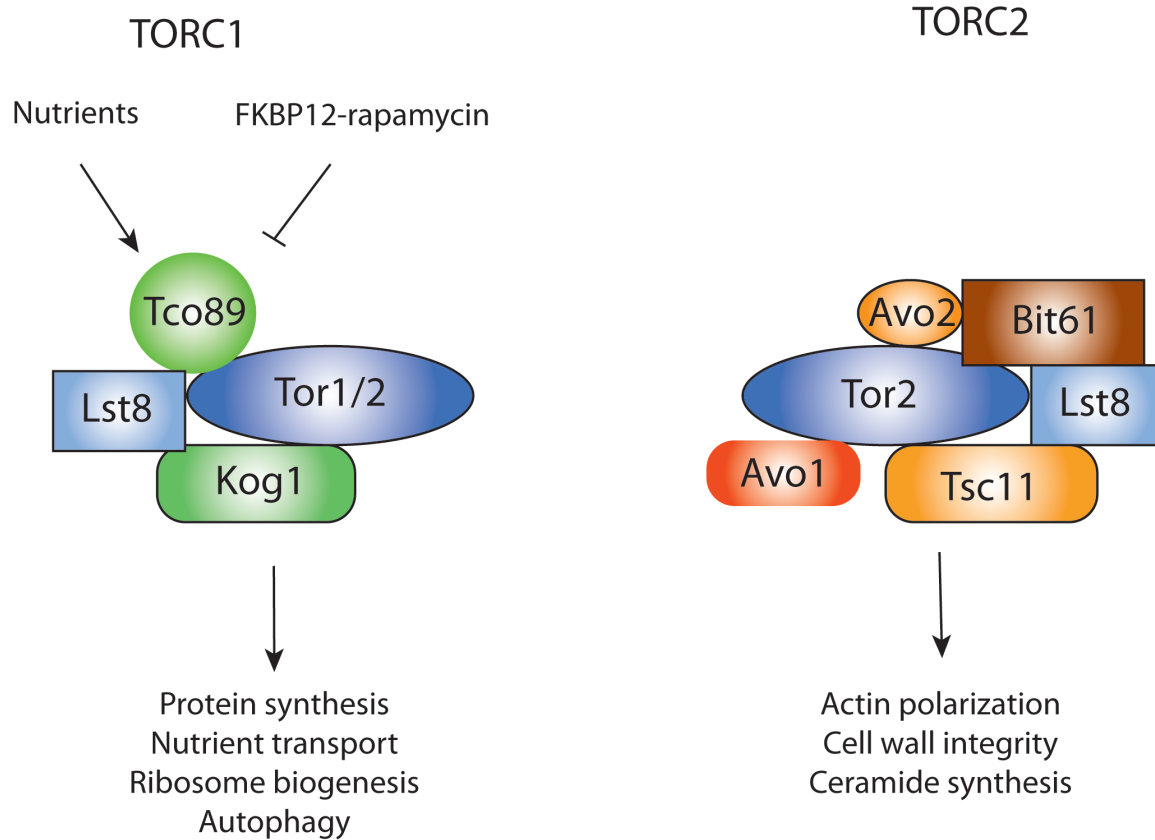
Figure 1-2). TORC1 and TORC2 signaling in budding yeast. TOR signaling controls both spatial and temporal aspects of cell growth. TORC1 responds to nutrients to increase anabolic processes and cell size. TORC2 regulates actin polarization and cell wall synthesis in a cell cycle dependent manner

The FKB12-rapamycin sensitive TORC1 contains either TOR1 or TOR2. TORC1 is activated in response to nutrients and regulates both catabolic and anabolic processes(*19*). TORC1 signaling can be divided into two signaling branches: one that inhibits scavenging mechanisms and utilization of energy stores, and a second that up-regulates protein synthesis and nutrient storage. TOR activation inhibits the transcription factors Gln3 and Gcn4, which are required for nitrogen scavenging and amino acid biosynthesis, respectively(*20*). Repression of these transcription factors is mediated through regulation of protein phosphatase-2A (PP2A) and other PP2A-related protein phosphatases via TORC1. This is coupled to a repression of autophagy via hyper-phosphorylation of Atg13, which is a regulatory subunit of the autophagosome(*21*). Through these, as well as other mechanisms, TORC1 activation leads to a repression of cellular recycling processes. The repression of cellular recycling is coupled to an up-regulation of cell growth and nutrient uptake. TORC1 regulates global protein synthesis, and thereby cell size, via expression of ribosomal genes as well as stabilization of the 5'-cap dependent translation initiation factor eIF4G(*22, 23*). TORC1 up-regulates nutrient uptake via control of amino acid permease translocation to the plasma membrane mediated via Lst8(*24*). Lst8, a component of TORC1, controls amino acid permease sorting within the late secretory pathway.

The function of TORC2 is not as well characterized as its counterpart TORC1. However it is clear that activation of TORC2 leads to polarization of the actin cytoskeleton, which promotes cell division(*25*). The TORC2-dependent polarization of the actin cytoskeleton is dependent on the small GTPase Rho1. The mechanism by which TORC2 activates Rho1 to polarize the actin cytoskeleton remains somewhat ambiguous. However TORC2 activates the AGC kinase Ypk2 via direct phosphorylation of the hydrophobic and turn motifs(*11*). It has also been shown that expression of a constitutively active Ypk2 is able to suppress a loss of TORC2. These data taken together suggest that TORC2 phosphorylates Ypk2, which in turn leads to Rho1 activation and actin polarization. Ypk2 phosphorylation also leads to an up-regulation of de novo ceramide biosynthesis, which may have a role in regulating endocytosis(*26*). TORC2 can also indirectly mediate actin polarization through activation of two related kinases, Slm1 and Slm2. Through coordination of all of these signaling pathways, TORC2 functions as a regulator of spatial growth in *s. cerevisiae*.

In order to study the essential function of *TOR2*, mutants have been constructed that allow for the acute disruption of Tor2 activity. Strains harboring a temperature sensitive allele of *TOR2* (*tor2^{ts}*) arrest growth at the restrictive temperature (37° C)(*27*). This is due to a lack of functional TORC2 and decreased activation of Rho1. As expected, this growth arrest can be suppressed by over-expression of proteins that activate Rho1. The growth arrest of the *tor2^{ts}* is also suppressed by growth on nonfermentative carbon sources (galactose,

raffinose, which are fermentable but do not elicit glucose repression) but not on nonfermentable carbon sources (glycerol, ethanol). Unexpectedly, treatment with cell wall/cell membrane perturbing agents, which cause cell integrity stress, can also abrogate the *tor2^ts* phenotype. The mechanism underlying the connection between nonfermentative carbon sources, cell wall stress and suppression of the *tor2^ts* remains unresolved. These data suggest the presence of signaling modalities that integrate input from cell integrity stress and metabolism to control cell growth. Properly coordinating these disparate signaling inputs into a concerted drive towards growth requires a complex interconnected signaling network.

Per-Arnt-Sim kinase (PSK1/PSK2)

In recent years many advances have come in our understanding of the inputs that are required for complex cell autonomous decision-making. One recent advance was the discovery and initial characterization of PAS kinase(*28, 29*). PAS kinase consists of an N-terminal PAS domain and a C-terminal kinase domain. PAS domains have been well characterized in prokaryotic systems to function as molecular sensors of indicators of cellular metabolic status. The PAS domain is able to bind to and inhibit the kinase domain in *cis*. This raises the intriguing possibility that the PAS domain is able to directly sense metabolic changes within the cell to regulate kinase activity. This idea is supported by the observation that PAS kinase does not require activation loop phosphorylation in

order to be active(*30*). The small molecule(s) that regulate the PAS and kinase domain interaction remain to be elucidated. However, in a PAS kinase null strain (*psk1Δ psk2Δ)* there is a dramatic increase in glycogen content at the expense of cell wall glucan, indicating an inability to properly regulate glucose flux(*12*).

In *S. cerevisiae* there are two PAS kinase paralogs, *PSK1* and *PSK2* (referred to together as PAS kinase). PAS kinase can be activated by multiple inputs including cell integrity stress and cellular nutrient status (Fig 1-3)(*31*). Over-expression of Wsc1, an integral cell membrane protein, can lead to an activation of PAS kinase. This may be due to a direct interaction between Wsc1 and PAS kinase or it may be that Wsc1 over-expression leads to cell integrity stress that is responsible for PAS kinase activation. The details of cell integrity stress activation of PAS kinase remain to be resolved. However activation leads to phosphorylation of Ugp1 at serine-11. Ugp1 is the enzyme responsible for the synthesis of UDP-glucose, which is the glucosyl donor for glycogen and cell wall glucan production(*32*). Phosphorylation of Ugp1 does not affect enzymatic activity, but rather the utilization of UDP-glucose. In the phosphorylated state Ugp1 produces UDP-glucose that is partitioned preferentially toward production of cell wall glucans. PAS kinase-dependent phosphorylation of Ugp1 increases production of cell wall glucans in order to stabilize the cell wall in response to cell integrity stress(*12*).
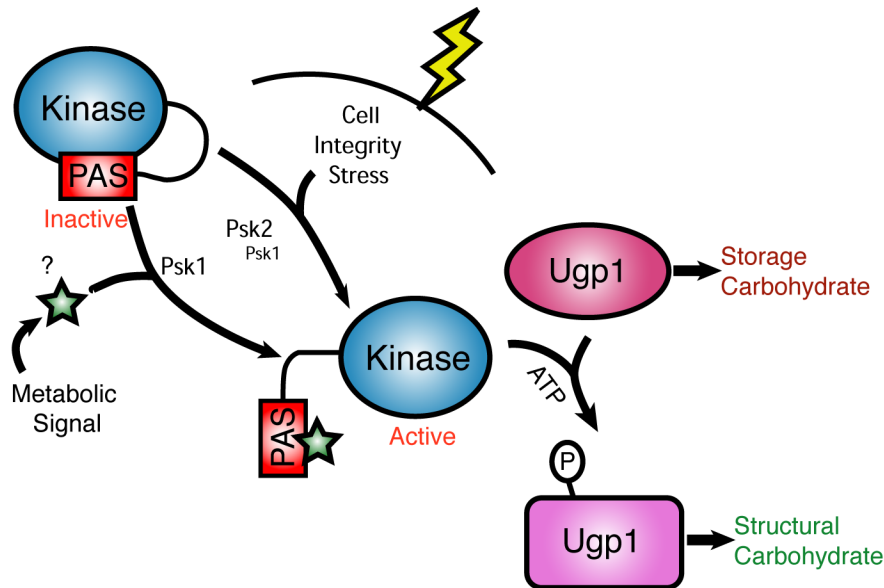
Figure 1-3). PAS kinase signaling in budding yeast. PAS kinase is activated by metabolic signals (nonfermentative carbon sources) as well as cell integrity stress (SDS, calcifluor white, congo red). Activation of PAS kinase leads to phosphorylation of the metabolic enzyme Ugp1. PAS kinase-dependent phosphorylation of serine-11 of Ugp1 induces a switch in glucose partitioning from storage (glycogen) to utilization (cell wall glucans).

Yeasts are able to utilize a diverse array of carbon sources in order to extract the energy needed to grow. However in order to efficiently utilize available nutrients the cell must be able to dynamically regulate various metabolic programs(*33*). The preferred carbon source for yeast is glucose, which they ferment to ethanol. Growth on glucose leads to repression of metabolic programs involved in mitochondrial function as well as metabolism of alternative carbons sources. In response to growth on nonfermentative carbon sources, or carbon sources that do not activate glucose repression, PAS kinase is activated. Non-fermentative activation of PAS kinase is dependent on SNF1/AMPK(*31*). However it is unclear if this is a direct or indirect effect of SNF1 activation. Activation of PAS kinase in response to these nutrient cues also leads to phosphorylation of Ugp1. When glucose is limiting in the environment it is presumably more efficient to use what is available to build cell wall rather than to store it as glycogen.

All PAS kinase mutant phenotypes are completely phenocopied by introducing the Ugp1 serine-11 to alanine mutation (Ugp1-S11A), which prevents PAS kinase-dependent Ugp1 phosphorylation. This indicates that the effects of PAS kinase on glucose utilization are primarily mediated through Ugp1 phosphorylation. However integrating PAS kinase function into broader signaling networks has remained elusive.

UDP-glucose pyrophosphorylase (UGP1)

UDP-glucose pyrophosphorylase (Ugp1) is the enzyme that catalyzes the production of UDP-glucose from UTP and glucose-1-phosphate (Figure 1-4A)(*32*). In plants Ugp1 functions as a monomer, while in prokaryotes, slime molds and mammals it forms an octamer consisting of identical subunits(*34*). The high conservation of Ugp1 is due to the necessity of UDP-glucose as the glucosyl donor for many cellular reactions (Figure 1-4B). In yeast UDP-glucose is used as a glucosyl donor for β-glucan synthesis, glycogen synthesis, trehalose production and N-glycosylation of proteins within the endoplasmic reticulum. Ugp1 enzymatic activity is essential in *S. cerevisiae*, which has complicated studies into its possible function aside from UDP-glucose synthesis. Ugp1 is phosphorylated on serine-11 by PAS kinase, which does not affect enzymatic activity. However phosphorylation does induce a conformational change(*12*). This conformational change in Ugp1 is associated with an increase in cell wall glucan production and a decrease in glycogen synthesis. To date Ugp1 is the only verified *in vivo* target of PAS kinase phosphorylation.

Suppressor-Of-SIT4 deletion (SSD1)

Suppressor-of-Sit4 deletion (SSD1) encodes a protein of 1250 amino acids. Ssd1 has an RNase H domain that is lacking critical catalytic residues for RNase activity and has not been shown to have RNase activity. Ssd1 can bind to RNA *in vivo(10)*. *SSD1* contains a common polymorphism at tyrosine 698,

A)

Glucose-1-phosphate   +   UTP $\xrightleftharpoons{\text{Ugp1}}$ UDP-glucose   +   Pi

B)   UDP-glucose

Glycogen   trehalose   B-glucan   N-glycosylation   galactose utilization
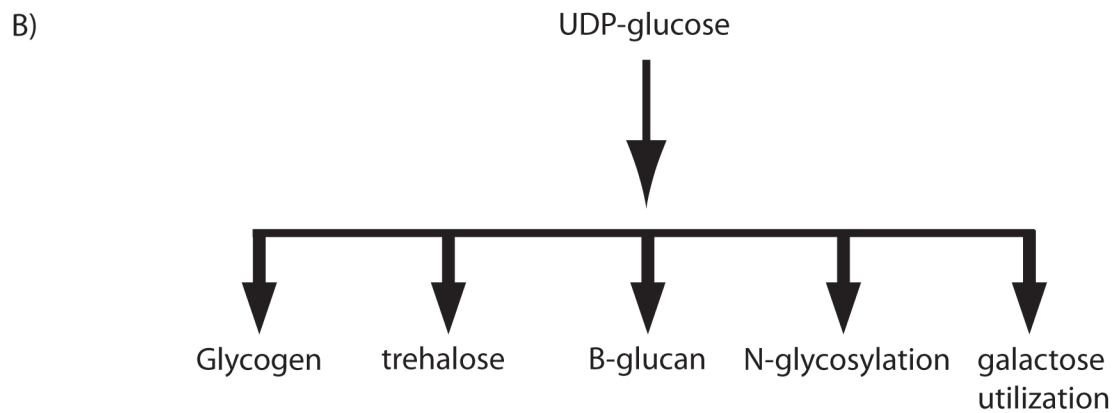
Figure 1-4). Reaction catalyzed by Ugp1. Ugp1 catalyzes the formation of UDP-glucose from UTP and glucose-1-phosphate. (B) UDP-glucose can be used as a building block form synthesis of essential cellular components.

which causes a premature stop codon in some *S. cerevisiae* lab strains. It has

been proposed that this premature stop codon has caused *SSD1* to be over-

represented in yeast genetic screens and has thereby complicated the study of

its proper cellular function, as shown in Table 1-1(*1*). Cells lacking *SSD1* have an

increase in cell wall mannan, chitin and decreased concentrations of glucans(*35*).

These data indicate that Ssd1 may have a function in cell wall regulation.

However, these results may just be a consequence of the RNA binding capacity

of Ssd1.

Ssd1 has been shown recently to bind mRNA and thereby suppress

protein(*10, 36*). The RNA bound via Ssd1 primarily consisted of cell wall lysis

enzymes. These enzymes are critical to facilitate cell wall remodeling that is

required to accommodate cell division. However if these genes were expressed

in a manner that is either temporally or spatially inappropriate it could be very

detrimental. Ssd1 insures that these specific mRNAs are expressed in a spatially

and temporally regulated manner. The inhibition of translation by Ssd1 is

negatively regulated by Cbk1 phosphorylation. Cbk1 localizes to the bed neck

and daughter cell, during mitosis. This localization ensures that the mRNAs

responsible for expression of cell wall lysis genes are only expressed at the site

of cell division. This regulation of expression may also be critical for daughter-cell

specific protein expression. Interestingly, Ssd1 contains eight phosphorylation

sites clustered at the N-terminus of the protein that contain the PAS kinase

Table 1-1). Genetic interactions of SSD1. Reported effects of addition of SSD1 are shown. Ts, suppresses a ts phenotype; sl, suppresses synthetic lethality between gene and (gene x); G, improves growth; L, suppresses lethality; D, causes death. Adapted from reference (*1*)

Gene	Function	interaction
ARL1	Membrane trafficking	ts
BCK1	Protein kinase involved in cell wall integrity	ts
BEM2	GTPase-activating protein required for polarized cell growth	ts
BUL1	Protein that binds ubiquitin ligase	ts
CBK1	Protein kinase involved in cell morphogenesis	
CBC2	component of cap binding complex	sl (sto1)
CCR4	Transcriptional regulator of glucose-repressed and cell wall genes	ts
CDC28	Cylcin-dependent protein kinase	ts
CET1	mRNA capping enzyme	ts
CLN1/2	G1 cyclins	G
CYR1	Adenylate cyclase	ts
DHH1	ATP-dependent RNA helicase	sl (elm1)
ELM1	Serine/threonine protein kinase that regulates psuedohyphal growth	sl (dhh1)
HDF1	component of DNA end-joining repair pathway	ts
JNM1	Protein required for proper nuclear migration during mitosis	ts
LAS1	Essential gene required for bud formation and morphogenesis	ts
LUV1	Protein involved in protein sorting in the late golgi	sl (rbl2)
MEP1/2	Ammonium permeases involved in regulating psuedohyphal growth	G
MPT5	Protein required for high temperature growth and normal life span	ts
PAG1	Protein that functions with Cbk1p to regulate cell morphogenesis	D
PPH21/22	catalytic subunits of the protein phosphatase 2A	ts
PRP18	U5 snRNA-associated protein	ts
PRP22	Pre-mRNA splicing factor	ts
RBL2	Putative tubulin cofactor A	sl (luv1)
RDS3	Spliceosome component	ts
RLM1	transcription factor downstream of MPK1	ts
RPC31	RNA polymerase III	ts
RPD3	Histone deacetylase component of the Rpd3-Sin3 complex	sl (swi6)
RPT4	Proteosome ATPase	ts
RRD1	Phosphotyrosyl phosphotase activator	sl (rrd2)
RRD2	Protein involved in rapamycin sensitivity	sl(rrd1)
SDS3	Component of the Rpd3-Sin3 histone deacetylase	sl (swi6)
SIN3	Component of the Rpd3-Sin3 histone deacetylase	sl (swi6)
SIT4	Phosphatase required for G1-S transition	L
SLC5	Unknown	ts
SLG1	Protein required for maintenance of cell wall integrity	ts
SLT2	MAP kinase that functions downstream of BCK1/SLK1	ts
SLY1	Protein involved in vesicle trafficking	ts
SMC2	Subunit of condensing protein complex	ts
SMC4	Subunit of condensing protein complex	ts
SNP1	U1 snRNA-associated protein	ts
STO1	Component of cap-binding complex	sl (cbc2)
SWI4	Cell-cycle-specific transcription factor	sl (mpt5)
SWI6	Cell-cycle-specific transcription factor	sl (mpt5)
U5AI	U5 snRNA	ts
YPT1	GTP-binding protein involved in the secretory pathway	ts
YPT6	GTP-binding protein involved in the secretory pathway	ts

phosphorylation consensus sequence. Six of the eight sites have a histidine at

the -5 position in relation to the phosphorylated residue, which is the preferred

amino acid for PAS kinase phosphorylation. Preference for histidine at -5 is

unusual and is only shared by Cbk1. These sites have been shown to be

important for the regulation of Ssd1. If the eight sites (serine or threonine) are

mutated to the nonphosphorylatable alanine, over-expression of this mutant is

lethal. This seems to be due to a thickening of the cell wall, such that the cells

can no longer divide. This is consistent with Ssd1 regulating the expression of

cell wall lysis genes.

ROM2-RHO1

Rho1 is a small GTPase of the Rho/Rac subfamily of Ras-like GTPases.

In the active state Rho1 is bound to GTP. The intrinsic GTPase activity of Rho1 is

regulated by GTPase activating proteins (GAPs) Bem2, Sac7, Bag2 and Rdi1,

which leads to hydrolyses of GTP to GDP (Figure 1-5)(*37*). GTP hydrolyses

causes inactivation of Rho1. Guanine nucleotide exchange factors (GEFs)

catalyze the exchange of GDP for GTP in order to activate Rho1 signaling(*38*).

Active Rho1 mediates its effects on the cell through activation of downstream

effectors(*39-41*). Rho1 activates protein kinase C (PKC), which leads to

activation of the mitogen-activated protein kinase (MAPK) cascade composed of

BCK1, MKK1/2 and MPK1. Activation of this cascade controls actin cytoskeleton
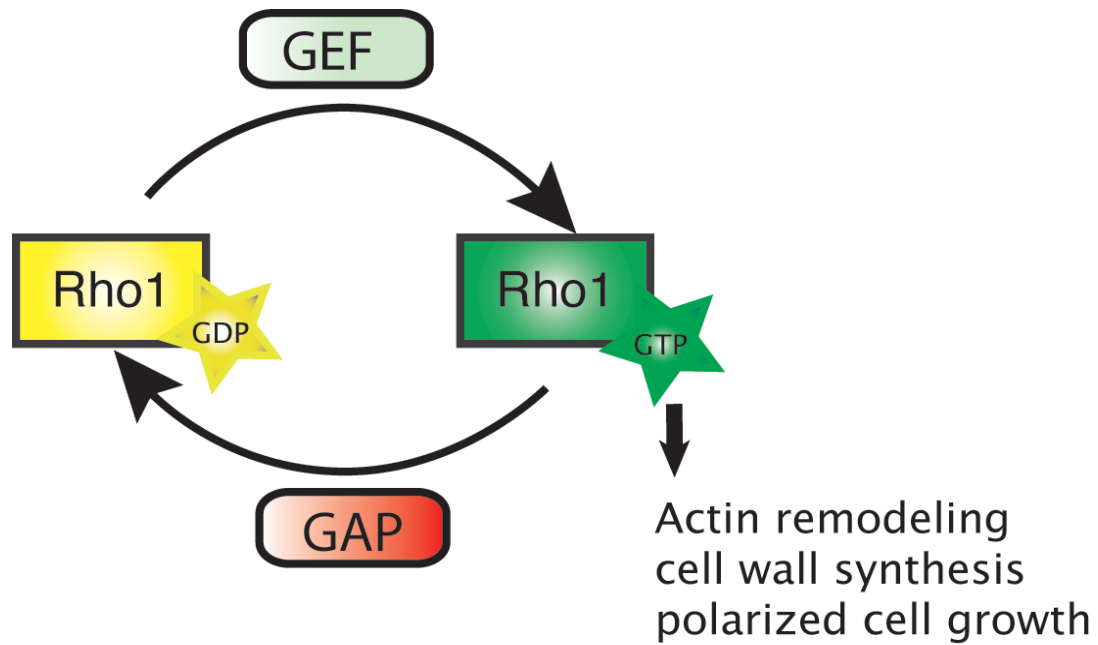
Figure 1-5). Schematic of Rho1 activation. GTP-bound Rho1 is inactivated by GTPase activating proteins (GAP), which activates the intrinsic GTPase activity of Rho1. GDP-bound Rho1 is activated by guanine nucleotide exchange factors (GEF), which catalyzes the exchange of GDP for GTP. GTP-bound Rho1 activates multiple downstream effectors that lead to actin polarization and cell wall synthesis.

organization as well as cell wall biogenesis genes. Rho1 also binds to and activates the integral plasma membrane protein Fks1, the enzyme responsible for the synthesis of β-1,3-glucan, to directly control cell wall biogenesis. Rho1 also associates with Bni1, involved in cortical actin organization and Skn7, a two-component system transcription factor that elicits an oxidative stress response.

Not all Rho1 effectors are activated in response to Rho1 activation. The downstream effectors that are activated by Rho1 depend, at least partially, on which Rho1 GEF is responsible for activation(*41*). There are three verified Rho1 GEFs in *S. cerevisiae*: Rom1, Rom2 and Tus1. Tus1 and Rom2 are partially redundant in the context of TORC2 signaling. However it is still unclear exactly which downstream Rho1 effectors are essential for TORC2 function. It may be that TORC2 can preferentially activate specific Rho1 signaling pathways via differential GEF activation. TORC2 is able to activate both MAPK signaling and Fks1 function downstream of Rho1. Notably, it has been shown that an *fks1Δ* mutant partially suppresses a *tor2^{ts}* (*27*). These data indicate that Fks1 is dispensable for TORC2 activity and that cell wall synthesis regulation is not an essential function of TORC2.

Discovery of a novel signaling pathway

The *tor2^{ts}* mutant can be suppressed by cell integrity stress, created chemically by treatment with detergent or cell wall perturbing agents (i.e., congo red) or genetically by deletion of genes involved in cell wall

production/maintenance. However the mechanism responsible for this suppression has never been elucidated. Understanding this pathway is important for understanding how the cell responds to stress and the signaling mechanisms that promote cell growth. In Chapter 2 we describe the discovery of a novel signaling pathway that can respond to cell stress to promote growth. This pathway is required for cell integrity stress to suppress the $tor2^{ts}$ mutant and involves the formation of a novel signaling complex that includes the PAS kinase phosphorylation dependent association of Ugp1, Rom2 and Ssd1 (Figure 1-6).

Central control of energy homeostasis

In higher eukaryotes appetite and nutrient utilization are influenced via neuronal inputs. These responses are regulated in the brain, more specifically through the arcuate nucleus (ARC) of the hypothalamus(*42*). The ARC releases neuropeptides, which signal to the paraventricular nucleus (PVN), the dorsomedial nucleus (DMN) and the ventralmedial nucleus (VMN), which can directly modulate feeding behavior(*43-45*). Within the ARC there are two populations of neurons: orexigenic (appetite inducing) and anorexigenic (appetite inhibitory) neurons. The orexigenic population includes neuropeptide Y (NPY) and agouti-related protein (AgRP) expressing neurons. The anorexigenic population includes pro-opiomelanocortin (POMC, precursor of melanocyte-stimulating hormone α-MSH) and cocaine and amphetamine-regulated transcript protein (CART) expressing neurons.
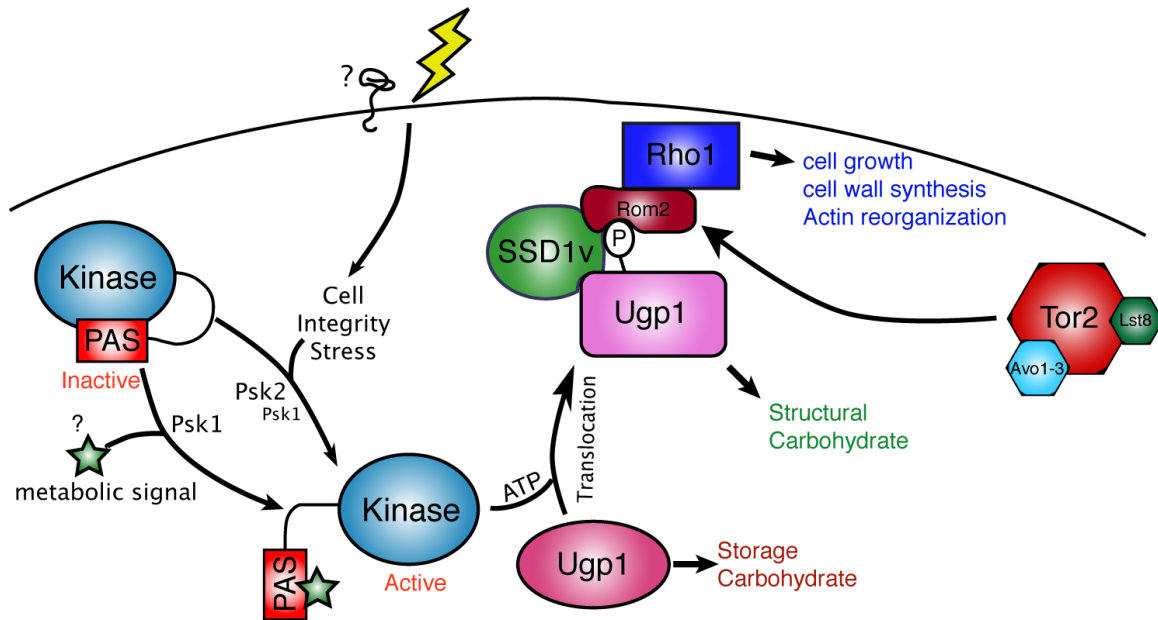
Figure 1-6). Schematic of PAS kinase suppression of the _tor2^ts_. PAS kinase phosphorylates Ugp1, which induces a translocation from the cytoplasm to the cell periphery. At the cell periphery P-Ugp1 nucleates the formation of a complex that includes Rom2 and Ssd1. Complex formation leads to activation of Rho1 and suppression of the _tor2^ts_.

Feeding activates POMC neurons, which stimulates the release of α-MSH and CART. Both, α-MSH and CART, bind to the melanocortin receptor 4 (MC4R) within the PVN to inhibit feeding behavior. α-MSH release leads to inhibition of glucose secretion from the liver, which is critical to maintain blood glucose in a narrow physiological range and inhibits the release of orexigenic neuropeptides. Conversely, release of AgRP directly antagonizes the binding of α-MSH to MC4R contributing the opposing effects of NPY/AgRP and POMC neurons on energy homeostasis. NPY release from the ARC leads to an increase in feeding behavior, hepatic glucose production and lipogenesis. In order for the ARC to effectively regulate feeding behavior it must receive input from the whole body. The nutrient status of the body is conveyed to the ARC via secreted proteins from peripheral tissues.

Endocrine regulation of energy homeostasis

In order for the central nervous system to appropriately regulate whole-body metabolism and energy intake it must receive inputs from the peripheral tissues of the body, which is accomplished primarily through secreted hormones. These are inputs from peripheral tissues that impinge upon the hypothalamus and central control of energy homeostasis. As with any global metabolic regulation the system has to be able to effectively integrate signals from various sources of energy, including food intake, circulating nutrients and energy storage,

which is accomplished primarily through the gut, pancreas and adipose tissue, respectively.

One endocrine organ that impinges on hypothalamic signaling is the pancreas. The pancreas responds to circulating blood glucose levels to release either insulin or glucagon into the blood stream. Under conditions of high circulating blood glucose concentrations the β-cells of the pancreas secrete insulin. Secretion of insulin from the pancreas is tightly coupled to an increase in intracellular ATP concentration(*46*). Insulin then binds to the insulin receptor (IR), which is expressed ubiquitously including neurons within the hypothalamus. Insulin release causes an increase in glucose uptake and utilization by peripheral tissues and suppresses gluconeogenesis within the liver(*47*). This allows the increase in blood glucose to be cleared via uptake within the peripheral tissue. Insulin also functions as a growth factor via promotion of amino acid uptake, protein synthesis and cell growth(*48*). Insulin acts within the hypothalamus to suppress energy intake via activation of the IR within the ARC(*49*). Insulin is a major regulator of dietary glucose utilization and energy homeostasis.

When blood glucose levels fall, the α-cells within the pancreas secrete glucagon. Glucagon elicits a switch from glucose uptake and utilization to mobilization of energy stores(*50*). Within the liver, the switch in substrate utilization is also coupled to an increase in gluconeogenesis and glucose secretion in order to sustain blood glucose levels. This is essential for organs

such as the brain and red blood cells, which are heavily dependent on glucose for energy production.

Adipose tissue is not only a storage depot for fat, but also an endocrine organ(*51*). White adipose tissue releases the anorectic hormone leptin. Circulating levels of leptin correlate positively with total body adiposity. Leptin promotes satiety through activation of the leptin receptor within the hypothalamus. Leptin simultaneously binds to NPY/AgRP neurons to inhibit the release of orexigenic signals and POMC neurons to stimulate the release of anorectic neuropeptides. Peripheral tissues also express the leptin receptor, which when activated promotes fatty acid oxidation. Leptin receptor activation within the liver inhibits gluconeogenesis and glucose secretion.

White adipose tissue also releases adiponectin, another hormone. Circulating plasma adiponectin levels negatively correlate with fat mass. Adiponectin has been shown to function as an insulin sensitizer in genetic models of obesity, such as ob/ob mice. This is mediated through activation of the AMPK signaling network, which leads to an increase in fatty acid oxidation and glucose uptake by peripheral tissues(*52*). Adiponectin also modulates central control of feeding through the hypothalamus. Activation of the adiponectin receptor in the hypothalamus leads to a decrease in energy expenditure and increase in food intake through the NPY/AgRP expressing neurons(*51*).

The gut releases a several hormones with anorectic effects. These include cholecystokinin, glucagon-like pepride-1 (GLP-1), oxyntomodulin (OXM),

pancreatic polypeptide (PP), peptide tyrosine tryrosine (PYY) and islet amyloid

peptide (IAP)(*53-55*). The mechanism by which each of these hormones elicits

an effect has not been completely elucidated. However the postprandial

expression and release of each of these hormones indicates that they are likely

satiety signals. Many of these peptides affect gastric emptying and digestive

enzyme release into the gut. GLP-1 is able to stimulate insulin release from the

pancreas(*56*). These anorectic hormones slow digestion, increase nutrient

absorption and elicit a satiety signal within the brain. However the mechanism of

action within the hypothalamus has not been fully elucidated.

Ghrelin is the only known orexigenic peptide that is released by the gut

and circulating levels increase before meals (*57*). The ghrelin receptor (GHS-R

1a) is primarily expressed within the AgRP/NPY neurons and activation

massively up-regulates expression of the neuropeptides NPY and AgRP(*58*).

The increase in NPY/AgRP leads to an increase in food intake. Ghrelin has no

direct effect on expression of the anorexigenic POMC mRNA. However it does

appear to indirectly inhibit the firing of the POMC expressing neurons.

Interestingly, the intracellular signaling modalities that regulate feeding

behavior within the brain are ubiquitously expressed within all tissue types(*2, 3*).

The ancient intracellular nutrient responsive modalities are even found within the

unicellular *s. cerevisiae*. Multicellular organisms' more complex mechanisms of

regulation have been grafted onto these ancient nutrient regulation systems.

These cell-autonomous mechanisms of energy regulation will be briefly reviewed below.

Cell autonomous signaling mechanisms

The endocrine system elicits its effects on the organism through intracellular activation of metabolic signaling pathways(*5*). Many of these intracellular signaling mechanisms are highly conserved through evolution(*59*). These mechanisms allow the cell to integrate whole body metabolism with the local microenvironment of the cell. The overall health of the organism is dictated by intracellular decisions that are made in response to extracellular inputs. Misregulation of these response mechanisms can lead to many pathological outcomes including obesity or cancer. Specifically, cell autonomous metabolic decisions are primarily guided by a few well-characterized signaling pathways. The master regulators of cellular metabolism are generally characterized by an ability to integrate multiple inputs and then propagate the output signal. Two of the best-characterized regulators of cellular energy status are TOR and AMPK, two highly conserved protein kinases(*2, 3*).

A fundamental cellular requirement is that cells couple availability of nutrients to growth factor signaling in order to drive growth only when there are sufficient nutrients to undergo cell division. Under conditions of low ATP and high AMP, AMPK acts as an energy checkpoint within the cell to stop cell growth and activate ATP-producing cellular processes(*7*). AMPK is a highly conserved

heterotrimeric protein kinase complex that consists of one catalytic (α) subunit

and two regulatory (β and γ) subunits. In mammals there are multiple paralogs of

each subunit, which increases the heterogeneity of the AMPK complex allowing

for variation in complex distribution and sensitivity. However the redundancy of

the subunits has made study of AMPK on an organismal level difficult. The

AMPKα1-/- AMPKα2-/- mice are embryonic lethal at 10.5 days postfertilization,

indicating an essential role for AMPK in development. The AMPKα1-/- has no

detectable metabolic phenotype, which could be due to redundancy with

AMPKα2. AMPKα2-/- results in mild insulin resistance and impaired glucose

tolerance that is associated with an insulin secretion defect(*60, 61*). This effect

seems to be due to the role of AMPK in the autonomic nervous system because

cells isolated from AMPKα2-/- function normally in isolation(*61*). The AMPKβ1 -/-

mice have reduced food intake and adiposity on a high fat diet(*62*). These data

generated from the knockout mice, which are complicated because of

redundancy, indicate that AMPK is critical for normal energy homeostasis.

 In order to understand the role of AMPK in energy homeostasis cell culture

systems and model organisms have provided a clear biochemical understanding

of AMPK function. As intracellular AMP levels increase AMP binds directly to the

tandem repeats of crystathionine-B-synthase domains of the γ-subunit(*63*).

Binding of AMP is thought to prevent dephosphorylation of a critical activation

loop threonine (Thr172) of the α-subunit. Phosphorylation of this threonine is

absolutely required for activation of the kinase. Activation of AMPK leads to

inhibition of glycogen synthesis, lipid synthesis and gluconeogenesis (Figure 1-7)(*2*). This inhibition is coordinated with up-regulation of lipid oxidation, glycolysis, mitochondrial activity and mitochondrial biogenesis.

Hepatic metabolism plays a central role in whole body energy homeostasis and is a major site for storage and distribution of glucose. AMPK activation, within the liver, induces a switch from lipid synthesis to lipid oxidation(*64*). The switch is mediated by phosphorylation and inhibition of Acetyl-CoA carboxylase (ACC). Inhibition of ACC produces a drop in intracellular malonyl-CoA levels. Malonly-CoA is a precursor for fatty acid synthesis and is also a potent inhibitor of mitochondrial β-oxidation by inhibition of carnitine palmitoyltransferase (CPT1)(*65*). Within skeletal muscle AMPK promotes mitochondrial biogenesis at least in part through activation of the transcription factors PPAR-gamma coactivator (PGC-1α) and peroxisome proliferator-activated receptor (PPAR-δ)(*66*). The animal knockout data taken together with the cell culture data indicate that AMPK plays a critical function in energy metabolism through effects on lipid oxidation, glycolysis and mitochondrial function. AMPK function is partially tissue specific. However AMPK activation universally leads to up-regulation of energy producing processes.

Mammalian Target of Rapamycin (mTOR) is a conserved serine/threonine kinase that is a master regulator of cell size and growth(*3*). Similar to *S. cerevisiae,* mTOR forms two functionally distinct complexes, mTORC1 and mTORC2(*67, 68*). In mammals mTORC1 consists of four proteins: raptor
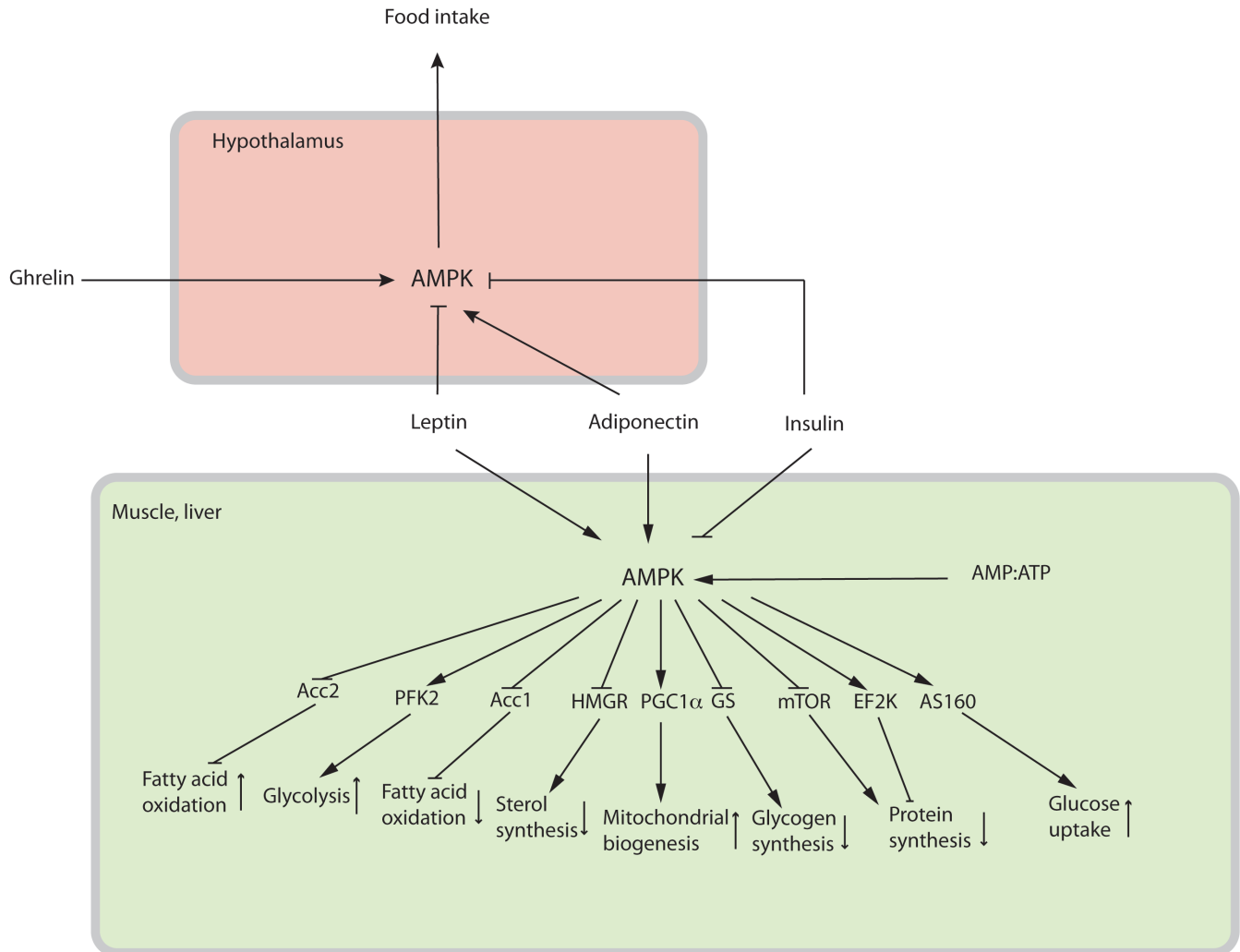
Figure 1-7). Overview of AMPK signaling in the hypothalamus and peripheral tissues. AMPK responds to a decrease in energy availability to stimulate energy production and inhibit energy consumption. Adapted from reference (*2*)

(regulatory associated protein of mTOR), PRAS40, mLST8 and mTOR. Growth factors and nutrients both activate mTORC1. There are two well-characterized mTORC1 downstream targets: 4EBP1 and the p70 ribosomal S6 kinase (S6K)(*69*). Phosphorylation of 4EBP1 by mTORC1 suppresses 4EBP1's inhibition of the translation initiation factor eIF4E (Figure 1-8)(*70*). Phosphorylation of 4EBP1 and S6K leads to an increase in protein translation, including expression of specific cell growth regulators such as HIF-1α and c-myc. S6K activation also controls lipid synthesis through post-transcriptional regulation of the sterol regulatory element-binding protein 1c (SREBP1c)(*71*). Chronic mTORC1 activation, as in the case of hyperglycemia, hyperlipidemia and hyperinsulinemia, lead to direct phosphorylation and degradation of components of insulin signaling(*72*). This negative feedback loop that suppresses insulin signaling might be responsible for some insulin resistance found in diabetics.

The mouse knockout of mTOR is embryonic lethal(*73*). However S6K knockout mice, an effector of mTORC1 that acts to integrate nutrient and insulin signals, have several metabolic defects(*72, 74*). Specifically, the mice are hypoinsulinemic, glucose intolerant and have reduced β-cell mass. On a high fat diet (HFD), S6K-/- mice have an increase in circulating free fatty acids and glucose but they remain insulin sensitive. The insulin sensitivity appears to be due to a lack of the negative feedback loop from S6K to IRS1. The effect of the S6K-/- indicates that mTOR signaling is required to properly utilize nutrients.
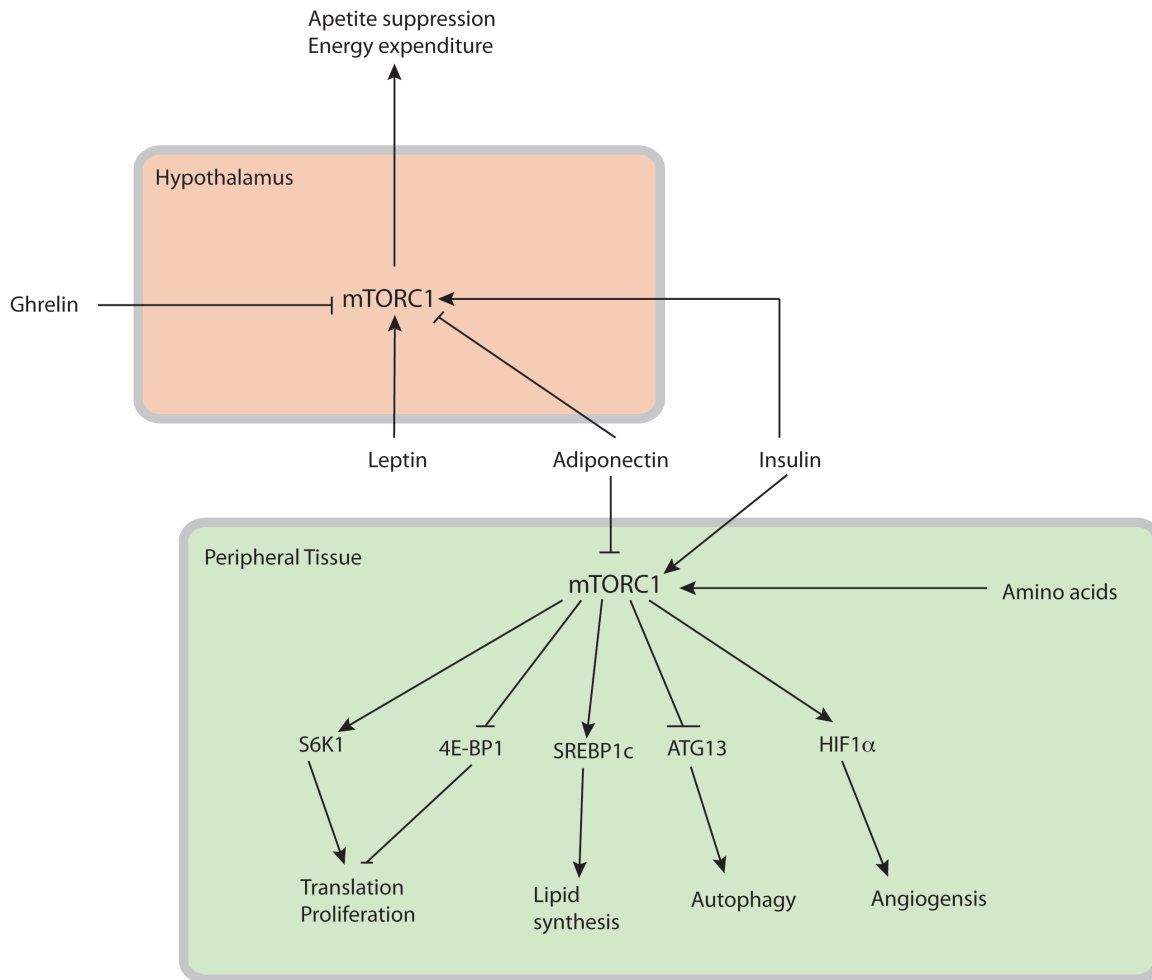
Figure 1-8). Overview of mTORC1 signaling. In response to nutrient replete conditions mTORC1 up-regulates anabolic processes and inhibits catabolic processes. Growth factor signaling also activates mTORC1, which drives an increase in cell size primarily through translation.

Identification and characterization of these two key metabolic kinases (AMPK, mTOR) have led to an increase in our understanding of growth and energy homeostatsis. This understanding has also produced novel treatments for a myriad of pathologies from obesity to cancer. Metformin has become a highly prescribed drug for many obesity related pathologies and is a potent activator of AMPK. Rapamycin(*75*) and other second generation drugs(*76*) are used for the treatment of some cancers as well as an immunosuppressant prior to organ transplantation(*77*). These drugs are selective inhibitors of mTORC1 signaling. As our understanding of the molecular events that occur within the cell increases, so does our ability to treat the pathologies that stem from malfunctions in that system. We have phenotypically characterized the mouse knockout of PAS kinase (PASK-/-) and shown that PASK is required for normal energy homeostasis. The PASK-/- mice are resistant to diet-induced obesity when challenged with a HFD and are hypermetabolic as measured by indirect calrimetry. On a HFD the PASK-/- are resistant to hepatosteatosis. The hypermetabolic phenotype of the PASK deficient mice can be replicated in a cell culture model. These data indicate that PASK functions in a cell autonomous mechanism to regulate energy homeostasis.

References

1. Kaeberlein, M., Andalis, A. A., Liszt, G. B., Fink, G. R., and Guarente, L. (2004) Saccharomyces cerevisiae SSD1-V confers longevity by a Sir2p-independent mechanism, *Genetics 166*, 1661-1672.

2. Hardie, D. G. (2007) AMP-activated/SNF1 protein kinases: conserved guardians of cellular energy, *Nat Rev Mol Cell Biol 8*, 774-785.

3. Zoncu, R., Efeyan, A., and Sabatini, D. M. (2011) mTOR: from growth signal integration to cancer, diabetes and ageing, *Nat Rev Mol Cell Biol 12*, 21-35.

4. Levin, B. E., Magnan, C., Dunn-Meynell, A., and Le Foll, C. (2011) Metabolic sensing and the brain: who, what, where, and how?, *Endocrinology 152*, 2552-2557.

5. Hardie, D. G. (2008) AMPK: a key regulator of energy balance in the single cell and the whole organism, *Int J Obes (Lond) 32 Suppl 4*, S7-12.

6. Ma, X. M., and Blenis, J. (2009) Molecular mechanisms of mTOR-mediated translational control, *Nat Rev Mol Cell Biol 10*, 307-318.

7. Shaw, R. J. (2009) LKB1 and AMP-activated protein kinase control of mTOR signalling and growth, *Acta Physiol (Oxf) 196*, 65-80.

8. Hao, H. X., Cardon, C. M., Swiatek, W., Cooksey, R. C., Smith, T. L., Wilde, J., Boudina, S., Abel, E. D., McClain, D. A., and Rutter, J. (2007) PAS kinase is required for normal cellular energy balance, *Proc Natl Acad Sci U S A 104*, 15466-15471.

9. Hardie, D. G. (2007) AMP-activated/SNF1 protein kinases: conserved guardians of cellular energy, *Nat Rev Mol Cell Biol 8*, 774-785.

10. Jansen, J. M., Wanless, A. G., Seidel, C. W., and Weiss, E. L. (2009) Cbk1 regulation of the RNA-binding protein Ssd1 integrates cell fate with translational control, *Curr Biol 19*, 2114-2120.

11. Kamada, Y., Fujioka, Y., Suzuki, N. N., Inagaki, F., Wullschleger, S., Loewith, R., Hall, M. N., and Ohsumi, Y. (2005) Tor2 directly phosphorylates the AGC kinase Ypk2 to regulate actin polarization, *Mol Cell Biol 25*, 7239-7248.

12. Smith, T. L., and Rutter, J. (2007) Regulation of glucose partitioning by PAS kinase and Ugp1 phosphorylation, *Mol Cell 26*, 491-499.

13. Loewith, R., Jacinto, E., Wullschleger, S., Lorberg, A., Crespo, J. L., Bonenfant, D., Oppliger, W., Jenoe, P., and Hall, M. N. (2002) Two TOR complexes, only one of which is rapamycin sensitive, have distinct roles in cell growth control, *Mol Cell 10*, 457-468.

14. Wullschleger, S., Loewith, R., and Hall, M. N. (2006) TOR signaling in growth and metabolism, *Cell 124*, 471-484.

15. Schmidt, A., Kunz, J., and Hall, M. N. (1996) TOR2 is required for organization of the actin cytoskeleton in yeast, *Proc Natl Acad Sci U S A 93*, 13780-13785.

16. Yamochi, W., Tanaka, K., Nonaka, H., Maeda, A., Musha, T., and Takai, Y. (1994) Growth site localization of Rho1 small GTP-binding protein and its involvement in bud formation in Saccharomyces cerevisiae, *J Cell Biol 125*, 1077-1093.

17. Helliwell, S. B., Wagner, P., Kunz, J., Deuter-Reinhard, M., Henriquez, R., and Hall, M. N. (1994) TOR1 and TOR2 are structurally and functionally similar but not identical phosphatidylinositol kinase homologues in yeast, *Mol Biol Cell 5*, 105-118.

18. Kunz, J., Schneider, U., Howald, I., Schmidt, A., and Hall, M. N. (2000) HEAT repeats mediate plasma membrane localization of Tor2p in yeast, *J Biol Chem 275*, 37011-37020.

19. Crespo, J. L., and Hall, M. N. (2002) Elucidating TOR signaling and rapamycin action: lessons from Saccharomyces cerevisiae, *Microbiol Mol Biol Rev 66*, 579-591, table of contents.

20. Beck, T., and Hall, M. N. (1999) The TOR signalling pathway controls nuclear localization of nutrient-regulated transcription factors, *Nature 402*, 689-692.

21. Noda, T., and Ohsumi, Y. (1998) Tor, a phosphatidylinositol kinase homologue, controls autophagy in yeast, *J Biol Chem 273*, 3963-3966.

22. Martin, D. E., Soulard, A., and Hall, M. N. (2004) TOR regulates ribosomal protein gene expression via PKA and the Forkhead transcription factor FHL1, *Cell 119*, 969-979.

23. Berset, C., Trachsel, H., and Altmann, M. (1998) The TOR (target of rapamycin) signal transduction pathway regulates the stability of

translation initiation factor eIF4G in the yeast Saccharomyces cerevisiae, *Proc Natl Acad Sci U S A 95*, 4264-4269.

24. Chen, E. J., and Kaiser, C. A. (2003) LST8 negatively regulates amino acid biosynthesis as a component of the TOR pathway, *J Cell Biol 161*, 333-347.

25. Schmidt, A., Bickle, M., Beck, T., and Hall, M. N. (1997) The yeast phosphatidylinositol kinase homolog TOR2 activates RHO1 and RHO2 via the exchange factor ROM2, *Cell 88*, 531-542.

26. Aronova, S., Wedaman, K., Aronov, P. A., Fontes, K., Ramos, K., Hammock, B. D., and Powers, T. (2008) Regulation of ceramide biosynthesis by TOR complex 2, *Cell Metab 7*, 148-158.

27. Helliwell, S. B., Howald, I., Barbet, N., and Hall, M. N. (1998) TOR2 is part of two related signaling pathways coordinating cell growth in Saccharomyces cerevisiae, *Genetics 148*, 99-112.

28. Rutter, J., Probst, B. L., and McKnight, S. L. (2002) Coordinate regulation of sugar flux and translation by PAS kinase, *Cell 111*, 17-28.

29. Rutter, J., Michnoff, C. H., Harper, S. M., Gardner, K. H., and McKnight, S. L. (2001) PAS kinase: an evolutionarily conserved PAS domain-regulated serine/threonine kinase, *Proc Natl Acad Sci U S A 98*, 8991-8996.

30. Kikani, C. K., Antonysamy, S. A., Bonanno, J. B., Romero, R., Zhang, F. F., Russell, M., Gheyi, T., Iizuka, M., Emtage, S., Sauder, J. M., Turk, B. E., Burley, S. K., and Rutter, J. (2010) Structural bases of PAS domain-regulated kinase (PASK) activation in the absence of activation loop phosphorylation, *J Biol Chem 285*, 41034-41043.

31. Grose, J. H., Smith, T. L., Sabic, H., and Rutter, J. (2007) Yeast PAS kinase coordinates glucose partitioning in response to metabolic and cell integrity signaling, *EMBO J 26*, 4824-4830.

32. Daran, J. M., Dallies, N., Thines-Sempoux, D., Paquet, V., and Francois, J. (1995) Genetic and biochemical characterization of the UGP1 gene encoding the UDP-glucose pyrophosphorylase from Saccharomyces cerevisiae, *Eur J Biochem 233*, 520-530.

33. Polakis, E. S., and Bartley, W. (1966) Changes in the intracellular concentrations of adenosine phosphates and nicotinamide nucleotides

during the aerobic growth cycle of yeast on different carbon sources, *Biochem J 99*, 521-533.

34. Roeben, A., Plitzko, J. M., Korner, R., Bottcher, U. M., Siegers, K., Hayer-Hartl, M., and Bracher, A. (2006) Structural basis for subunit assembly in UDP-glucose pyrophosphorylase from Saccharomyces cerevisiae, *J Mol Biol 364*, 551-560.

35. Wheeler, R. T., Kupiec, M., Magnelli, P., Abeijon, C., and Fink, G. R. (2003) A Saccharomyces cerevisiae mutant with increased virulence, *Proc Natl Acad Sci U S A 100*, 2766-2770.

36. Kurischko, C., Kim, H. K., Kuravi, V. K., Pratzka, J., and Luca, F. C. (2011) The yeast Cbk1 kinase regulates mRNA localization via the mRNA-binding protein Ssd1, *J Cell Biol 192*, 583-598.

37. Schmidt, A., Schmelzle, T., and Hall, M. N. (2002) The RHO1-GAPs SAC7, BEM2 and BAG7 control distinct RHO1 functions in Saccharomyces cerevisiae, *Mol Microbiol 45*, 1433-1441.

38. Ozaki, K., Tanaka, K., Imamura, H., Hihara, T., Kameyama, T., Nonaka, H., Hirano, H., Matsuura, Y., and Takai, Y. (1996) Rom1p and Rom2p are GDP/GTP exchange proteins (GEPs) for the Rho1p small GTP binding protein in Saccharomyces cerevisiae, *EMBO J 15*, 2196-2207.

39. Nonaka, H., Tanaka, K., Hirano, H., Fujiwara, T., Kohno, H., Umikawa, M., Mino, A., and Takai, Y. (1995) A downstream target of RHO1 small GTP-binding protein is PKC1, a homolog of protein kinase C, which leads to activation of the MAP kinase cascade in Saccharomyces cerevisiae, *EMBO J 14*, 5931-5938.

40. Qadota, H., Python, C. P., Inoue, S. B., Arisawa, M., Anraku, Y., Zheng, Y., Watanabe, T., Levin, D. E., and Ohya, Y. (1996) Identification of yeast Rho1p GTPase as a regulatory subunit of 1,3-beta-glucan synthase, *Science 272*, 279-281.

41. Helliwell, S. B., Schmidt, A., Ohya, Y., and Hall, M. N. (1998) The Rho1 effector Pkc1, but not Bni1, mediates signalling from Tor2 to the actin cytoskeleton, *Curr Biol 8*, 1211-1214.

42. Cone, R. D. (2005) Anatomy and regulation of the central melanocortin system, *Nat Neurosci 8*, 571-578.

43. Coll, A. P. (2007) Effects of pro-opiomelanocortin (POMC) on food intake and body weight: mechanisms and therapeutic potential?, *Clin Sci (Lond) 113*, 171-182.

44. McCrimmon, R. J., Shaw, M., Fan, X., Cheng, H., Ding, Y., Vella, M. C., Zhou, L., McNay, E. C., and Sherwin, R. S. (2008) Key role for AMP-activated protein kinase in the ventromedial hypothalamus in regulating counterregulatory hormone responses to acute hypoglycemia, *Diabetes 57*, 444-450.

45. Coll, A. P., and Loraine Tung, Y. C. (2009) Pro-opiomelanocortin (POMC)-derived peptides and the regulation of energy homeostasis, *Mol Cell Endocrinol 300*, 147-151.

46. Seino, S., Shibasaki, T., and Minami, K. (2011) Dynamics of insulin secretion and the clinical implications for obesity and diabetes, *J Clin Invest 121*, 2118-2125.

47. Kaestner, K. H., Christy, R. J., and Lane, M. D. (1990) Mouse insulin-responsive glucose transporter gene: characterization of the gene and trans-activation by the CCAAT/enhancer binding protein, *Proc Natl Acad Sci U S A 87*, 251-255.

48. Nave, B. T., Ouwens, M., Withers, D. J., Alessi, D. R., and Shepherd, P. R. (1999) Mammalian target of rapamycin is a direct target for protein kinase B: identification of a convergence point for opposing effects of insulin and amino-acid deficiency on protein translation, *Biochem J 344 Pt 2*, 427-431.

49. Belgardt, B. F., Okamura, T., and Bruning, J. C. (2009) Hormone and glucose signalling in POMC and AgRP neurons, *The Journal of Physiology 587*, 5305-5314.

50. Berglund, E. D., Lee-Young, R. S., Lustig, D. G., Lynes, S. E., Donahue, E. P., Camacho, R. C., Meredith, M. E., Magnuson, M. A., Charron, M. J., and Wasserman, D. H. (2009) Hepatic energy state is regulated by glucagon receptor signaling in mice, *J Clin Invest 119*, 2412-2422.

51. Galic, S., Oakhill, J. S., and Steinberg, G. R. (2010) Adipose tissue as an endocrine organ, *Molecular and cellular endocrinology 316*, 129-139.

52. Schraw, T., Wang, Z. V., Halberg, N., Hawkins, M., and Scherer, P. E. (2008) Plasma adiponectin complexes have distinct biochemical characteristics, *Endocrinology 149*, 2270-2282.

53.   Burcelin, R., Serino, M., and Cabou, C. (2009) A role for the gut-to-brain GLP-1-dependent axis in the control of metabolism, *Curr Opin Pharmacol 9*, 744-752.

54.   Smith, G. P., and Gibbs, J. (1992) Are gut peptides a new class of anorectic agents?, *Am J Clin Nutr 55*, 283S-285S.

55.   Cummings, D. E., and Overduin, J. (2007) Gastrointestinal regulation of food intake, *J Clin Invest 117*, 13-23.

56.   Drucker, D. J. (2006) The biology of incretin hormones, *Cell Metab 3*, 153-165.

57.   Tschop, M., Smiley, D. L., and Heiman, M. L. (2000) Ghrelin induces adiposity in rodents, *Nature 407*, 908-913.

58.   Date, Y., Murakami, N., Toshinai, K., Matsukura, S., Niijima, A., Matsuo, H., Kangawa, K., and Nakazato, M. (2002) The role of the gastric afferent vagal nerve in ghrelin-induced feeding and growth hormone secretion in rats, *Gastroenterology 123*, 1120-1128.

59.   Kahn, B. B., Alquier, T., Carling, D., and Hardie, D. G. (2005) AMP-activated protein kinase: ancient energy gauge provides clues to modern understanding of metabolism, *Cell Metab 1*, 15-25.

60.   Jorgensen, S. B., Viollet, B., Andreelli, F., Frosig, C., Birk, J. B., Schjerling, P., Vaulont, S., Richter, E. A., and Wojtaszewski, J. F. (2004) Knockout of the alpha2 but not alpha1 5'-AMP-activated protein kinase isoform abolishes 5-aminoimidazole-4-carboxamide-1-beta-4-ribofuranosidebut not contraction-induced glucose uptake in skeletal muscle, *J Biol Chem 279*, 1070-1079.

61.   Viollet, B., Andreelli, F., Jorgensen, S. B., Perrin, C., Geloen, A., Flamez, D., Mu, J., Lenzner, C., Baud, O., Bennoun, M., Gomas, E., Nicolas, G., Wojtaszewski, J. F., Kahn, A., Carling, D., Schuit, F. C., Birnbaum, M. J., Richter, E. A., Burcelin, R., and Vaulont, S. (2003) The AMP-activated protein kinase alpha2 catalytic subunit controls whole-body insulin sensitivity, *J Clin Invest 111*, 91-98.

62.   Dzamko, N., van Denderen, B. J., Hevener, A. L., Jorgensen, S. B., Honeyman, J., Galic, S., Chen, Z. P., Watt, M. J., Campbell, D. J., Steinberg, G. R., and Kemp, B. E. (2010) AMPK beta1 deletion reduces

appetite, preventing obesity and hepatic insulin resistance, *J Biol Chem 285*, 115-122.

63.   Sanders, M. J., Grondin, P. O., Hegarty, B. D., Snowden, M. A., and Carling, D. (2007) Investigating the mechanism for AMP activation of the AMP-activated protein kinase cascade, *Biochem J 403*, 139-148.

64.   Hardie, D. G., and Pan, D. A. (2002) Regulation of fatty acid synthesis and oxidation by the AMP-activated protein kinase, *Biochem Soc Trans 30*, 1064-1070.

65.   Bird, M. I., and Saggerson, E. D. (1984) Binding of malonyl-CoA to isolated mitochondria. Evidence for high- and low-affinity sites in liver and heart and relationship to inhibition of carnitine palmitoyltransferase activity, *Biochem J 222*, 639-647.

66.   Zong, H., Ren, J. M., Young, L. H., Pypaert, M., Mu, J., Birnbaum, M. J., and Shulman, G. I. (2002) AMP kinase is required for mitochondrial biogenesis in skeletal muscle in response to chronic energy deprivation, *Proc Natl Acad Sci U S A 99*, 15983-15987.

67.   Kim, D. H., Sarbassov, D. D., Ali, S. M., King, J. E., Latek, R. R., Erdjument-Bromage, H., Tempst, P., and Sabatini, D. M. (2002) mTOR interacts with raptor to form a nutrient-sensitive complex that signals to the cell growth machinery, *Cell 110*, 163-175.

68.   Sarbassov, D. D., Ali, S. M., Kim, D. H., Guertin, D. A., Latek, R. R., Erdjument-Bromage, H., Tempst, P., and Sabatini, D. M. (2004) Rictor, a novel binding partner of mTOR, defines a rapamycin-insensitive and raptor-independent pathway that regulates the cytoskeleton, *Curr Biol 14*, 1296-1302.

69.   Holz, M. K., Ballif, B. A., Gygi, S. P., and Blenis, J. (2005) mTOR and S6K1 mediate assembly of the translation preinitiation complex through dynamic protein interchange and ordered phosphorylation events, *Cell 123*, 569-580.

70.   Hara, K., Yonezawa, K., Kozlowski, M. T., Sugimoto, T., Andrabi, K., Weng, Q. P., Kasuga, M., Nishimoto, I., and Avruch, J. (1997) Regulation of eIF-4E BP1 phosphorylation by mTOR, *J Biol Chem 272*, 26457-26463.

71.   Duvel, K., Yecies, J. L., Menon, S., Raman, P., Lipovsky, A. I., Souza, A. L., Triantafellow, E., Ma, Q., Gorski, R., Cleaver, S., Vander Heiden, M. G., MacKeigan, J. P., Finan, P. M., Clish, C. B., Murphy, L. O., and

Manning, B. D. (2010) Activation of a metabolic gene regulatory network downstream of mTOR complex 1, *Mol Cell 39*, 171-183.

72. Um, S. H., Frigerio, F., Watanabe, M., Picard, F., Joaquin, M., Sticker, M., Fumagalli, S., Allegrini, P. R., Kozma, S. C., Auwerx, J., and Thomas, G. (2004) Absence of S6K1 protects against age- and diet-induced obesity while enhancing insulin sensitivity, *Nature 431*, 200-205.

73. Gangloff, Y. G., Mueller, M., Dann, S. G., Svoboda, P., Sticker, M., Spetz, J. F., Um, S. H., Brown, E. J., Cereghini, S., Thomas, G., and Kozma, S. C. (2004) Disruption of the mouse mTOR gene leads to early postimplantation lethality and prohibits embryonic stem cell development, *Mol Cell Biol 24*, 9508-9516.

74. Aguilar, V., Alliouachene, S., Sotiropoulos, A., Sobering, A., Athea, Y., Djouadi, F., Miraux, S., Thiaudiere, E., Foretz, M., Viollet, B., Diolez, P., Bastin, J., Benit, P., Rustin, P., Carling, D., Sandri, M., Ventura-Clapier, R., and Pende, M. (2007) S6 kinase deletion suppresses muscle growth adaptations to nutrient availability by activating AMP kinase, *Cell Metab 5*, 476-487.

75. Cloughesy, T. F., Yoshimoto, K., Nghiemphu, P., Brown, K., Dang, J., Zhu, S., Hsueh, T., Chen, Y., Wang, W., Youngkin, D., Liau, L., Martin, N., Becker, D., Bergsneider, M., Lai, A., Green, R., Oglesby, T., Koleto, M., Trent, J., Horvath, S., Mischel, P. S., Mellinghoff, I. K., and Sawyers, C. L. (2008) Antitumor activity of rapamycin in a Phase I trial for patients with recurrent PTEN-deficient glioblastoma, *PLoS Med 5*, e8.

76. Janes, M. R., Limon, J. J., So, L., Chen, J., Lim, R. J., Chavez, M. A., Vu, C., Lilly, M. B., Mallya, S., Ong, S. T., Konopleva, M., Martin, M. B., Ren, P., Liu, Y., Rommel, C., and Fruman, D. A. (2010) Effective and selective targeting of leukemia cells using a TORC1/2 kinase inhibitor, *Nat Med 16*, 205-213.

77. Ferrer, I. R., Araki, K., and Ford, M. L. (2011) Paradoxical aspects of rapamycin immunobiology in transplantation, *Am J Transplant 11*, 654-659.

CHAPTER 2

PAS KINASE REGULATES CELL SURVIVAL AND GROWTH IN RESPONSE TO STRESS

Caleb M. Cardon, Thomas Beck, Michael N. Hall, and Jared Rutter

Abstract

In a high copy suppressor screen of a mutant of the *S. cerevisiae* Target of Rapamycin 2 (*tor2)* gene, we isolated *PSK1* and *PSK2*, paralogous yeast genes encoding two serine/threonine kinases, referred together as PAS kinase. We also show that post-translational activation of PAS kinase, either by cell integrity stress or growth on nonfermentative carbon sources, suppresses the *tor2* mutation. Suppression of the *tor2* mutant by PAS kinase activation requires phosphorylation of the metabolic enzyme Ugp1 on serine-11. Ugp1 phosphorylation nucleates the formation of a complex that induces Rho1 activation. In addition to phospho-Ugp1, this complex contains Rom2, a Rho1 guanine nucleotide exchange factor, and Ssd1, a poorly characterized RNA binding protein. Activation of PAS kinase-dependent Ugp1 phosphorylation, therefore, promotes two processes that are required for cell growth and stress resistance. First, as shown previously, Ugp1 phosphorylation leads to the synthesis of cell wall material through an alteration in glucose partitioning. Second, through the formation of a signaling complex, it leads to polarized cell growth through Rho1 activation This complex potentially integrates the metabolic and signaling responses required for cell growth and survival in suboptimal conditions.

Introduction

Organisms must monitor their environment in order to respond appropriately to changes in nutrient levels, temperature, and toxins. One of the most critical decisions made by organisms is whether to stimulate or arrest growth given the current environmental situation. In multicellular organisms, this decision depends upon inputs from neighboring cells, hormonal cues and neuronal signaling. In this context making the wrong growth decision at a cellular level can lead to pathological consequences, including cancer. Cells from multicellular organisms also have autonomous mechanisms to measure nutrient availability, which integrated with extrinsic signals, enables making appropriate growth decisions.

Two evolutionarily conserved kinases that participate in this sensing and response are the 5'-AMP-activated protein kinase (AMPK) (*1*) and the Target of Rapamycin (TOR)(*2, 3*). AMPK is activated when intracellular energy in the form of ATP is depleted and promotes a switch from ATP consumption to ATP production(*4*). One primary aspect of this switch is a cessation of cell growth and division. The TOR protein kinase is activated under nutrient replete conditions and leads to an increase in protein translation and cell growth (*2, 5*). As such, it has been called a master regulator of cell and organismal size in most organisms.

The *S. cerevisiae* genome contains two closely related TOR genes, *TOR1* and *TOR2*. The protein products of these two genes function in two distinct protein complexes termed TOR complex 1 (TORC1) and TOR complex 2

(TORC2)(*6-8*). TORC1, which contains either Tor1 or Tor2 as well as Kog1, Tco89 and Lst8, regulates protein synthesis and cell size in response to nutrient availability. TORC1 function is sensitive to inhibition by rapamycin. TORC2, which contains Tor2 (but not Tor1), Avo1, Avo2, Avo3, Bit61 and Lst8, is essential for cell division and cell cycle-dependent polarization of the actin cytoskeleton (*9-11*). TORC2 function is not directly sensitive to rapamycin. TORC2 regulates polarized cell growth at least partially through activation of the small GTPase Rho1 (*12*). Rho1 regulates many downstream signaling pathways including Protein Kinase C (Pkc1)-mediated activation of MAPK signaling, activation of cell wall synthesis via Fks1 and polarization of the actin cytoskeleton to enable cell growth and division (*13-16*). As stated in Chapter 1 strains harboring a temperature sensitive allele of *TOR2* (*tor2^{ts}*) arrest growth at the restrictive temperature (37° C) due to lack of TORC2 activity and decreased activation of Rho1(*6*). The lethality caused by a *tor2^{ts}* mutant can be suppressed by proteins that activate Rho1, or growth nonfermentative carbon sources but not nonfermentable carbon sources. Unexpectedly, cell integrity stress can also suppress the *tor2^{ts}* phenotype (*17*). However the cellular mechanism connecting nonfermentative carbon sources, cell wall stress and suppression of the *tor2^{ts}* remains unresolved. These data suggest the presence of signaling networks that can integrate input from cell integrity and metabolic signals to control cell growth.

The recent past has seen many advances in our understanding of the diversity of inputs that are recognized by cell autonomous nutrient sensors and of

those sensors themselves. One advance was the discovery and initial

characterization of PAS kinase, which is required for normal energy balance in

organisms from *S. cerevisiae* to mice (*18, 19*). However, the mechanisms

whereby PAS kinase signaling integrates into broader cellular signaling networks

have remained undiscovered. The *S. cerevisiae* genome contains two closely

related and partially redundant PAS kinase paralogs, *PSK1* and *PSK2* (referred

to together as PAS kinase). Cell integrity stress activates PAS kinase via the

WSC family of cell membrane sensors (*20*). Cellular nutrient status can also

activate PAS kinase through an interaction with the Snf1/AMPK signaling

pathway. Psk1 and Psk2 both phosphorylate serine-11 of Ugp1, the enzyme

responsible for the synthesis of UDP-glucose, which is the glucose donor for

glycogen and cell wall glucan production. Surprisingly, phosphorylation at serine-

11 does not affect the enzymatic activity of Ugp1, but rather the destination of the

glucose moiety from UDP-glucose (*21*). In the unphosphorylated state, Ugp1

synthesizes UDP-glucose that is used preferentially for the synthesis of glycogen.

In the phosphorylated state, Ugp1 produces UDP-glucose that is partitioned

preferentially toward production of cell wall glucans. Therefore, a PAS kinase null

strain (*psk1Δ psk2Δ)* exhibits a dramatic increase in glycogen content at the

expense of cell wall glucan, indicating an inability to properly regulate glucose

flux. All PAS kinase mutant phenotypes are completely phenocopied by mutating

Ugp1 serine-11 to alanine (Ugp1-S11A), which prevents Ugp1 phosphorylation.

This indicates that the effects of PAS kinase on glucose partitioning are primarily mediated through Ugp1 phosphorylation.

In a screen for multicopy suppressors of the lethality of a $tor2^{ts}$ mutant, we discovered both *PSK1* and *PSK2*. We found that the signaling mechanism by which PAS kinase suppresses the $tor2^{ts}$ requires phosphorylation of Ugp1. We show that phosphorylated Ugp1 enables the formation of a signaling complex, containing phosphorylated Ugp1, Ssd1 and Rom2, which leads to the activation of Rho1. The activation of Rho1, in response to PAS kinase dependent phosphorylation of Ugp1, stimulates cell survival and growth. Thus, we describe a signaling pathway by which PAS kinase signals for cell growth in coordination with its previously described progrowth effects on glucose partitioning.

Results

PAS kinase is both necessary and sufficient

for suppression of the $tor2^{ts}$

Due to its role in enabling cell growth and division as a component of TORC2, Tor2 is essential for viability (*6*). Because a *tor2* deletion mutant is inviable, we have utilized a temperature-sensitive $tor2^{ts}$ mutant to conduct a high copy suppressor screen for novel genes that enable suppression of the lethality caused by a $tor2^{ts}$. This screen should reveal genes that are downstream of Tor2 or genes that can activate similar growth pathways, but do so independently of Tor2. We used a 2-micron library constructed from the *S. cerevisiae* genome to

discover genomic fragments that could suppress the $tor2^{ts}$. We recovered

genomic fragments that contained *RHO2, PSK1* and *PSK2,* all of which

suppressed the growth defect of the $tor2^{ts}$ strain at the restrictive temperature

(Figure 2-1A). Overexpression of *RHO2* is very likely to suppress the $tor2^{ts}$ by

functioning analogous in a manner analogous to *RHO1* (*12*), but it was unclear

how *PSK1* or *PSK2* could suppress. To determine if PAS kinase alone is

sufficient to suppress the $tor2^{ts}$, we assayed suppression by the isolated, full-

length *PSK1* or *PSK2* expressed from their endogenous promoters.

Overexpression of either *PSK1* or *PSK2* was sufficient to support growth of the

$tor2^{ts}$ at the restrictive temperature. This suppression requires kinase activity as a

PSK2 kinase domain mutant (K870R) was completely unable to promote growth

of the $tor2^{ts}$ mutant (Figure 2-1B). As with the other functions of PAS kinase (*20*),

PSK2 might be the predominant gene in this signaling pathway given its more

pronounced suppression relative to *PSK1*.

Given that all of the known *psk1Δ psk2Δ* phenotypes are completely

phenocopied by the *UGP1-S11A* allele, we wanted to test whether Ugp1

phosphorylation is necessary for suppression. In the presence of the

unphosphorylatable Ugp1-S11A protein neither *PSK1* nor *PSK2* could suppress

the $tor2^{ts}$, showing that Ugp1 phosphorylation is necessary for PAS kinase-

Figure 2-1). PAS kinase-dependent suppression of the *tor2^ts^* requires kinase activity and Ugp1 phosphorylation. Strains of the indicated genotype were grown to saturation and serially diluted in water. These diluted samples were then spotted onto synthetic minimal media lacking uracil and incubated at the indicated temperature for two days. (A) Plasmids that contain all or part of *RHO2, PSK1* and *PSK2* were recovered from a high copy suppressor screen of the *tor2^ts^* (B) *PSK1* and *PSK2* are able to suppress the *tor2^ts^* which is dependent on kinase activity. High copy plasmids that contain full length *PSK1, PSK2* or *PSK2* kinase dead (K870R) were expressed from their endogenous promoters and assayed for an ability to suppress the *tor2^ts^*. (C) PAS kinase-dependent suppression requires Ugp1 phosphorylation on serine-11. Neither *PSK1* nor *PSK2* can suppress the *tor2^ts^* in the presence of the Ugp1-S11A mutation.

A
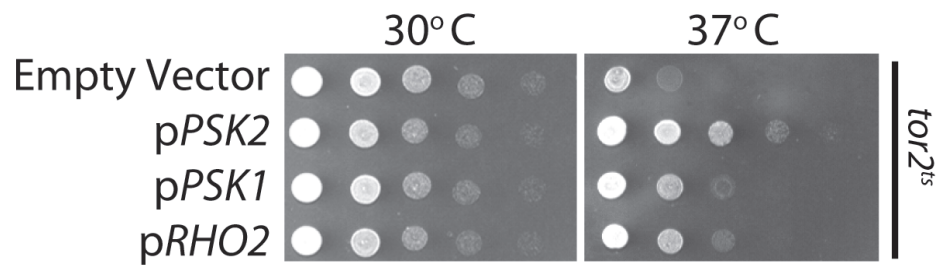
B
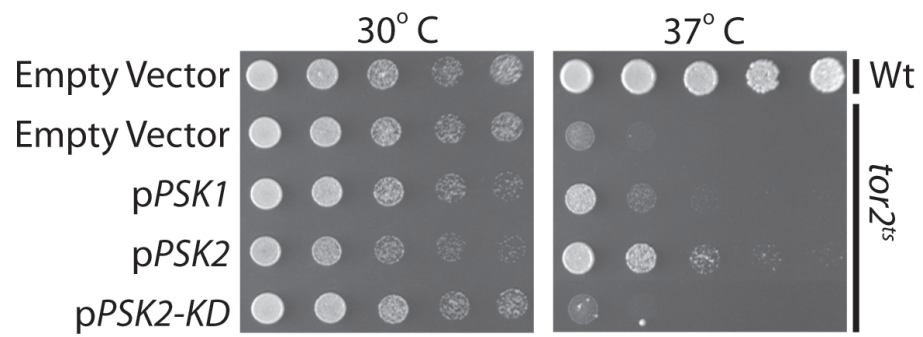
C
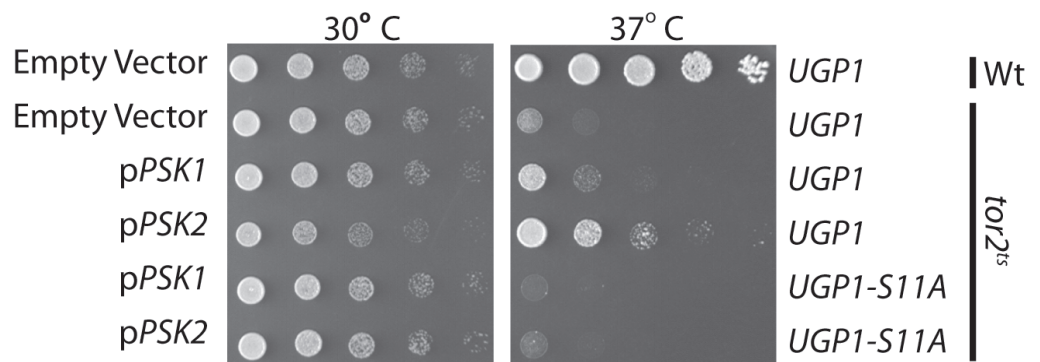
dependent suppression (Figure 2-1C). We have previously shown that S11E and S11D mutants of Ugp1 do not mimic the phosphorylated state, but rather mimic constitutively unphosphorylated state. These acidic mutations showed a similar effect in $tor2^{ts}$ suppression. Specifically, they fail to enable suppression by *PSK2* overexpression (data not shown). As a result, we remain unable to determine the sufficiency of Ugp1 phosphorylation for $tor2^{ts}$ suppression.

PAS kinase activation suppresses the $tor2^{ts}$

and increases Ugp1 phosphorylation

The $tor2^{ts}$ mutant is unable to grow at high temperature (37° C) presumably because of decreased functional TORC2. The $tor2^{ts}$ mutant can be suppressed by supplementation of 1 M sorbitol in the media (see supporting information for this Chapter)(*6*), indicating that the lethality of the $tor2^{ts}$ is due to cell wall instability and cell lysis. In light of this observation, it is surprising that treatment with agents that destabilize the cell membrane or cell wall (e.g., calcofluor white, congo red, SDS, Tween) suppress rather than exacerbate the $tor2^{ts}$ mutant phenotype (*17*). The mechanism by which cell integrity stress suppresses the $tor2^{ts}$ is unknown, but we speculated that PAS kinase might be involved because it is activated by cell integrity stress (*20*) and suppresses the $tor2^{ts}$ when over-expressed. Therefore, we tested the necessity of PAS kinase for suppression of the $tor2^{ts}$ by cell integrity stress. Given that Psk2 responds more robustly to cell integrity stress and that Psk2 over-expression more fully

suppresses the $tor2^{ts}$ when compared to Psk1, we focused primarily on the role

of *PSK2* in these studies. As expected, the $tor2^{ts}$ phenotype was suppressed by

the addition of 0.005% SDS to the media (Figure 2-2A). The $tor2^{ts}$ strain also

containing the *psk2Δ* mutation, however, was not able to grow on the SDS

supplemented media (Figure 2-2A). Consistent with the known role of Psk2 in

cell integrity stress response, the *psk2Δ* mutant showed a modest growth defect

in the on SDS supplemented media. As with PAS kinase over-expression, PAS

kinase-dependent suppression via cell integrity stress is dependent on

phosphorylation of Ugp1 at serine-11 (Figure 2-2A). Therefore, in the presence of

normal Tor2 signaling, Psk2 activation is not required for viability under cell

integrity stress, but becomes essential upon Tor2 inactivation. Thus, activation of

PAS kinase via two independent mechanisms, cell integrity stress and over-

expression, enables suppression of the $tor2^{ts}$ mutant phenotype.

In addition to cell integrity stress, we have previously shown that PAS

kinase is activated by growth on nonfermentative carbon sources(*20*). Given that

either PAS kinase over-expression or activation in response to cell integrity

stress suppresses the $tor2^{ts}$, we asked whether other PAS kinase activating

stimuli could likewise suppress the phenotype. As in Figure 2-2B, the $tor2^{ts}$

phenotype was suppressed by growth on either nonfermentative carbon source,

raffinose or galactose, both of which cause PAS kinase activation. Deletion of

PSK2 or the presence of Ugp1-S11A, however, attenuates this phenotype

suppression. Taken together, we have shown that three independent means of

Figure 2-2). Activation of PAS kinase by either SDS or nonfermentative carbon sources suppresses the *tor2^ts^*. Strains of the indicated genotype were grown to saturation and serially diluted in water. The dilutions were then plated onto minimal glucose media lacking uracil unless otherwise indicated. (A) Suppression of the *tor2^ts^* via SDS is dependent on PAS kinase and Ugp1 phosphorylation. Strains were grown to saturation and then serially diluted onto YPA media supplemented with 0.005% SDS.
(B) Suppression of the *tor2^ts^* via growth on nonfermentative carbon sources is dependent on PAS kinase and Ugp1 phosphorylation. Strains were grown to saturation and then serially diluted on the indicated carbon source. (C) PAS kinase activation via over-expression, cell integrity stress (SDS, 37˚C) or non-fermentative carbon sources (raffinose, galactose) increase Ugp1 phosphorylation. Western blot is one representative experiment and bar graph is the average of four experiments.
Wild-type strain was grown to saturation then back diluted to an OD$_{600}$ ~0.2 in indicated media. SDS or heat shock treatment for 3 hours were grown in YPAD media. *PSK2* over-expression culture was grown in SD-ura and was incubated at 37˚ C for 3 hours prior to harvest.

A

	YPAD	0.005% SDS
Wt		
psk2Δ		
tor2^{ts}		
tor2^{ts} psk2Δ		

Wt		
tor2^{ts}		
tor2^{ts} UGP1-S11A		
UGP1-S11A		

30° C   37° C

B

	Glucose	Galactose	Raffinose
Wt				*Wt*
Wt			
UGP1-S11A				*tor2^{ts}*
psk2Δ			
psk2Δ				*Wt*

30° C   37° C

C

P-Ugp1
Ugp1
PGK

— | PSK2 O/E | — | 37° C 3 hrs | 0.02% SDS | galactose | raffinose

SD-Ura   YPA

P-Ugp1/Pgk
P-Ugp1/Ugp1
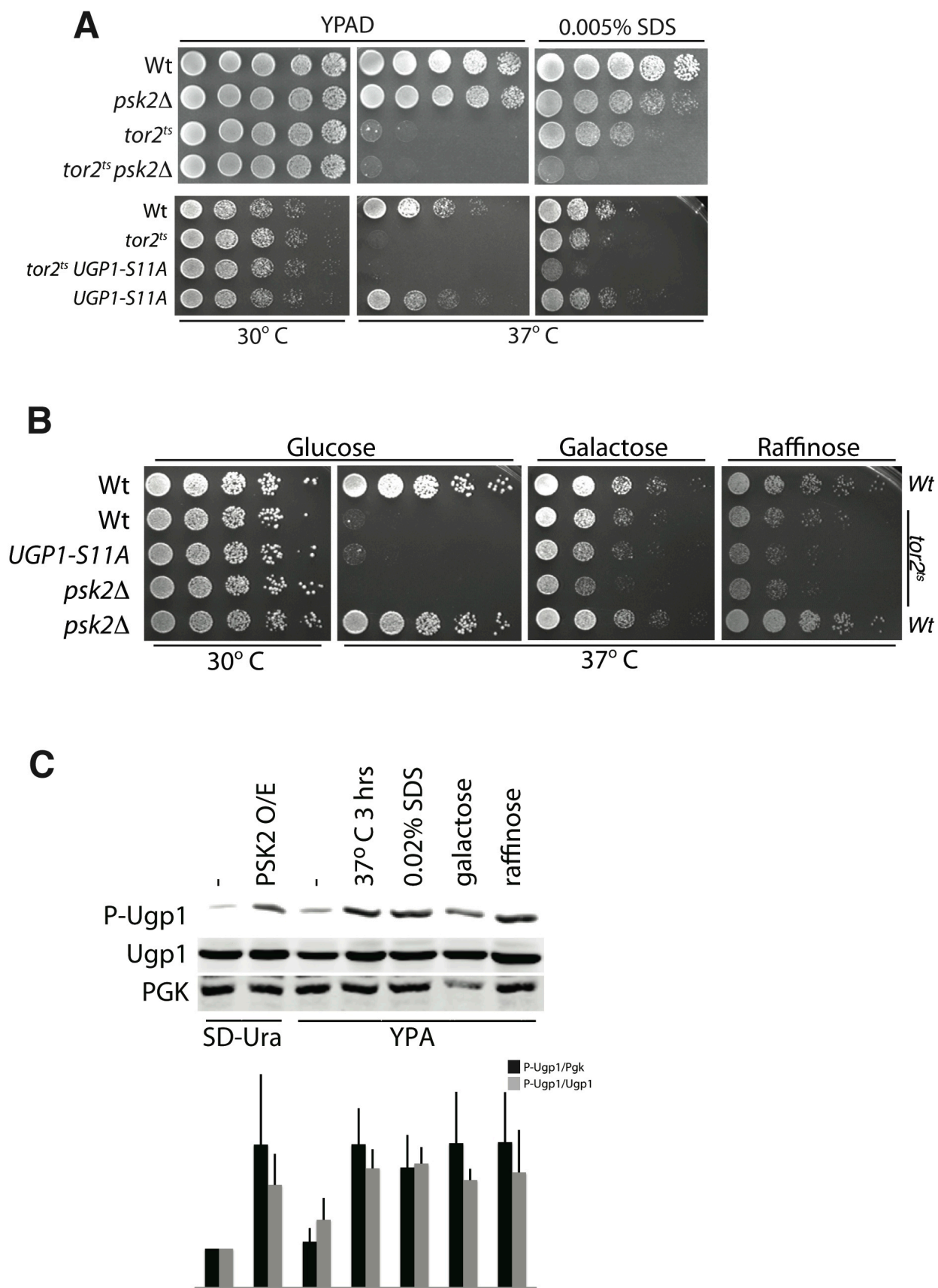
stress or nonfermentative carbon sources, all cause suppression of the $tor2^{ts}$

phenotype.

Three distinct conditions that are expected to cause increased PAS kinase

activity suppress the $tor2^{ts}$. Activated PAS kinase phosphorylates Ugp1 at serine-

11, which leads to an increase in the production cell wall glucan. In order to

confirm that these suppressing conditions actually do lead to an increase in Ugp1

phosphorylation we performed immunoblots using an antibody specific for

phospho(Ser11)-Ugp1. As seen in Figure 2-2C, each of these three conditions,

overexpression of *PSK1* or *PSK2*, cell integrity stress or nonfermentative carbon

sources, also lead to an increase in Ugp1 phosphorylation. Together, these data

suggest that activation of PAS kinase is sufficient to suppress the $tor2^{ts}$ and

suppression requires Ugp1 phosphorylation.

SSD1 is required for the _tor2^{ts}_ suppression

by PAS kinase

During the course of our studies of the suppression of the $tor2^{ts}$ phenotype by

PAS kinase, which to this point were all conducted in the JK9 strain background,

we made the surprising observation that PAS kinase was completely unable to

suppress the $tor2^{ts}$ in the W303 strain background (Figure 2-3A-right panel). We

reasoned that determining the key difference between the JK9 and W303 strains

should provide insight into the genetic pathway underlying PAS kinase-

dependent suppression. To uncover the genetic basis for this distinction, we took

Figure 2-3). *SSD1* **is required for PAS kinase to suppress the** *tor2^{ts}*. **Strains were grown to saturation in selective media.** The strains were then serially diluted in water; dilutions were then plated on minimal glucose media lacking uracil or uracil and methionine. (A) *SSD1v* is required for PAS kinase to suppress the *tor2^{ts}*. The deletion was made in the Jk9 strain and the wild-type copy was expressed in the W303 strain from its endogenous promoter on a CEN plasmid. Strains were grown at 37° C for 3 days (B) nonphosphorylatable (Ssd1-8A) or phosphomimetic (Ssd1-8D, Ssd1-8E) Ssd1 do not affect PAS kinase-dependent suppression. Ssd1-8A/8D/8E were expressed from a 2-micron plasmid with a minimal *CYC1* promoter. (C) Ssd1 associates with Ugp1 in a phosphorylation-dependent manner with a peak of association at 3 hours of heat shock at 37° C. Ssd1-HA was expressed from its endogenous promoter on a CEN plasmid. The *tor2^{ts}* strain expressing Ssd1-HA was grown on synthetic glucose media lacking uracil to log phase. Crude cell lysates were then subjected to immunoprecipitation using anti-HA conjugated agarose beads. Strains were heat shocked at 37° C for 3 hours unless otherwise indicated. Ssd1 was detected using anti-HA antibody and Ugp1 was detected with an antibody to endogenous Ugp1.
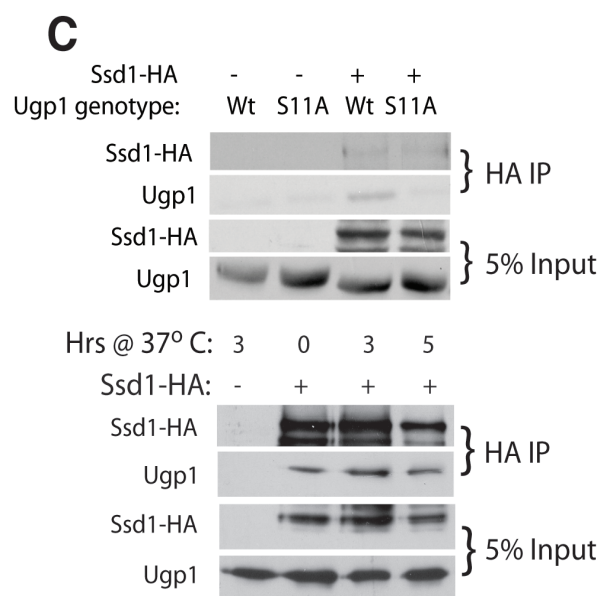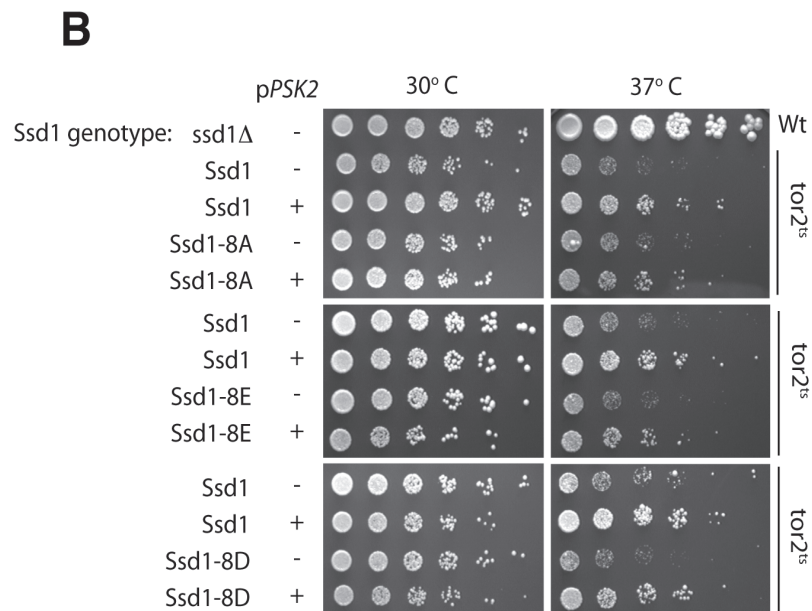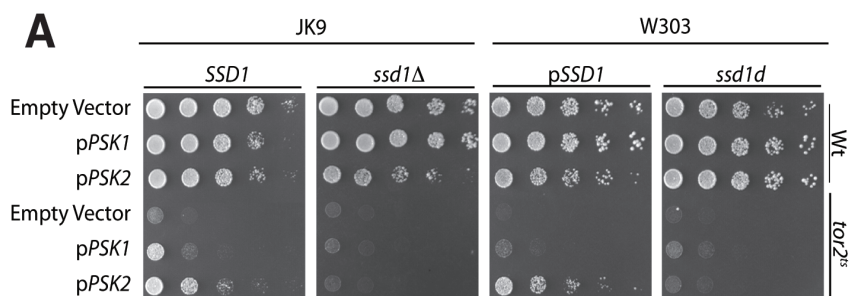
a candidate gene approach by examining known polymorphisms that vary between the two strains. Many laboratory *S. cerevisiae* strains have a mutation (*ssd1d*) that causes a premature stop codon in the *SSD1* gene (*22*). *SSD1* has been implicated genetically in many different cellular functions, but the biochemical function of Ssd1 has remained elusive (*23-32*). It has homology to the RNase II family of enzymes, but it lacks residues that are critical for catalytic activity. Clues of Ssd1 biochemical function have come from recent studies showing that Ssd1 controls post-transcriptional gene expression through direct RNA binding (*24, 33*).

The W303 strain contains the nonfunctional *ssd1d* allele, while JK9 contains wild-type *SSD1*. To determine whether this mutation is the key difference preventing suppression of the *tor2^{ts}* by PAS kinase activation in the W303 strain, we complemented the *ssd1d* mutation with a plasmid containing the wild-type *SSD1* gene. When wild-type *SSD1* is provided, PAS kinase is now able to suppress the *tor2^{ts}* phenotype in the W303 strain background (Figure 2-3A). Conversely, deletion of the wild-type copy of *SSD1* in the JK9 strain prevents PAS kinase suppression of the *tor2^{ts}* defect. These data indicate that *SSD1* is necessary for PAS kinase to suppress the *tor2^{ts}* and is epistatic to PAS kinase.

Previously it has been shown that the function of Ssd1 in post-transcriptional gene regulation is regulated via phosphorylation at eight N-terminal sites(*24*). Six of these important phosphorylation sites are a perfect match for the PAS kinase consensus phosphorylation motif (HXRXX[S/T])(*34*).

While Ugp1 phosphorylation is required for the PAS kinase-dependent *tor2^ts^*

suppression, we wanted to experimentally determine whether Ssd1

phosphorylation at these sites might also play a role. Mutants of Ssd1 wherein

the 8 phosphorylatable residues are mutated to alanine (Ssd1-8A) or a

phosphomimetic amino acid (Ssd1-8D, Ssd1-8E) were generated. Over-

expression of unphosphorylatable Ssd1 was previously observed to cause

toxicity (*24*), which was shown to be due to its role in gene expression. As

expected, we also observed that overexpression of Ssd1-8A caused toxicity,

which was not observed when Ssd1 was either phosphorylatable at these sites or

contained phosphomimetic substitutions (see Supporting Information for this

Chapter). All of these *SSD1* mutants, like the wild-type, enabled suppression of

the *tor2^ts^* phenotype when expressed at endogenous levels (Figure 2-3B). These

data indicate that phosphorylation of Ssd1 at these eight sites does not play a

significant role in PAS kinase-dependent suppression of the *tor2^ts^* phenotype.

This suggests that the role of Ssd1 in *tor2^ts^* suppression is distinct from its role in

post-transcriptional regulation of gene expression.

Ugp1 and Ssd1 physically interact in a

phosphorylation-dependent manner

We have previously described the likely mechanism whereby Ugp1

phosphorylation controls glucose partitioning (*21*), specifically through the

localization of Ugp1 to the cell periphery where its UDP-glucose product is

preferentially used for cell wall glucan synthesis. How Ugp1 phosphorylation enables suppression of the *tor2^{ts}* phenotype and why Ssd1 is required for this effect was not known. We speculated that these two proteins might physically interact to nucleate a novel signaling complex. We expressed a C-terminally HA-tagged Ssd1 at endogenous levels (native promoter/CEN plasmid) and tested for a possible interaction with Ugp1. Because Ugp1 phosphorylation was critical in the *tor2^{ts}* strain at 37°C, we performed the co-immunoprecipitations under these conditions. As shown in Figure 2-3C, immunoprecipitation of Ssd1-HA also pulls down wild-type Ugp1. Ugp1 is an abundant protein and control immunoprecipitations often show trace levels of Ugp1, but specific interactions can be detected above this background. We would expect this interaction to be dependent upon Ugp1 phosphorylation and tested that by co-immunoprecipitation in a strain expressing the S11A mutant of Ugp1 from the endogenous locus. Unlike the wild-type, we detected no interaction of the S11A mutant of Ugp1 with Ssd1-HA under any condition (Figure 2-3C). Because of the various other cellular roles that both Ugp1 and Ssd1 play in both growth and stress response, we wanted to determine if this association was dynamically regulated in response to a temperature increase. We tested the interaction in cultures grown at 37° C for 0, 3 and 5 hours (Figure 2-3C). Complex formation is enhanced in response to the temperature shift, but it returns to basal levels after 5 hours at 37° C. These data taken together indicate that Ssd1 and Ugp1 form a heat stress-responsive complex that is dependent upon Ugp1 phosphorylation.
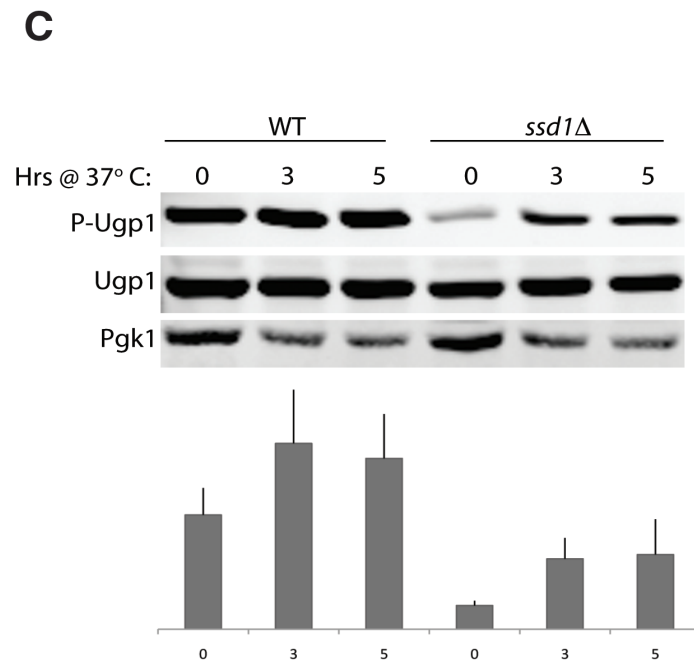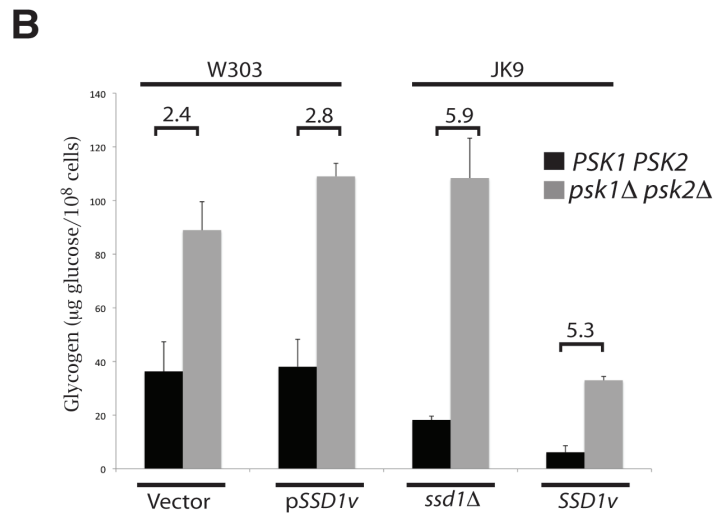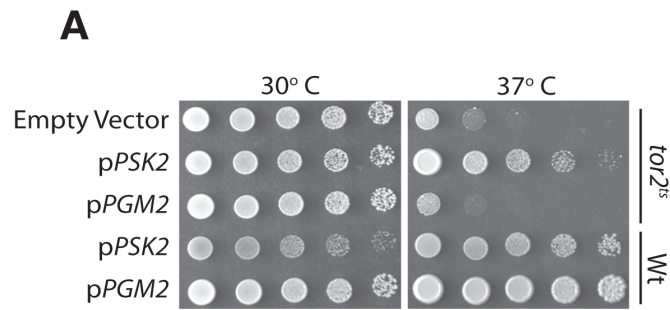
The *tor2^ts* suppression effect of Ugp1

phosphorylation is independent of

glucose partitioning

One of the lethal defects of the *tor2^ts* mutant is instability of the cell wall as evidenced by the fact that it can be rescued by supplementation with the osmotic stabilizer sorbitol (*6*)(see Supporting Information for this Chapter). Also, we have previously shown that phosphorylation of Ugp1 promotes increased cell wall glucan production at the expense of glycogen synthesis, with the effect of increased cell wall stability (*21*). We have shown herein that phosphorylation of Ugp1 also causes suppression of the *tor2^ts* mutant phenotype. Taken together, these data led to the possibility that suppression of the *tor2^ts* via PAS kinase overexpression or activation was simply due to glucose partitioning being altered in favor of cell wall glucan production. Alternatively, Ugp1 might have a distinct phosphorylation-dependent role in cellular signaling that enables *tor2^ts* suppression. This question cannot be answered directly as an inactive mutant of Ugp1 does not enable viability of a *ugp1Δ* strain, due to the essential role of Ugp1 in producing UDP-glucose (*35*). We have conducted two experiments, however, that suggest that the *tor2^ts* suppression role of Ugp1 is distinct from its role in glucose partitioning. First, we have previously shown that overexpression of phosphoglucomutase-2 (*PGM2*) is sufficient to suppress a growth defect caused by loss of Ugp1 phosphorylation(*19*). Pgm2 is the enzyme responsible for the conversion of glucose-6-phosphate to glucose-1-phosphate, which is the

glucose donor for UDP-glucose synthesis by Ugp1. When it is overexpressed, the increased UDP-glucose synthesis enables cell wall production and stabilization, even in the absence of Ugp1 phosphorylation (*36*). If cell wall glucan synthesis were sufficient for *tor2^{ts}* suppression, *PGM2* overexpression should suppress. As shown in Figure 2-4A, however, *PGM2* overexpression had no effect on the temperature sensitivity of the *tor2^{ts}* mutant.

Second, if Ugp1 phosphorylation regulates glucose partitioning and *tor2^{ts}* suppression through the same mechanism, then these two functions should be equally dependent upon *SSD1*. We have previously shown that *tor2^{ts}* suppression by Psk2 overexpression is completely dependent upon *SSD1*. To determine whether PAS kinase-dependent regulation of glucose partitioning was dependent upon *SSD1*, we measured glycogen levels in wild-type and *psk1Δ psk2Δ* mutants in both the JK9 and W303 backgrounds both with and without *SSD1*. Our lab has shown previously that the *psk1Δ psk2Δ* exhibits glycogen levels that are dramatically higher than wild-type levels, concomitant with a decrease in cell wall production (*21*). The fold increase in glycogen content in the *psk1Δ psk2Δ* mutant relative to wild-type was not significantly different in either the JK9 or the W303 strain with or without functional *SSD1* (Figure 2-4B). While the effects of PAS kinase deletion were identical in each genetic condition, there was an overall decrease in glycogen content in the JK9 strain with *SSD1*. This must be due to a genetic interaction between *SSD1* and a gene other than PAS kinase that differs between the two strains.

Figure 2-4). The metabolic function of Ugp1 is separable from its signaling role. (A) *PGM2* over-expression, which increases Ugp1 substrate availability, is not able to suppress the *tor2^ts^*. Strains were grown to saturation and then serially diluted in water. The dilutions were incubated at the indicated temperature for 2 days. (B) *SSD1* is not required for PAS kinase to regulate glycogen storage. Fold change between Wt and *psk1Δpsk2Δ* for each *SSD1* genotype is indicated above bars. Indicated strains were grown at 30° C to an OD_{600} ~1.0 and were harvested by centrifugation. The strains were assayed for glycogen content as described. (C) Deletion of *SSD1* from the Jk9 strain results in a decrease in Ugp1 phosphorylation. Quantification of four individual experiments is represented on the bar graph below a representative blot. P-Ugp1 signal was normalized to total Ugp1. Strains were grown at 30° C and then shifted for the indicated time to 37° C.

A

	30° C	37° C	
Empty Vector			
pPSK2			tor2ts
pPGM2			
pPSK2			Wt
pPGM2			

B

C

Hrs @ 37° C:

P-Ugp1

Ugp1

Pgk1

These data, taken together with the *PGM2* data, suggest that there is a bifurcation in the PAS kinase pathway at the point of Ugp1 phosphorylation. Suppression of the *tor2^{ts}* via phosphorylation of Ugp1 requires Ssd1. However, the ability of Ugp1 phosphorylation to enact the switch from production of UDP-glucose for glycogen to use in cell wall glucans is independent of Ssd1. These data would indicate that Ssd1 is not required for Ugp1 phosphorylation but may be necessary downstream of phosphorylation for the signaling function of Ugp1. Consistent with this observation, PAS kinase-dependent phosphorylation of Ugp1 still responds to heat shock in the absence of Ssd1 (Figure 2-4C). However, the ssd1Δ consistently has a decrease in total phospho-Ugp1. These data indicate that Ssd1 is not required for Ugp1 phosphorylation in response to PAS kinase activation, but it may be required to fully stabilize the phosphorylated form. *SSD1* appears to be epistatic to Ugp1 phosphorylation, however, as *SSD1* overexpression is not sufficient to suppress the *tor2^{ts}* (data not shown).

PAS kinase suppression causes Rom2-dependent Rho1 activation
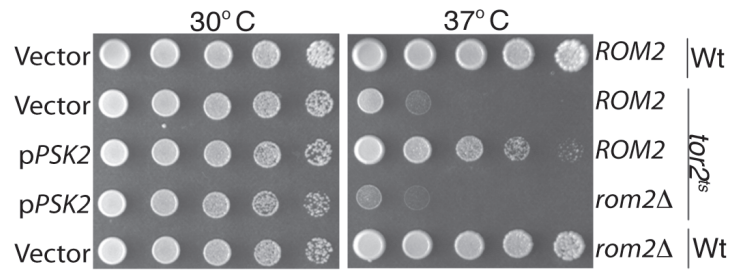
Tor2 mediates the majority of its effects on cell growth and actin reorganization through activation of the small GTPase Rho1(*37*). Rho1 controls activation of the MAP kinase pathway, cortical actin polarization, cell wall synthesis and budding(*14-16*). Because of the critical role of Rho1 in mediating the effects of Tor2 activation on growth, we postulated that the ability of PAS

kinase to suppress the *tor2^ts* might also be dependent on Rho1 activation, which is usually caused by guanine nucleotide exchange factors (GEFs). The *S. cerevisiae* genome encodes three GEFs for Rho1, *ROM1*, *ROM2* and *TUS1*(*38, 39*). To determine whether Rho1 activation by one of these GEFs was required for suppression of the *tor2^ts* by PAS kinase, we examined suppression in strains each lacking one GEF. While deletion of *ROM1* and *TUS1* had no effect on PAS kinase-dependent *tor2^ts* suppression (see Supporting Information for this Chapter), it was completely abolished by deletion of *ROM2* (Figure 2-5A). Because Rom2, like Ssd1, is required for suppression and Ssd1 physically interacts with Ugp1, we wanted to determine whether Rom2 might also be a component of this complex. A FLAG-tagged Rom2 protein expressed from the endogenous *ROM2* locus precipitated wild-type Ugp1 (Figure 2-5B). As with Ssd1, however, we detected no interaction between Rom2 and an S11A mutant of Ugp1 (Figure 2-5B).

Because of the dynamic nature of the Ssd1-Ugp1 interaction in response to high temperature, we examined the kinetics of the Rom2-Ugp1 interaction. The kinetics of the association between Rom2 and Ugp1 are very similar to Ssd1 and Ugp1. The degree of association peaks at about 3 hours at 37° C, and the interaction returns to or below baseline by 5 hours (Figure 2-5C). However, unlike Ssd1, Rom2 total protein levels markedly decrease after 5 hours at 37° C. To more systematically assess protein abundance, we grew cultures at 37° C and

Figure 2-5). Rom2 is required for PAS kinase-dependent suppression and forms a complex with Ugp1. (A) Rom2 is necessary for *PSK2* over-expression to suppress the *tor2^ts*. Indicated strains were grown to stationary phase and then serially diluted in water. Dilutions were then spotted onto synthetic medium lacking uracil and grown at indicated temperature for 2 days. (B) Rom2 interacts with Ugp1 in a phosphorylation-dependent manner. Strains containing Rom2-FLAG at the endogenous locus with or without the Ugp1-S11A allele were grown to log phase and then subjected to anti-FLAG immunoprecipitation. (C) Rom2 interacts with Ugp1 in response to heat shock. Immunoprecipitations were performed on a Rom2-FLAG strain using anti-FLAG beads and blotted for Ugp1. (D) *PSK2* over-expression leads to increased Rho1 activity. Strains were grown to mid-log phase and GTP-bound Rho1 was immunoprecipitated with RBD beads. Biological replicates were loaded in adjacent lanes.

A

30° C   37° C

Vector		ROM2	Wt
Vector		ROM2	
pPSK2		ROM2	tor2ts
pPSK2		rom2Δ	
Vector		rom2Δ	Wt

B

Rom2-Flag:	-	-	+	+
Ugp1 Genotype:	WT	S11A	WT	S11A

Rom2-Flag
Ugp1   } FLAG IP

Rom2-Flag
Ugp1   } 5% Input

C

Hrs @ 37 C:	3	0	3	5
Rom2-Flag:	-	+	+	+

Rom2
Ugp1   } FLAG IP

Rom2
Ugp1   } 5% Input

D

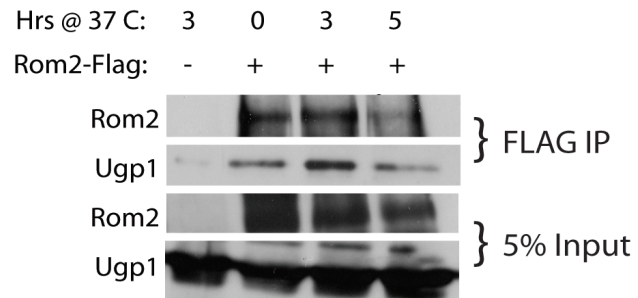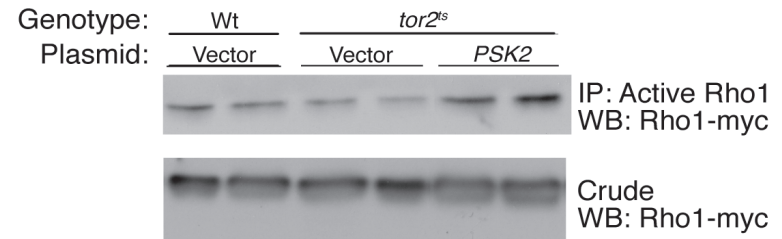| Genotype:	Wt	tor2ts	
Plasmid:	Vector	Vector	PSK2

IP: Active Rho1
WB: Rho1-myc

Crude
WB: Rho1-myc

70
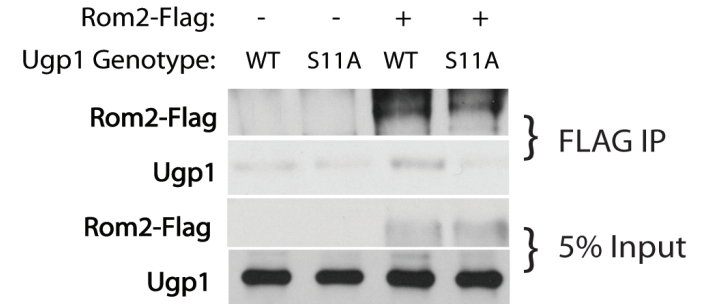
harvested samples every hour for 7 hours. We then blotted for Rom2, Ugp1, and

Ssd1 to determine if there was a decrease in protein levels for any of them over

the course of the heat shock. Rom2 protein levels decrease significantly after

about 4 hours at 37° C (see Supporting Information for this Chapter). Ssd1 levels

decrease similarly after about 4 hours. Ugp1 levels remain stable over the course

of the heat shock treatment, but Ugp1 phosphorylation peaks after 1-2 hours at

37°C and then gradually decreases over the remainder of the time-course (see

Supporting Information for this Chapter) These data taken together suggest that

Ugp1-Ssd1-Rom2 form a dynamic complex in response to Ugp1 phosphorylation.

This complex is likely the signaling complex that enables $tor2^{ts}$ suppression by

PAS kinase activation.

The majority of the effects of TORC2 are mediated via activation of Rho1

through one of its GEFs (*12, 37*). As PAS kinase suppression of the $tor2^{ts}$

requires *ROM2* and Rom2 interacts with Ssd1 and phospho-Ugp1, we

speculated that this Rom2 complex promotes Rho1 activation and thereby

bypasses the requirement for Tor2 activity. Therefore, we determined whether

PSK2 overexpression was sufficient to activate Rho1 in the $tor2^{ts}$ mutant strain.

Levels of GTP-bound (active) Rho1 were determined by isolation with RBD-

conjugated beads and Western blot (*40, 41*). As expected, the $tor2^{ts}$ has

attenuated levels of active Rho1 when compared to wild-type cells (Figure 2-5D).

Overexpression of *PSK2* in the $tor2^{ts}$ mutant, however, increased the levels of

GTP-bound Rho1 to roughly wild type levels. Therefore, PAS kinase

overexpression causes Ugp1 phosphorylation, the formation of a

Ugp1/Ssd1/Rom2 complex and the activation of Rho1. Through this pathway,

PAS kinase enables suppression of the $tor2^{ts}$ mutant phenotype and promotes

cell growth in response to nonideal conditions.

Discussion

Activation of PAS kinase, via over-expression, cell integrity stress or

growth on nonfermentative carbon sources, increases Ugp1 phosphorylation and

enables suppression of the $tor2^{ts}$. Ugp1 phosphorylation nucleates the formation

of a very unusual signaling complex, specifically a complex that contains a

metabolic enzyme (Ugp1), a degenerate RNase (Ssd1) and a Rho1 GEF (Rom2)

and possibly other proteins. Interestingly, the roles of Ugp1 and Ssd1 within this

complex appear to be separable from their defined roles in glucose utilization (*20,
21*) and translational repression (*24, 33*), respectively. We found that this

complex appears to activate Rho1, thereby playing an important role in cellular

growth control.

As relates to its Rho1 activation function, the proximal active component of

this complex is likely to be Rom2, due to its known role as a Rho1 guanine

nucleotide exchange factor (GEF) (*17*). Rho1 has at least four downstream

effectors. It binds to and activates Pkc1 (*37*), which activates the MAP kinase

signaling cascade. Rho1 activates cell wall synthesis by binding to and activating

Fks1, the β-1,3-glucan synthase (*15*). Finally, Rho1 interacts with Bni1, a formin

family member (*16*) and Skn7 a two-component signaling factor (*42*).

Interestingly activation of Rho1 does not always produce equivalent activation of

all of the downstream effectors. Instead Rho1 activation can preferentially

activate specific downstream effectors, which is at least partially dependent on

the activating GEF. PAS kinase-dependent suppression of the *tor2^{ts}* appears to

function exclusively through Rom2, and not Rom1 or Tus1, two other verified

Rho1 GEFs. Dependence on Rom2 is probably due to its unique ability to

assemble in the Ugp1-Ssd1 complex. The *tor2^{ts}* strain arrests growth with a

disorganized actin cytoskeleton (*37*), which can be suppressed by over-

expression of Pkc1. However over-expression of the other Rho1 downstream

effectors, Bni1, Fks1 or Skn7, are not able to suppress the *tor2^{ts}*. These data,

and the fact that growth on sorbitol suppresses the *tor2^{ts}*, indicate that the lethal

defects of the *tor2^{ts}* strain are lack of actin organization and cell lysis probably

due to cell wall defects. Given that PAS kinase activation can suppress the *tor2^{ts}*

it must be that PAS kinase signaling acts to repair one or both of these defects

through the activation of Rho1. This could be accomplished by Rho1-dependent

activation of Pkc1 and actin rearrangement, activation of Fks1 and cell wall

synthesis, or both. It remains to be determined which Rho1 downstream effectors

are regulated by PAS kinase activation and which are required for *tor2^{ts}*

suppression.

Ssd1 is required for PAS kinase to suppress the *tor2^{ts}*. The role of Ssd1 in

this signaling pathway remains unclear. Its physical interaction with Ugp1 in a

phosphorylation dependent manner, however, strongly suggests that its suppressing function is a component of the Ugp1/Rom2 complex. Two possible roles for Ssd1 in this complex are: 1) to stabilize the phosphorylated form of Ugp1; or 2) to function as a scaffold for the Rom2-Ugp1 association. Ssd1 clearly does increase the phosphorylation of Ugp1, presumably through preventing dephosphorylation. This effect, however, could be a secondary effect of binding with Ssd1 and Rom2. The model of Ssd1 as a scaffold is particularly attractive, because it would bring together Ugp1, the recipient of the activating phosphorylation signal, and Rom2, which likely provides the Rho1 activation output.

The RNA binding capacity of Ssd1 raises the intriguing possibility that the complex also contains RNA. The complex may function to regulate specific mRNA stability, localization or translation or, alternatively, RNA may play a structural or regulatory role within the complex. Unlike the described role of Ssd1 in translational repression (*24*), the function of Ssd1 in suppression of the *tor2^{ts}* is totally unaffected by phosphorylation on the known eight N-terminal residues. These data indicate that the two roles of Ssd1 are separable and likely totally distinct activities. One is regulated by phosphorylation at the N-terminus and involves regulation of mRNA translation. The second involves complex formation with Ugp1 and Rom2, which is independent of N-terminal phosphorylation. This duality may enable coordination between the cell wall synthesis/actin polarization

required for cell division and the spatially regulated expression of cell wall degrading enzymes that are needed for cell separation.

The primary mechanism by which PAS kinase regulates this complex appears to be phosphorylation of Ugp1. Therefore, the phosphorylation of Ugp1 plays at least two cellular roles. First, it causes the preferential partitioning of UDP-glucose toward cell wall biosynthesis at the expense of glycogen storage (*21*). This function is independent of Ssd1. This effect is probably due to a phosphorylation-dependent conformational change, which promotes localization of the protein to the cell periphery. Second, Ugp1 phosphorylation nucleates the formation of a signaling complex that includes Ssd1 and Rom2. While these two effects are separable due to differential Ssd1 dependence, they may be related indirectly. The PAS kinase-dependent translocation of Ugp1, which might be the mechanism of glucose partitioning, may also be required for the formation of the Ugp1-Ssd1-Rom2 complex. Peripheral localization would bring the complex into proximity with Rho1, which is known to localize to the cell periphery (*43*). The two functions of Ugp1 may both be dependent on translocation and may allow Ugp1 to simultaneously produce UDP-glucose at the cell periphery and activate the Fks1 protein, which is responsible for the incorporation of UDP-glucose in cell wall biogenesis. This is the first evidence that Ugp1, thought only to catalyze the formation of UDP-glucose, has a distinct signaling function. It remains to be determined, however, whether this signaling function is dependent upon the enzymatic activity of Ugp1 or Ugp1 simply plays a scaffolding role within the

complex. If enzymatic activity is required, it would be very interesting to determine the role of UDP-glucose in the complex. This is a difficult question to answer given that the enzymatic activity of Ugp1 is required for cell viability and that Ugp1 forms a stable octamer (*35*). However future studies will ultimately shed light on the molecular basis of the signaling activity of this metabolic enzyme.

The physiological significance of PAS kinase activation remains to be elucidated. One possibility is that PAS kinase is simply activated in response to various forms of stress, both structural and metabolic, and acts to stabilize the cell wall. This is accomplished by phosphorylation of Ugp1, which directly promotes cell wall production, and also activates Rho1, which leads to an increase in cell wall biogenesis via activation of Fks1. On the other hand, PAS kinase activation might function to enable growth under nonideal conditions. Rho1 activation leads to polarization of the actin cytoskeleton in coordination with cell growth and division. A progrowth role for PAS kinase is supported by the observation that an *fks1Δ* mutation suppresses the *tor2^{ts}*(*6*). If PAS kinase were suppressing the *tor2^{ts}* by simple upregulation of cell wall synthesis, deletion of *FKS1* should exacerbate and not suppress the *tor2^{ts}* phenotype. This proposed progrowth role is further supported by the fact that PAS kinase is a positive regulator of protein synthesis in yeast (*19*), which is clearly a progrowth function. In mammalian systems, PASK is activated in nutrient replete conditions to elicit the appropriate cellular response (*18*). Specifically, PASK kinase promotes

insulin synthesis in pancreatic β-cells, represses oxidative metabolism in skeletal

muscle and upregulates lipid synthesis and storage in the liver. These data

support a role for PAS kinase in mediating nutrient-responsive anabolism, which

has been conserved through evolution.

Herein we detail a novel signaling network that connects PAS kinase and

TOR signaling. There are many similarities between PAS kinase and TOR in *S.*

cerevisiae and in mammals. First, TOR has been clearly demonstrated to

respond to nutrient replete conditions, both locally and globally, in order to elicit a

progrowth response (*6*). This function is analogous to the role for PAS kinase as

described herein and elsewhere. Second, PAS kinase and TOR both have two

closely related paralogs in *S. cerevisiae* (*PSK1, PSK2* and *TOR1, TOR2*), but

higher organisms only have one of each gene. Third, mice lacking PAS kinase

and mice lacking S6K1, a downstream target of Tor signaling, have a strikingly

similar phenotype (*18, 44*). Specifically, they are both hypermetabolic, are

resistant to diet-induced obesity and have ß-cell insufficiency. These similarities

could be coincidental, but it is also possible that these two highly-conserved

nutrient sensing kinases have a closer relationship. While we have shown that

PAS kinase and TORC2 function in parallel pathways in *S. cerevisiae* to activate

Rho1, their functions in higher organisms might be in more direct coordination.

The cell autonomous decision to grow and divide must be responsive to

environmental cues. In particular, it must integrate the nutritional environment to

assure that sufficient energy sources and building blocks are available. Because

of the potential catastrophic consequences of mishandling this decision, cells have evolved multiple cellular energy sensors to detect the nutritional environment and signal appropriately. We have shown that PAS kinase functions in parallel to TORC2 to enable cell survival and growth under stress conditions.

Methods

Saccharomyces cerevisiae strain JRY626 (MAT*a Leu2 Ura3 Trp1 His4*) was used as the JK9 parental strain and wild type strain. JRY421 (MAT*a/α His3 Lys2 Met15 Ura3 Trp1 Leu2*) was used as the W303 parental diploid, temperature sensitive strains were isolated via sporulation and dissection. Deletion mutant strains and strains expressing chromosomal-integrated FLAG-tagged proteins were generated by standard PCR-based homologous recombination methods in diploids, followed by sporulation and tetrad dissection (Longtine et al., 1998). Yeast were transformed by the lithium acetate method, and grown at 30°C in SD medium (0.67% yeast nitrogen base, 2% glucose) with amino acids unless otherwise indicated. Complete strain and plasmid information is given in the Supporting Information for this Chapter.

Glycogen assay was performed as previously described. Briefly, UGPase activity was determined by the rate of formation of glucose-1-phosphate from UDP-glucose in an NADP-linked glucose-6-phosphate dehydrogenase assay as previously described (*35*). The reaction mixture contained 50 mM Tris (pH 8.0), 10 mM dithiothreitol, 10 mM $MgCl_2$, 0.2 mM NADP, 10 mM glucose-1,6-biphosphate, 2 mM UDP-glucose, 0.6 U phosphoglucomutase, 0.5 U glucose-6-

phosphate dehydrogenase, 10 mM Na-pyrophosphate, and sample (whole-cell lysate). Assay was read at 340 nm in a 1 cm path cuvette in an Ultraspec 2000 spectrophotometer (Amersham Pharmacia). Glycogen content was assayed as previously described (*19*).

For Ugp1-Rom2 and Ugp1-Ssd1 co-immunoprecipitation experiments, the indicated strains were grown to log phase, harvested, resuspended and lysed in 600 ul of IP buffer (25 mM KOAc, 25 mM HEPES pH 7.4, 0.2 mM EDTA, 0.2 mM EGTA, 10% glycerol, 0.02% NP-40, protease inhibitor cocktail (Sigma), PhoSTOP (Roche)). Cleared cell lysates were incubated with either anti-FLAG or anti-HA conjugated (Sigma) beads for 2 hours at 4 C. The mixture was then rinsed 2 times in IP buffer. The beads were then resuspended in IP buffer and transferred into a spin column (Sigma). The beads were then rinsed 3 times in wash buffer (50 mM KOAc, 25 mM HEPES pH 7.4, 0.2 mM EDTA, 0.2 mM EGTA, 10% glycerol, 0.02% NP-40, protease inhibitor cocktail, PhoSTOP). The beads are then incubated with FLAG or HA peptide for 1 hour at room temperature and the elution is mixed with Laemelli's loading buffer. The samples were then analyzed by western blot.

Active Rho1 was assayed as previously described with modification (*40, 41*). Rho1-HA expressing cells were grown to log phase, harvested and lysed in IP buffer (25 mM HEPES-KOH pH 7.9, 100 mM KOAc, 0.2 mM EDTA, 0.2 mM EGTA, 0.1% NP-40, 10% glycerol, protease inhibitor cocktail (Sigma), phoSTOP (Roche)). Cleared cell lysates were normalized using the Bradford assay.

Normalized cell lysates were incubated with GST-tagged RBD preconjugated to beads (cytoskeleton) for 2 hour at 4° C. Pelleted beads were washed three times with IP buffer. Protein bound to the beads was eluted using 1X Laemilli's buffer and subjected to 12% SDS-PAGE. Rho1 was detected using HA monoclonal antibody.

References

1.   Hardie, D. G. (2007) AMP-activated/SNF1 protein kinases: conserved guardians of cellular energy, *Nat Rev Mol Cell Biol 8*, 774-785.

2.   Sengupta, S., Peterson, T. R., and Sabatini, D. M. (2010) Regulation of the mTOR complex 1 pathway by nutrients, growth factors, and stress, *Mol Cell 40*, 310-322.

3.   Zoncu, R., Efeyan, A., and Sabatini, D. M. (2011) mTOR: from growth signal integration to cancer, diabetes and ageing, *Nat Rev Mol Cell Biol 12*, 21-35.

4.   Hardie, D. G. (2008) AMPK and Raptor: matching cell growth to energy supply, *Mol Cell 30*, 263-265.

5.   Wullschleger, S., Loewith, R., and Hall, M. N. (2006) TOR signaling in growth and metabolism, *Cell 124*, 471-484.

6.   Helliwell, S. B., Howald, I., Barbet, N., and Hall, M. N. (1998) TOR2 is part of two related signaling pathways coordinating cell growth in Saccharomyces cerevisiae, *Genetics 148*, 99-112.

7.   Loewith, R., Jacinto, E., Wullschleger, S., Lorberg, A., Crespo, J. L., Bonenfant, D., Oppliger, W., Jenoe, P., and Hall, M. N. (2002) Two TOR complexes, only one of which is rapamycin sensitive, have distinct roles in cell growth control, *Mol Cell 10*, 457-468.

8.   Helliwell, S. B., Wagner, P., Kunz, J., Deuter-Reinhard, M., Henriquez, R., and Hall, M. N. (1994) TOR1 and TOR2 are structurally and functionally similar but not identical phosphatidylinositol kinase homologues in yeast, *Mol Biol Cell 5*, 105-118.

9.   Kunz, J., Henriquez, R., Schneider, U., Deuter-Reinhard, M., Movva, N. R., and Hall, M. N. (1993) Target of rapamycin in yeast, TOR2, is an essential phosphatidylinositol kinase homolog required for G1 progression, *Cell 73*, 585-596.

10.   Schmidt, A., Kunz, J., and Hall, M. N. (1996) TOR2 is required for organization of the actin cytoskeleton in yeast, *Proc Natl Acad Sci U S A 93*, 13780-13785.

11.   Wullschleger, S., Loewith, R., Oppliger, W., and Hall, M. N. (2005) Molecular organization of target of rapamycin complex 2, *J Biol Chem 280*, 30697-30704.

12.   Schmidt, A., Bickle, M., Beck, T., and Hall, M. N. (1997) The yeast phosphatidylinositol kinase homolog TOR2 activates RHO1 and RHO2 via the exchange factor ROM2, *Cell 88*, 531-542.

13.   Nonaka, H., Tanaka, K., Hirano, H., Fujiwara, T., Kohno, H., Umikawa, M., Mino, A., and Takai, Y. (1995) A downstream target of RHO1 small GTP-binding protein is PKC1, a homolog of protein kinase C, which leads to activation of the MAP kinase cascade in Saccharomyces cerevisiae, *EMBO J 14*, 5931-5938.

14.   Kamada, Y., Qadota, H., Python, C. P., Anraku, Y., Ohya, Y., and Levin, D. E. (1996) Activation of yeast protein kinase C by Rho1 GTPase, *J Biol Chem 271*, 9193-9196.

15.   Qadota, H., Python, C. P., Inoue, S. B., Arisawa, M., Anraku, Y., Zheng, Y., Watanabe, T., Levin, D. E., and Ohya, Y. (1996) Identification of yeast Rho1p GTPase as a regulatory subunit of 1,3-beta-glucan synthase, *Science 272*, 279-281.

16.   Kohno, H., Tanaka, K., Mino, A., Umikawa, M., Imamura, H., Fujiwara, T., Fujita, Y., Hotta, K., Qadota, H., Watanabe, T., Ohya, Y., and Takai, Y. (1996) Bni1p implicated in cytoskeletal control is a putative target of Rho1p small GTP binding protein in Saccharomyces cerevisiae, *EMBO J 15*, 6060-6068.

17.   Bickle, M., Delley, P. A., Schmidt, A., and Hall, M. N. (1998) Cell wall integrity modulates RHO1 activity via the exchange factor ROM2, *EMBO J 17*, 2235-2245.

18.   Hao, H. X., Cardon, C. M., Swiatek, W., Cooksey, R. C., Smith, T. L., Wilde, J., Boudina, S., Abel, E. D., McClain, D. A., and Rutter, J. (2007) PAS kinase is required for normal cellular energy balance, *Proc Natl Acad Sci U S A 104*, 15466-15471.

19.   Rutter, J., Probst, B. L., and McKnight, S. L. (2002) Coordinate regulation of sugar flux and translation by PAS kinase, *Cell 111*, 17-28.

20.   Grose, J. H., Smith, T. L., Sabic, H., and Rutter, J. (2007) Yeast PAS kinase coordinates glucose partitioning in response to metabolic and cell integrity signaling, *EMBO J 26*, 4824-4830.

21.   Smith, T. L., and Rutter, J. (2007) Regulation of glucose partitioning by PAS kinase and Ugp1 phosphorylation, *Mol Cell 26*, 491-499.

22.   Uesono, Y., Toh-e, A., and Kikuchi, Y. (1997) Ssd1p of Saccharomyces cerevisiae associates with RNA, *J Biol Chem 272*, 16103-16109.

23.   Chen, C. Y., and Rosamond, J. (1998) Candida albicans SSD1 can suppress multiple mutations in Saccharomyces cerevisiae, *Microbiology 144 (Pt 11)*, 2941-2950.

24.   Jansen, J. M., Wanless, A. G., Seidel, C. W., and Weiss, E. L. (2009) Cbk1 regulation of the RNA-binding protein Ssd1 integrates cell fate with translational control, *Curr Biol 19*, 2114-2120.

25.   Kaeberlein, M., Andalis, A. A., Liszt, G. B., Fink, G. R., and Guarente, L. (2004) Saccharomyces cerevisiae SSD1-V confers longevity by a Sir2p-independent mechanism, *Genetics 166*, 1661-1672.

26.   Kaeberlein, M., and Guarente, L. (2002) Saccharomyces cerevisiae MPT5 and SSD1 function in parallel pathways to promote cell wall integrity, *Genetics 160*, 83-95.

27.   Li, L., Lu, Y., Qin, L. X., Bar-Joseph, Z., Werner-Washburne, M., and Breeden, L. L. (2009) Budding yeast SSD1-V regulates transcript levels of many longevity genes and extends chronological life span in purified quiescent cells, *Mol Biol Cell 20*, 3851-3864.

28.   Luukkonen, B. G., and Seraphin, B. (1999) A conditional U5 snRNA mutation affecting pre-mRNA splicing and nuclear pre-mRNA retention identifies SSD1/SRK1 as a general splicing mutant suppressor, *Nucleic Acids Res 27*, 3455-3465.

29.   Mir, S. S., Fiedler, D., and Cashikar, A. G. (2009) Ssd1 is required for thermotolerance and Hsp104-mediated protein disaggregation in Saccharomyces cerevisiae, *Mol Cell Biol 29*, 187-200.

30.   Moriya, H., and Isono, K. (1999) Analysis of genetic interactions between DHH1, SSD1 and ELM1 indicates their involvement in cellular morphology determination in Saccharomyces cerevisiae, *Yeast 15*, 481-496.

31.   Tsuchiya, E., Matsuzaki, G., Kurano, K., Fukuchi, T., Tsukao, A., and Miyakawa, T. (1996) The Saccharomyces cerevisiae SSD1 gene is involved in the tolerance to high concentration of Ca2+ with the participation of HST1/NRC1/BFR1, *Gene 176*, 35-38.

32. Uesono, Y., Fujita, A., Toh-e, A., and Kikuchi, Y. (1994) The MCS1/SSD1/SRK1/SSL1 gene is involved in stable maintenance of the chromosome in yeast, *Gene 143*, 135-138.

33. Kurischko, C., Kim, H. K., Kuravi, V. K., Pratzka, J., and Luca, F. C. (2011) The yeast Cbk1 kinase regulates mRNA localization via the mRNA-binding protein Ssd1, *J Cell Biol 192*, 583-598.

34. Kikani, C. K., Antonysamy, S. A., Bonanno, J. B., Romero, R., Zhang, F. F., Russell, M., Gheyi, T., Iizuka, M., Emtage, S., Sauder, J. M., Turk, B. E., Burley, S. K., and Rutter, J. (2010) Structural bases of PAS domain-regulated kinase (PASK) activation in the absence of activation loop phosphorylation, *J Biol Chem 285*, 41034-41043.

35. Daran, J. M., Dallies, N., Thines-Sempoux, D., Paquet, V., and Francois, J. (1995) Genetic and biochemical characterization of the UGP1 gene encoding the UDP-glucose pyrophosphorylase from Saccharomyces cerevisiae, *Eur J Biochem 233*, 520-530.

36. Masuda, C. A., Xavier, M. A., Mattos, K. A., Galina, A., and Montero-Lomeli, M. (2001) Phosphoglucomutase is an in vivo lithium target in yeast, *J Biol Chem 276*, 37794-37801.

37. Helliwell, S. B., Schmidt, A., Ohya, Y., and Hall, M. N. (1998) The Rho1 effector Pkc1, but not Bni1, mediates signalling from Tor2 to the actin cytoskeleton, *Curr Biol 8*, 1211-1214.

38. Ozaki, K., Tanaka, K., Imamura, H., Hihara, T., Kameyama, T., Nonaka, H., Hirano, H., Matsuura, Y., and Takai, Y. (1996) Rom1p and Rom2p are GDP/GTP exchange proteins (GEPs) for the Rho1p small GTP binding protein in Saccharomyces cerevisiae, *EMBO J 15*, 2196-2207.

39. Schmelzle, T., Helliwell, S. B., and Hall, M. N. (2002) Yeast protein kinases and the RHO1 exchange factor TUS1 are novel components of the cell integrity pathway in yeast, *Mol Cell Biol 22*, 1329-1339.

40. Kimura, K., Tsuji, T., Takada, Y., Miki, T., and Narumiya, S. (2000) Accumulation of GTP-bound RhoA during cytokinesis and a critical role of ECT2 in this accumulation, *J Biol Chem 275*, 17233-17236.

41. Kono, K., Nogami, S., Abe, M., Nishizawa, M., Morishita, S., Pellman, D., and Ohya, Y. (2008) G1/S cyclin-dependent kinase regulates small GTPase Rho1p through phosphorylation of RhoGEF Tus1p in Saccharomyces cerevisiae, *Mol Biol Cell 19*, 1763-1771.

42. Alberts, A. S., Bouquin, N., Johnston, L. H., and Treisman, R. (1998) Analysis of RhoA-binding proteins reveals an interaction domain conserved in heterotrimeric G protein beta subunits and the yeast response regulator protein Skn7, *J Biol Chem 273*, 8616-8622.

43. Yamochi, W., Tanaka, K., Nonaka, H., Maeda, A., Musha, T., and Takai, Y. (1994) Growth site localization of Rho1 small GTP-binding protein and its involvement in bud formation in Saccharomyces cerevisiae, *J Cell Biol 125*, 1077-1093.

44. Pende, M., Kozma, S. C., Jaquet, M., Oorschot, V., Burcelin, R., Le Marchand-Brustel, Y., Klumperman, J., Thorens, B., and Thomas, G. (2000) Hypoinsulinaemia, glucose intolerance and diminished beta-cell size in S6K1-deficient mice, *Nature 408*, 994-997.

Supporting Information

Table 2-S1). Strains and plasmids used

Strain	Background	Genotype	mating type
JRY625	JK9	wildtype	diploid
JRY626	JK9	wildtype	a haploid
JRY627	Jk9	tor2::ADE2-3 tor2-21::YCplac111	a haploid
JRY932	JK9	psk1::KanMX4	diploid
JRY933	JK9	psk2::HphMX4	diploid
JRY940	JK9	tor2::ADE2-3 tor2-21::YCplac111 psk2::KanMX4	diploid
JRY950	JK9	tor2::ADE2-3 tor2-21::YCplac111 UGP1-S11A:TRP1	a haploid
JRY951	JK9	tor2::ADE2-3 tor2-21::YCplac111 psk2::KanMX4	a haploid
JRY952	JK9	psk2::KanMX4	a haploid
JRY953	JK9	UGP1-S11A:TRP1	a haploid
JRY1115	JK9	tor2::ADE2-3 YCplac111::tor2-21 rom2::HphMX4 ssd1::KanMX4 UGP1S11A:TRP1	a haploid
JRY1119	JK9	tor2::ADE2-3 tor2-21::YCplac111 ssd1::KanMX4	a haploid
JRY1123	JK9	ssd1::KanMX4	a haploid
JRY1118	JK9	tor2::ADE2-3 tor2-21::YCplac111 rom2::HphMX4	a haploid
JRY1122	JK9	rom2::HphMX4	α haploid
JRY649	W303	tor2::HphMX tor2-21:YCplac111	a haploid
JRY652	W303	tor2-21:YCplac111	a haploid
JRY1735	JK9	tor2::ADE2-3/TOR2 tor2-21::YCplac111 ROM2/ROM2-FLAG:KanMX4 psk2::NatMX/PSK2	diploid
JRY1736	JK9	tor2::ADE2-3 tor2-21::YCplac111 ROM2-FLAG:KanMX4	a haploid
JRY1740	JK9	tor2::ADE2-3 tor2-21::YCplac111 ROM2-FLAG:KanMX4 UGP1-S11A:TRP1	a haploid
JRY1741	JK9	tor2::ADE2-3 tor2-21::YCplac111 ROM2-FLAG:KanMX4 UGP1-S11A:TRP1	diploid
JRY1737	JK9	tor2::ADE2-3 tor2-21::YCplac111	a haploid
JRY1739	JK9	tor2::ADE2-3 tor2-21::YCplac111 Ugp1-S11A:TRP1	a haploid

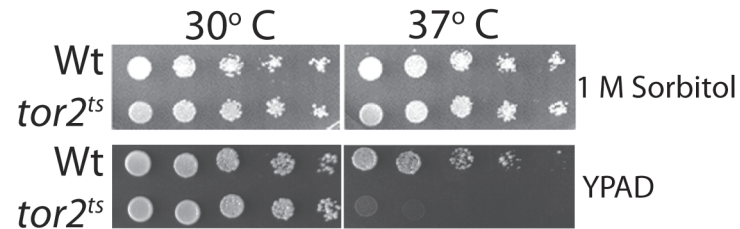| plasmid	gene	Yeast origin	selection
pRS426	empty vector	2u	URA3
pJR273	empty vector	2u	MET25
PJR1413A	PSK1	2u	URA3
pJR1413C	PSK2	2u	URA3
pJR1413D	PSK2-KD(K870R)	2u	URA3
pJR6115B	SSD1v	cen	MET25
pJR6115A	SSD1v	none	MET25
pJR1058B	PGM2	2u	URA3
pJR11159	SSD1-HA	cen	URA3
pJR9889A	Rho1-HA	cen	URA3
pJR5282	tor2-21	cen	LEU2

Figure 2-S1). 1 M sorbitol can suppress the *tor2*ᵗˢ. Indicated strains were grown to stationary phase YPAD. Serial dilutions of each strain were then plated onto synthetic dextrose plates supplemented with 1 M sorbitol. The plates were then incubated at the indicated temperature for 4 days.
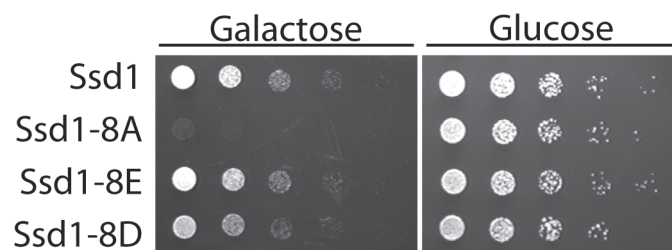

Figure 2-S2). Ssd1-8A, but not Ssd1-8D or Ssd1-8E, over-expression is lethal in the Jk9 strain. Ssd1-8A/8D/8E were over-expressed by a galactose inducible promoter. Strains were grown to stationary phase and serially diluted in water. The strains were then grown at 25° C for 3 days on synthetic galactose media.
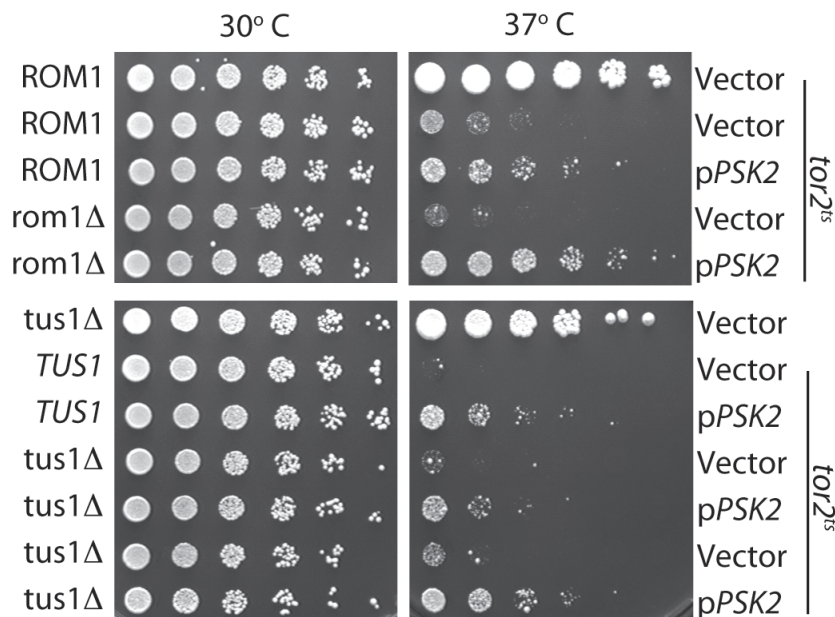
Figure 2-S3). Neither *ROM1* nor *TUS1* is required for PAS kinase to suppress the *tor2^ts*. Strains were grown to stationary phase and serially diluted in water. The strains were then grown at the indicated temperature for 2 days.
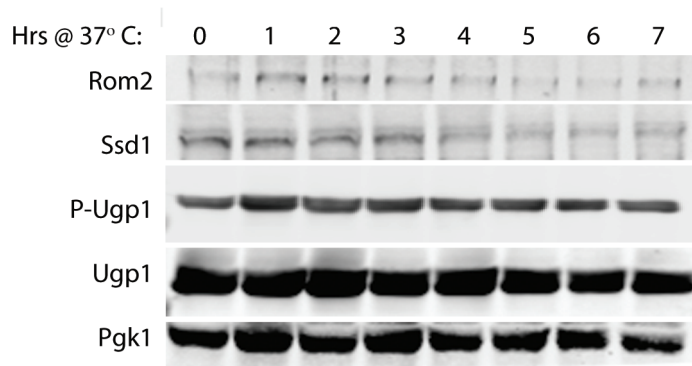

Figure 2-S4). Stability of Rom2 and Ssd1, but not Ugp1, decrease with extended heat shock. A strain containing Ssd1-HA and Rom2-FLAG was incubated at 37° C for the indicated time. Crude cell lysates were then prepared and subjected to western blot analysis.

CHAPTER 3

PAS KINASE IS REQUIRED FOR NORMAL CELLULAR ENERGY BALANCE

Huai-Xiang Hao, Caleb M. Cardon, Wojtek Swiatek, Robert C Cooksey, Tammy L. Smith, James Wilde, Sihem Boudina, E. Dale Abel, Donald A. McClain and Jared Rutter

The author's work is contained in Figure 5 as well as the supplementary data not included in the original manuscript.

PAS kinase is required for normal cellular energy balance

Huai-Xiang Hao*, Caleb M. Cardon*, Wojtek Swiatek*, Robert C. Cooksey†, Tammy L. Smith*, James Wilde*, Sihem Boudina†, E. Dale Abel†, Donald A. McClain†, and Jared Rutter*‡

*Department of Biochemistry and †Division of Endocrinology, Diabetes and Metabolism, University of Utah School of Medicine, Salt Lake City, UT 84112

The metabolic syndrome, a complex set of phenotypes typically associated with obesity and diabetes, is an increasing threat to global public health. Fundamentally, the metabolic syndrome is caused by a failure to properly sense and respond to cellular metabolic cues. We studied the role of the cellular metabolic sensor PAS kinase (PASK) in the pathogenesis of metabolic disease by using PASK$^{-/-}$ mice. We identified tissue-specific metabolic phenotypes caused by PASK deletion consistent with its role as a metabolic sensor. Specifically, PASK$^{-/-}$ mice exhibited impaired glucose-stimulated insulin secretion in pancreatic β-cells, altered triglyceride storage in liver, and increased metabolic rate in skeletal muscle. Further, PASK deletion caused nearly complete protection from the deleterious effects of a high-fat diet including obesity and insulin resistance. We also demonstrate that these cellular effects, increased rate of oxidative metabolism and ATP production, occur in cultured cells. We therefore hypothesize that PASK acts in a cell-autonomous manner to maintain cellular energy homeostasis and is a potential therapeutic target for metabolic disease.

metabolism | PAS domain | nutrient sensing | obesity

Because of changes in diet and lifestyle, the incidence of obesity and type 2 diabetes is increasing dramatically worldwide. Type 2 diabetes arises when pancreatic β-cells fail to secrete sufficient insulin to compensate for peripheral insulin resistance, a condition severely aggravated by obesity (1, 2). Type 2 diabetes is now widely viewed as a manifestation of a broader underlying metabolic disorder called the metabolic syndrome, which is characterized by hyperglycemia, hyperinsulinemia, dyslipidemia, hypertension, visceral obesity, and cardiovascular disease (3). The World Health Organization estimates that the current decade will witness a 46% increase in diabetes incidence worldwide (from 151 million to 221 million), with the vast majority of this increase being due to metabolic syndrome-related type 2 diabetes (4).

Cellular energy and nutrient sensors determine how cells respond to excessive nutrients, and aberrant nutrient and energy sensing is a contributing factor to metabolic syndrome development (5, 6). AMP-activated protein kinase (AMPK) and mammalian target of rapamycin (mTOR) are two well studied and evolutionarily conserved cellular energy and nutrient sensors. AMPK is activated in response to intracellular ATP depletion and acts to switch the cellular metabolic program from ATP consumption to ATP production (7). In contrast to AMPK, mTOR is activated by sufficient cellular energy or nutrients, particularly amino acids (8). Activation of mTOR stimulates cell growth by increasing protein synthesis through phosphorylation of ribosomal S6 kinase (S6K) and eIF4E-binding protein (9). Decreased AMPK activity and elevated mTOR activity have been linked with obesity, diabetes, and cancer (10–12).

Like AMPK and mTOR, PAS kinase (PASK) is a nutrient-responsive protein kinase conserved from yeast to humans. The PAS domain of PASK specifically interacts with the kinase catalytic domain and inactivates the kinase in cis (13). Based on biochemical and genetic data, a model has been proposed wherein a small metabolite activates PASK by directly interacting with the PAS domain and disrupting its interaction with the kinase domain (5, 14, 15). Studies in cultured pancreatic β-cells support a role for PASK in nutrient sensing and response. Specifically, PASK has been shown to be regulated by glucose both posttranslationally and at the level of gene expression, and PASK activity is required for glucose-stimulated insulin expression in Min-6 cells (16).

We sought to address the *in vivo* role of PASK in pancreatic β-cell function and energy homeostasis. Using PASK$^{-/-}$ mice (17), we demonstrate that PASK is required for normal β-cell insulin secretion. We also demonstrate that PASK deletion results in resistance to the phenotypes caused by a high-fat diet, including obesity, insulin resistance, and hepatic triglyceride accumulation. This protection is likely due to increased metabolic rate and energy expenditure in PASK$^{-/-}$ mice independent of the activity of AMPK, mTOR, and peroxisome proliferator-activated receptor γ coactivator 1 (PGC-1). Increased oxidative metabolism and ATP generation are also observed in cultured cells upon acute PASK knockdown by RNAi. These cellular effects, which recapitulate effects observed *in vivo*, support the hypothesis that PASK functions as a cell-autonomous regulator of cellular energy balance (14).

Results

Impaired Glucose-Stimulated Insulin Secretion (GSIS) in PASK$^{-/-}$ Mice. Previously, PASK was shown to be required for the induction of preproinsulin promoter activity by high glucose concentrations in cultured Min-6 β-cells (16). To examine GSIS in PASK$^{-/-}$ mice, we measured plasma insulin levels before and after an intraperitoneal glucose injection. As shown in Fig. 1A, insulin levels in PASK$^{-/-}$ mice are modestly but significantly lower than those in WT littermates at both 5 min and 45 min after glucose injection. This defect in insulin secretion is also manifest in isolated islets of Langerhans *in vitro*. Using islet perifusion experiments, we found PASK$^{-/-}$ islets to be defective in GSIS, particularly at higher glucose concentrations (Fig. 1B), but normal in depolarization-induced insulin secretion (data not shown). The total insulin secreted by PASK$^{-/-}$ islets in these experiments was 56% the total secreted by WT islets.

Defects in insulin secretion are often accompanied by alterations in islet morphology or β-cell mass. To determine whether these
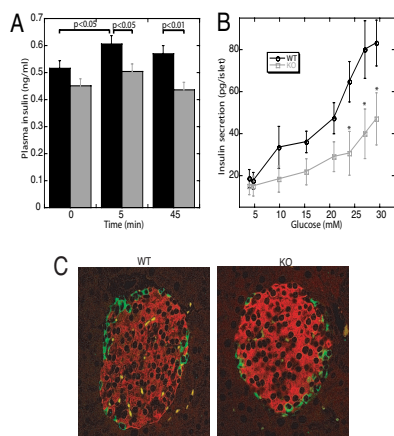
Fig. 1. Impaired insulin secretion but normal islet morphology in $PASK^{-/-}$ mice. (*A*) Plasma insulin concentrations before and after i.p. glucose injection into WT (black bars) and $PASK^{-/-}$ (gray bars) ($n = 24$ male mice per genotype, 12 weeks of age). (*B*) Perifusion of 15–17 isolated islets with a 3–30 mM glucose ramp in gassed Krebs buffer for 40 min ($n = 4$ female mice, 16 weeks of age). Area under the curve: $1,146 \pm 129$ for WT islets and 646 ± 171 for $PASK^{-/-}$ islets ($P < 0.05$). The experiment was performed twice with similar results. $*$, $P < 0.05$. Data shown represent the mean $\pm$ SD. (*C*) Immunostaining of pancreatic sections by using anti-insulin (red) and anti-glucagon (green) antibodies from 16-week-old male WT and $PASK^{-/-}$ mice.

Fig. 2. $PASK^{-/-}$ mice were protected from diet-induced glucose intolerance, insulin resistance, and obesity. (*A*–*D*) GTT and ITT with WT and $PASK^{-/-}$ mice fed with either NCD (*A* and *B*) or HFD (*C* and *D*). Plasma glucose levels were determined before and at indicated times after i.p. glucose (*A* and *C*) or insulin (*B* and *D*) injection. (*E* and *F*) Growth curves of WT and $PASK^{-/-}$ mice on NCD (*E*) or HFD (*F*) beginning at 12 weeks of age. All data represent the mean $\pm$ SEM for 12 male mice of each genotype. $*$, $P < 0.05$; $**$, $P < 0.01$.

parameters are affected in $PASK^{-/-}$ mice, we examined islet organization and morphology by glucagon and insulin double-immunostaining. No defect in islet morphology, size, or β-cell area was observed in $PASK^{-/-}$ mice (Fig. 1*C* and data not shown). We also observed no significant difference between WT and $PASK^{-/-}$ mice in Ins-1 or Ins-2 mRNA levels (see supporting information (SI) Fig. 6*A*) or in total pancreatic insulin (SI Fig. 6*B*). The expression levels of several genes involved in insulin transcription and GSIS, including Pdx-1, MafA, GLUT2, and glucokinase, were also unchanged in $PASK^{-/-}$ islets (data not shown). We therefore suggest that the GSIS defect observed in $PASK^{-/-}$ mice is likely a result of impaired β-cell glucose sensing.

Improved Glucose Tolerance, Increased Insulin Sensitivity, and Resistance to Obesity in High-Fat Diet (HFD)-Fed $PASK^{-/-}$ Mice. To assess whether PASK is required for the maintenance of glucose homeostasis, we performed a glucose tolerance test (GTT), in which plasma glucose levels were monitored over time after glucose injection. $PASK^{-/-}$ mice displayed a slight and statistically insignificant glucose intolerance (Fig. 2*A*). Insulin sensitivity, as measured by insulin tolerance test (ITT), was identical in WT and $PASK^{-/-}$ mice (Fig. 2*B*). When fed a HFD, C57BL/6J mice develop obesity and a set of symptoms reminiscent of the metabolic syndrome, including insulin resistance (18). To examine glucose homeostasis under this stress condition, we performed GTT and ITT experiments on HFD-fed WT and $PASK^{-/-}$ mice. Whereas HFD-fed WT mice developed glucose intolerance and insulin resistance, $PASK^{-/-}$ mice were completely protected from these effects (Fig. 2 *C* and *D*; compare with Fig. 2 *A* and *B*). As expected, fasting insulin levels of HFD-fed $PASK^{-/-}$ mice were substantially lower than the fasting insulin levels of WT mice (SI Fig. 7*A*).

$PASK^{-/-}$ mice were also protected from HFD-induced obesity. WT and $PASK^{-/-}$ mice were of similar weight on normal chow diet (NCD) (Fig. 2*E*), but the weight gain of $PASK^{-/-}$ mice on HFD was significantly less than that of WT littermates (Fig. 2*F*). After 8 weeks of HFD feeding, the body weight of $PASK^{-/-}$ mice was
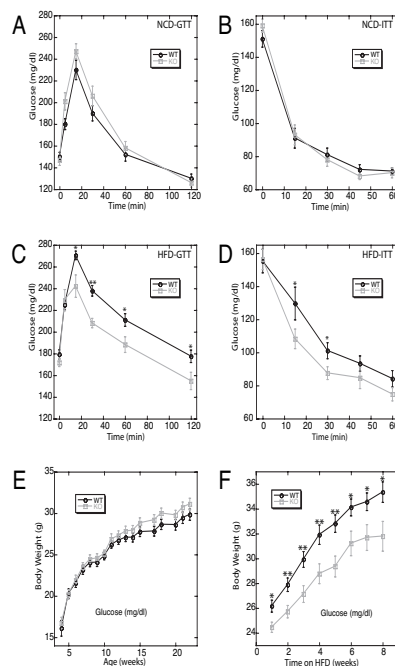
similar to NCD-fed WT or $PASK^{-/-}$ mice. Analysis of body composition by dual-energy x-ray absorptiometry showed that the difference in total body weight between WT and $PASK^{-/-}$ HFD-fed mice is completely accounted for by decreased fat mass in $PASK^{-/-}$ mice (SI Fig. 7*B*).

$PASK^{-/-}$ Mice Exhibit Increased Whole-Body Energy Expenditure and Increased Metabolic Rate in Skeletal Muscle. We hypothesized that the $PASK^{-/-}$ lean phenotype is responsible for the improved glucose tolerance and insulin sensitivity; therefore, we sought to understand the basis for this phenotype. Obesity is the result of an imbalance between energy intake (in the form of feeding) and energy expenditure (in the form of physical activity and basal metabolism) (19). We therefore measured O_2 consumption, CO_2 production, food intake, and locomotor activity by using metabolic chambers. Food intake and locomotor activity were similar, but $PASK^{-/-}$ mice consumed more O_2, produced more CO_2, and generated more heat than WT littermates (Fig. 3*A*). Relative to WT mice, HFD-fed $PASK^{-/-}$ mice have a slight substrate preference for carbohydrate over fat, as indicated by the respiratory quotient (0.91 ± 0.02 for WT mice and 0.93 ± 0.02 for $PASK^{-/-}$ mice, $P < 0.05$, night values). This hypermetabolic phenotype in $PASK^{-/-}$ mice was also manifest in permeabilized soleus muscle fibers, wherein we observed elevated ATP production from succinate in $PASK^{-/-}$ muscle (Fig. 3*B*).

One potential explanation for the observed increase in oxidative metabolism was an increase in mitochondrial mass in $PASK^{-/-}$ muscle. However, soleus muscle electron micrographs (Fig. 3*C*) and
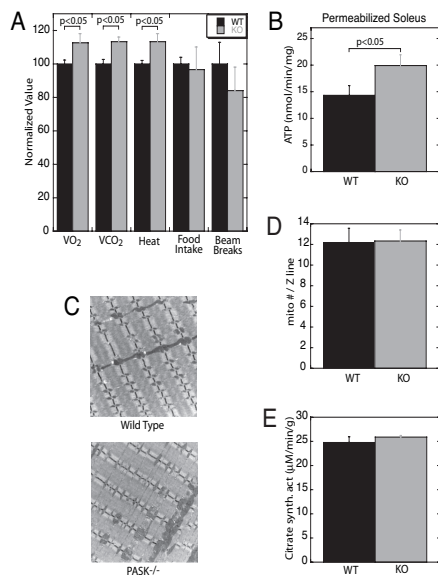
Fig. 3. $PASK^{-/-}$ mice exhibit increased metabolic rate without increased mitochondrial mass. (*A*) Metabolic chamber analysis of WT and $PASK^{-/-}$ mice (n = 3 male mice, 24 weeks of age). VO$_2$, O$_2$ consumption; VCO$_2$, CO$_2$ emission. Laser beam breaks are a measure of locomotor activity. For each parameter, the average of the WT value was set at 100%. The data presented are nighttime values (6 p.m. to 6 a.m.). Daytime values exhibited a similar difference between WT and $PASK^{-/-}$ mice. (*B*) Maximal ATP production rate in saponin-permeabilized soleus muscle fibers, measured in the presence of 1 mM exogenous ADP and succinate (n = 10 male mice, 16 weeks of age). (*C*) Representative electron micrographs of soleus muscle from 16-week-old WT and $PASK^{-/-}$ male mice. (Original magnification: ×8000.) Four sections from each animal and three animals per genotype were examined. (*D*) Quantification of mitochondrial number manually counted from 10 electron micrographs per genotype. The data presented are the mean ± SD and are normalized to Z line number. (*E*) Citrate synthase activity in soleus muscle extracts from WT and $PASK^{-/-}$ mice (n = 6 male mice, 16 weeks of age). The data presented are the mean ± SD.

Table 1. Normalized transcript levels in HFD-fed $PASK^{-/-}$ liver (WT set as 1)

Transcript	Normalized level in $PASK^{-/-}$		P value (vs. WT)
	Mean	SD	
Glut2	0.92	0.17	0.37
G6Pase	0.66	0.34	0.16
PEPCK	0.88	0.23	0.38
PGC-1α	0.88	0.17	0.24
PGC-1β	1.00	0.14	1.00
PPARα	0.90	0.12	0.17
LXRα	1.02	0.13	0.82
SREBP-1c	0.75	0.26	0.32
FAS	0.74	0.30	0.53
ACL	0.93	0.52	0.85
MCAD	0.79	0.42	0.46
LCAD	1.00	0.14	1.00
VLCAD	1.03	0.15	0.70

deletion affected AMPK or mTOR activity. We performed Western blots of WT and $PASK^{-/-}$ liver samples from NCD- and HFD-fed mice by using antibodies recognizing phospho-AMPK (Thr-172) and phospho-S6K (Thr-389), which are widely accepted as markers of AMPK and mTOR activity, respectively. As shown in Fig. 4*C*, we observed no difference between WT and $PASK^{-/-}$ liver under either NCD or HFD conditions. We also observed no change in phospho-AMPK and phospho-S6K in gastrocnemius muscle (data not shown), suggesting the function of PASK is independent of changes in the activity of the AMPK or mTOR pathways.
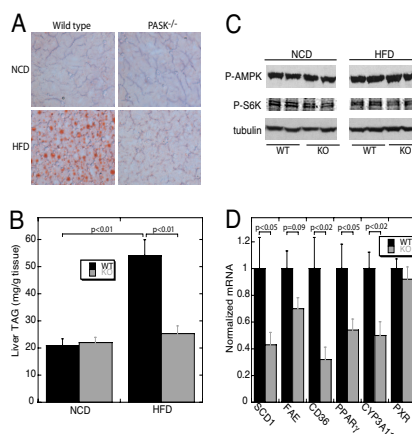
subsequent quantification of both mitochondrial number and area showed no difference between $PASK^{-/-}$ and WT soleus muscle (Fig. 3*D* and data not shown). Further, the activity of citrate synthase, a marker of mitochondrial density (20), was identical in $PASK^{-/-}$ and WT soleus muscle extracts (Fig. 3*E*). We also observed no difference in the mRNA levels of either PGC-1α or PGC-1β (Table 1), important transcriptional regulators of mitochondrial biogenesis (21, 22). We conclude that PASK deficiency leads to increased mitochondrial metabolism and ATP production that is independent of increased mitochondrial biogenesis.

$PASK^{-/-}$ Mice Exhibit Reduced Liver Triglyceride Accumulation. Diet-induced obesity is typically accompanied by increased lipid accumulation in peripheral tissues, which is strongly associated with the development of insulin resistance (23, 24). We examined liver lipid content both by histological oil red O staining (Fig. 4*A*) and by enzymatic triglyceride quantification (Fig. 4*B*). In both cases, HFD-fed $PASK^{-/-}$ mice were completely protected from the increased lipid accumulation observed in HFD-fed WT mice.

Increased AMPK activity and reduced mTOR pathway activity cause resistance to diet-induced obesity, as demonstrated by using transgenic and pharmacologic strategies (25, 26). Given their joint role as nutrient sensors, we sought to determine whether $PASK$

Fig. 4. Reduced triglyceride accumulation in $PASK^{-/-}$ livers on HFD. (*A*) Representative oil red O staining of liver cryosections from 24-week-old WT and $PASK^{-/-}$ male mice on NCD and HFD after an 8-h fast. (*B*) Liver triglyceride (triacyl glycerol, TAG) content in 24-week-old WT and $PASK^{-/-}$ mice on NCD and HFD harvested after an 8-h fast (n = 3–5 male mice). (*C*) Immunoblot analysis of phospho-AMPK (Thr-172), phospho-S6K (Thr-389), and tubulin (as loading control) levels in liver extracts from WT and $PASK^{-/-}$ mice on NCD and HFD. Results from two mice per group are shown. Total AMPK and S6K protein levels were also analyzed and found to be identical among the groups. (*D*) SCD1, fatty acid elongase (FAE), CD36, PPARγ, CYP3A11, and PXR mRNA levels in liver from WT and $PASK^{-/-}$ mice on HFD measured by quantitative RT-PCR. The data shown are the average of n = 6 per group with the WT value set as 1. RPL13A was used as the normalizer. All data presented are the mean ± SD.
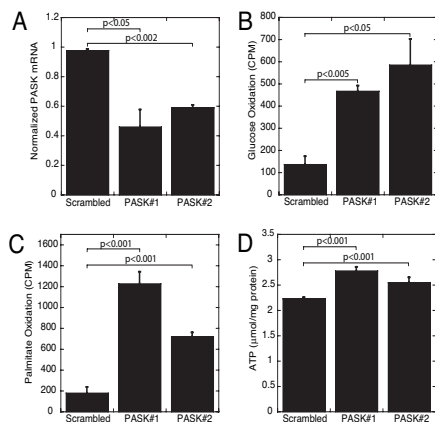
Fig. 5. Increased oxidative metabolism and cellular ATP content upon PASK silencing in L6 cells. (*A*) PASK mRNA levels in L6 clones expressing either scrambled or PASK shRNA in the absence of doxycycline. Data represent the mean ± SD of triplicates per group. (*B*) Measurement of $^{14}CO_2$ released from indicated L6 clones incubated in [^{14}C]glucose ($n = 3$). (*C*) Measurement of $^{14}CO_2$ released from indicated L6 clones incubated in [^{14}C]palmitate ($n = 3$). (*D*) Cellular ATP content measurement normalized to protein in extract.

We also determined the levels of transcripts related to lipid metabolism in liver from HFD-fed WT and $PASK^{-/-}$ mice. Levels of stearoyl-CoA desaturase 1 (SCD1) (27), long-chain fatty acid elongase (28), fatty acid transporter (CD36) (29), and the lipid-responsive nuclear hormone receptor peroxisome proliferator-activated receptor γ (PPARγ) (30) are all significantly decreased in $PASK^{-/-}$ liver (Fig. 4*D*). Lower expression of each of these genes is consistent with decreased hepatic lipid synthesis and triglyceride accumulation. The transcripts of other genes involved in fatty acid metabolism, including *FAS, ACC-1,* and *SREBP-1c,* showed no difference between WT and $PASK^{-/-}$ liver (Table 1).

The altered lipid accumulation and the pattern of gene expression observed in $PASK^{-/-}$ liver is strikingly similar, albeit opposite, to that observed in a transgenic mouse expressing a constitutively active pregnane X receptor (PXR) in liver (31). This observation raised the possibility that the PASK-dependent effects on lipid metabolism in liver might be mediated through a decrease in PXR expression or function. Indeed, we observed a decrease in the mRNA levels of a well established PXR target gene *CYP3A11* (32) in $PASK^{-/-}$ liver. The expression of the *PXR* gene itself is not altered by *PASK* deletion (Fig. 4*D*); therefore, if PASK does regulate PXR activity, it does so via a mechanism distinct from gene expression.

Acute PASK Silencing Increases Oxidative Metabolism in Cultured Cells. To address the possibility that the observed hypermetabolic phenotype in skeletal muscle is a secondary or adaptive response to *PASK* deletion in mice, we generated two independent L6 myoblast cell lines wherein we could acutely silence PASK expression by using short hairpin RNA (shRNA) upon doxycycline removal. As shown in Fig. 5*A*, these two clones both exhibit an ≈50% decrease in PASK mRNA upon doxycycline removal compared with the scrambled shRNA control. On PASK knockdown, we observed a large increase in both glucose and palmitate oxidation (Fig. 5 *B* and *C*). This increased substrate metabolism is accompanied by elevated steady-state levels of ATP, presumably a result of increased mitochondrial ATP production (Fig. 5*D*). We also generated L6-derived cells with constitutive knockdown of PASK and observed increased glucose oxidation and ATP levels (data not

shown). These data in cultured cells indicate that loss of PASK leads to an acute and cell-autonomous increase in mitochondrial metabolism and ATP production.

Discussion

Herein we describe a physiological role for PASK in regulating mammalian energy balance. $PASK^{-/-}$ mice are protected from HFD-induced obesity and from other metabolic perturbations that accompany HFD-induced obesity. Levels of insulin sensitivity and glucose tolerance in HFD-fed $PASK^{-/-}$ mice are nearly identical to the levels in NCD-fed WT or $PASK^{-/-}$ mice. These changes in organismal energy and glucose homeostasis are likely manifestations of an underlying alteration in metabolic regulation in individual cells and tissues. We have previously described a role for PASK in glucose-responsive processes in pancreatic β-cells (16). We show here that $PASK^{-/-}$ mice exhibit hypoinsulinemia *in vivo* and $PASK^{-/-}$ islets have impaired GSIS *in vitro*. These effects are not due to decreased insulin gene expression or altered islet morphology or mass, but likely to impaired β-cell glucose sensing. Another group did not observe this decrease in GSIS in $PASK^{-/-}$ mice (33).

We observed a striking protection from HFD-induced hepatic steatosis in $PASK^{-/-}$ mice. This is accompanied by a significant decrease in the transcript levels of SCD1, fatty acid elongase, CD36, and PPARγ. SCD1 is the rate-limiting enzyme in the synthesis of monounsaturated fatty acids, which are the major substrates for triglyceride synthesis (34). $SCD1^{-/-}$ mutant mice exhibit decreased liver triglyceride accumulation and fatty acid biosynthesis and are protected from HFD-induced obesity (35, 36). Fatty acid elongase is required for *de novo* fatty acid synthesis (37). CD36 (also known as fatty acid translocase) is a putative fatty acid transporter. Interestingly, *CD36* is a target gene of PPARγ (38); thus, the decreased expression of *CD36* could be secondary to the lower expression of PPARγ in $PASK^{-/-}$ liver. *PPARγ* expression has been shown to positively correlate with obesity in multiple mouse models (39). Decreased expression of each of these genes in liver is consistent with decreased lipid content observed in HFD-fed $PASK^{-/-}$ mice. These alterations in gene expression, and particularly a decrease in *CYP3A11* expression, are consistent with decreased PXR activity in $PASK^{-/-}$ liver (31). The expression of *PXR* is not different, however, suggesting that PASK might regulate PXR via direct phosphorylation, through altered abundance of a PXR agonist, or through other mechanisms. Alternatively, the PXR paralog CAR, which activates an overlapping set of genes, might be down-regulated upon *PASK* deletion. These hypotheses await further investigation.

Deletion of *PASK* leads to organismal hypermetabolism as measured by O_2 consumption, CO_2 production, and heat generation. This hypermetabolism is also exhibited in isolated permeabilized skeletal muscle, wherein we observed increased ATP production. A number of mouse models exhibit similar hypermetabolism. Three aspects of the $PASK^{-/-}$ phenotype make it unusual. First, the elevated metabolic rate is not caused by impaired metabolic efficiency and concomitantly increased substrate demand. In fact, we observed increased ATP production both in isolated $PASK^{-/-}$ skeletal muscle and in cultured cells upon acute *PASK* knockdown. Further, energy stress is not apparent, as there is no AMPK hyperactivation in liver or skeletal muscle from $PASK^{-/-}$ mice as measured by phosphorylation of either AMPK or ACC (Fig. 4*C* and data not shown). Second, the increased mitochondrial oxidative metabolism occurs without changes in mitochondrial mass or number or in PGC-1α or -β expression. Third, this phenotype seems to be a property of individual cells because it is recapitulated in L6 myoblasts upon acute *PASK* knockdown. Although the detailed mechanism for increased oxidative metabolism upon *PASK* loss is unclear, it is almost certainly due to changes in mitochondria. First, the *ex vivo* soleus ATP measurements were performed under conditions that measure mitochondrial ATP production. Second,

the observation that both glucose and palmitate oxidation were increased upon PASK knockdown suggests that the alteration lies downstream of where these two metabolic pathways converge, namely at the level of the mitochondrial tricarboxylic acid cycle.

We have previously proposed that PASK functions as a cell-autonomous nutrient sensor (5, 14). PASK is posttranslationally activated by elevated glucose medium in cultured β-cells (16), probably through allosteric control via its regulatory PAS domain (13, 15). PASK also is regulated by nutrient status at the level of gene expression (16). Taking these observations together, we conclude that PASK integrates multiple cues to monitor cellular energetic status. As inferred from the loss-of-function phenotype, the effect of PASK activation seems to be cell type specific and part of an appropriate nutrient response for each cell type analyzed. PASK activation in β-cells contributes to insulin secretion. PASK activation in hepatocytes increases the synthesis and accumulation of storage lipids such as triglycerides. PASK activation in skeletal muscle results in decreased ATP generation both from carbohydrate and fatty acid oxidation. We, therefore, propose a model wherein PASK acts as a sensor, integrator, and transducer of a metabolic sufficiency signal. The transduction pathway downstream of PASK is cell type specific but, at least in skeletal muscle, decreases mitochondrial oxidative metabolism and ATP production. When PASK is artificially lost, this metabolic sufficiency signal is not transduced and the result is chronically elevated mitochondrial metabolism, resulting in protection from ectopic HFD-induced lipid accumulation. As with the other well known metabolic sensory kinases AMPK and mTOR, we propose that PASK may be an important regulator of human metabolic disease.

Methods

Animals. $PASK^{-/-}$ mice were genotyped as described (17). After the fifth backcross into C57BL/6 (Charles River Laboratories, Wilmington, MA), 12- to 24-week-old males were used for all experiments except that the islet perifusion studies were performed on females. Mice were maintained on a NCD (3080; Harlan Teklad, Madison, WI) or a HFD from 12 weeks of age (45% fat by calories, D12451; Research Diets, New Brunswick, NJ). In each experiment, age-matched WT littermates were used as controls for $PASK^{-/-}$ mice. All procedures were approved by the institutional animal care and use committee of University of Utah.

Cell Culture. Rat L6 myoblasts were provided by Scott Summers (University of Utah, Salt Lake City, UT). Cells were maintained at 37°C under 5% CO_2 in DMEM supplemented with 10% FBS (HyClone, Logan, UT), 0.1 mg/ml penicillin and 0.1 mg/ml streptomycin (Life Technologies, Grand Island, NY).

GTT/ITT and Serum Insulin Measurement. For GTT and plasma insulin measurement, experimental animals were fasted for 6 h, after which glucose (1 g/kg body weight) was injected i.p. At the indicated times, tail vein blood was sampled for glucose determination with a glucometer (Bayer, Pittsburgh, PA) or for insulin measurement by using the Sensitive Rat Insulin RIA kit (Linco Research, St. Charles, MO). For ITT, human recombinant insulin (0.75 unit/kg of body weight; Novo-Nordisk, Copenhagen, Denmark) was injected i.p. to randomly fed mice and blood glucose levels were determined at the indicated times.

Islet Isolation and Perifusion. Islets of Langerhans were isolated from pancreas by using the intraductal liberase (Roche Applied Science, Indianapolis, IN) digestion method as described in ref. 40. Fifteen to 17 size-matched islets were individually handpicked and used for perifusion experiments as described (40). The glucose and released insulin in fractions of perifusion buffer were measured by using a Glucose Analyzer (Beckman Instruments, Fullerton, CA) and Sensitive Rat Insulin RIA kit (Linco Research), respectively.

Metabolic Chamber Studies. Indirect calorimetry was performed with a four-chamber Oxymax system (Columbus Instruments, Columbus, OH). Animals were allowed to adapt to the metabolic chamber for 4 h and then VO_2, VCO_2, heat production, food and water intake, and movement were measured every 15 min for 3 days from individually housed mice. Averaged data from 6 p.m. to 6 a.m. are expressed as night values and data from 6 a.m. to 6 p.m. are expressed as day values.

Mitochondrial Respiration Experiment. Soleus fibers were separated and then permeabilized by saponin. Maximal (ADP-stimulated) ATP production rate was determined by exposing fibers to 1 mM exogenous ADP and succinate as described (21).

Citrate Synthase Activity Assay. Citrate synthase activity was measured by the spectrophotometric method as described (41). In brief, frozen soleus muscle was homogenized on ice and citrate synthase was released from mitochondria by freezing and thawing the homogenate. The reaction was initiated by addition of oxaloacetate into 1 ml of diluted homogenate in reaction buffer containing acetyl-CoA, and then monitored at 412 nm for 3 min with an Ultrospec 3000 spectrophotometer (Amersham, Piscataway, NJ).

Histological Analysis. For immunostaining, dissected pancreata were fixed overnight at room temperature in 10% formalin, paraffin-embedded, and microtome-sectioned at 5 μm thickness. After deparaffinization and rehydration, the sections were sequentially treated with 3% H_2O_2, target retrieval solution (DAKO, Glostrup, Denmark), and blocking solution. The sections were then incubated with antiglucagon (Vector Laboratories, Burlingame, CA), followed by secondary antibody labeled with AlexaFluor 488 (Molecular Probes, Carlsbad, CA), and anti-insulin (DAKO), followed by AlexaFluor 594-labeled secondary antibody. Fluorescent confocal images were captured, overlaid, and analyzed by National Institutes of Health (NIH) ImageJ software. For electron microscopy analysis, soleus muscle was fixed in EM fixative, dehydrated in graded ethanol, and embedded in Poly Bed plastic resins for sectioning as described (21). Soleus mitochondrial number was quantified in blinded fashion from electron micrographs at the magnification of ×8000 and normalized to Z line number. For oil red O staining, frozen liver samples were embedded in OTC reagent (Tissue-Tek; Sakura Finetek, Hatfield, PA) and sectioned at 8 μm in cryostat. Cryosections were fixed in formaldehyde vapor at 50°C, incubated in 0.5% oil red O in isopropyl alcohol, and counterstained with hematoxylin (Sigma, St. Louis, MO). After rinsing in distilled water, liver sections were mounted with permanent aqueous mounting medium Gel/Mount (Biomeda, Foster City, CA) and photographed by using light microscopy at ×40 magnification. All images were acquired at the University of Utah Imaging Core Facility.

Liver Triglyceride Content Measurement. Quantitative analysis of liver triglyceride content was performed by saponification of liver in ethanolic KOH as described (42). After neutralization with $MgCl_2$, glycerol produced during hydrolysis was measured by a colorimetric assay with Free Glycerol Reagent and Glycerol Standard Solution (Sigma).

Western Blotting. Liver lysates were prepared by homogenizing 50–100 mg snap-frozen liver slices in cell lysis buffer (Cell Signaling Technology, Beverly, MA) by using a Tissue-Tearer rotor. After centrifugation at 20,000 × g for 30 min at 4°C, the supernatants were collected and protein concentrations were determined by Advanced Protein Assay Reagent (Cytoskeleton, Denver, CO). About 50 μg of protein from each sample was separated by SDS/PAGE, transferred to a PVDF membrane (Fisher, Waltham, MA), and blotted with indicated antibodies according to the manufacturer's

protocol. Phospho-AMPK (Thr-172), phospho-S6K (Thr-389), and tubulin antibodies were purchased from Cell Signaling Technology.

Real-Time Quantitative RT-PCR. Total RNA was extracted from tissues or cells by using RNAStat60 reagent (Tel-Test, Friendswood, TX) and purified with RNeasy Mini kit (Qiagen, Valencia, CA), according to the manufacturer's instructions. First-strand cDNA synthesis was carried out with SuperScript III reverse transcriptase (Invitrogen, Carlsbad, CA). Real-time PCR was performed on a LightCycler (Roche Diagnostics, Indianapolis, IN) by using the SYBR Green-based method as described (40). Melting curve analysis and a mock reverse transcribed control were included to ensure the specificity of the amplicons. Primer sequences for indicated transcripts are available on request.

Generation of Inducible PASK Knockdown Cells. pRevTet-Off-IN retroviral vector was purchased from Clontech (Mountain View, CA), and retrovirus was produced according to the manufacturer's instructions by using Fugene transfection reagent (Roche Applied Science) and Phoenix-Ampho retroviral packaging cell line (American Type Culture Collection, Manassas, VA). L6 cells were infected with the generated Tet-Off retrovirus in the presence of 6 mg/ml Polybrene, and 48 h after infection G418 was added to the medium at a final concentration of 200 μg/ml. After 2 weeks of selection, G418-resistant colonies were individually harvested by using cloning cylinders (Corning, Corning, NY) and screened for inducibility with pRevTRE-Luc (Clontech) virus. shRNA oligonucleotide duplexes containing sequences targeting rat PASK gene and a scrambled shRNA were designed by using Invitrogen web site software and cloned into tetracycline-regulated retroviral SIN-TREmiR30-PIG (TMP) vector (OPEN Biosystems, Huntsville, AL). Retrovirus expressing the inducible hairpins was generated and used to infect highly inducible Tet-Off L6 clones as verified by luciferase assay. Finally, 2 μg/ml puromycin as well as 2 μg/ml doxycycline was applied and puromycin-resistant clones were isolated as described above. PASK knockdown clones were screened by quantitative RT-PCR analysis of PASK mRNA levels in the absence and presence of doxycycline. PASK targeting hairpin sequence: GATGCCAAGACCACAGAGA and GCGCAGA-CAAGCTCAAAGA. Scrambled sequence: GCGCAGA-CAAGCTCAAAGA.

Glucose and Palmitate Oxidation Measurement. Glucose oxidation rates were determined according to previously described methods (43). In brief, triplicate samples of L6 cells were incubated with 500 μl of oxygenated Krebs–Ringer buffer containing 5 mM unlabeled glucose, 2 μCi of [U-^{14}C]glucose (MP Biochemicals, Aurora, OH), and 0.4% BSA (wt/vol) in a 24-well plate. A UniFilter-24 GF/B plate (Packard Instruments, Waltham, MA) was sealed with an adhesive sheet by using vacuum grease, and 200 μl of 10× hyamine hydroxide (PerkinElmer Sciences, Waltham, MA) was pipetted onto each filter for CO_2 capture. Finally, the 24-well plate was sealed with a rubber gasket. The apparatus was incubated with gentle shaking for 2 h at 37°C and the experiment was stopped by injecting 100 μl of 1 M perchloric acid per well. Filters were removed, and captured $^{14}CO_2$ was measured by scintillation counting. Control incubations lacking cells were included in each plate. For palmitate oxidation, the same procedure was used except using Krebs–Ringer buffer containing 1 mM glucose, 0.5 mM unlabeled palmitate, 1 μCi of [1-^{14}C]palmitate (MP Biochemicals), and 1 mM carnitine.

Cellular ATP Content Measurement. L6 cells were washed with PBS, harvested by trypsinization, and pelleted by centrifugation. The cells were then lysed in 1 M perchloric acid on ice to precipitate cellular proteins. After centrifugation at 20,000 × g for 10 min, the supernatant was transferred into a new tube and neutralized with an equal volume of 1 M KOH. The ATP content was measured by an ATP Determination kit (Invitrogen) according to the manufacturer's instructions.

Statistical Analysis. Data are presented as mean ± standard deviation unless otherwise indicated. A two-tailed equal variance t test was used to compare differences, and the null hypothesis was rejected at the 0.05 level.

1. Rhodes CJ (2005) *Science* 307:380–384.
2. Lazar MA (2005) *Science* 307:373–375.
3. Reaven GM (1988) *Diabetes* 37:1595–1607.
4. Zimmet P, Alberti KG, Shaw J (2001) *Nature* 414:782–787.
5. Lindsley JE, Rutter J (2004) *Comp Biochem Physiol B Biochem Mol Biol* 139:543–559.
6. Marshall S (2006) *Sci STKE* 2006:re7.
7. Hardie DG, Carling D, Carlson M (1998) *Annu Rev Biochem* 67:821–855.
8. Proud CG (2002) *Eur J Biochem* 269:5338–5349.
9. Gingras AC, Raught B, Sonenberg N (2001) *Genes Dev* 15:807–826.
10. Inoki K, Corradetti MN, Guan KL (2005) *Nat Genet* 37:19–24.
11. Winder WW, Hardie DG (1999) *Am J Physiol* 277:E1–E10.
12. Manning BD (2004) *J Cell Biol* 167:399–403.
13. Rutter J, Michnoff CH, Harper SM, Gardner KH, McKnight SL (2001) *Proc Natl Acad Sci USA* 98:8991–8996.
14. Rutter J (2002) *Science* 298:1567–1568.
15. Amezcua CA, Harper SM, Rutter J, Gardner KH (2002) *Structure (London)* 10:1349–1361.
16. da Silva Xavier G, Rutter J, Rutter GA (2004) *Proc Natl Acad Sci USA* 101:8319–8324.
17. Katschinski DM, Marti HH, Wagner KF, Shibata J, Eckhardt K, Martin F, Depping R, Paasch U, Gassmann M, Ledermann B, *et al.* (2003) *Mol Cell Biol* 23:6780–6789.
18. Surwit RS, Kuhn CM, Cochrane C, McCubbin JA, Feinglos MN (1988) *Diabetes* 37:1163–1167.
19. Spiegelman BM, Flier JS (2001) *Cell* 104:531–543.
20. Leek BT, Mudaliar SR, Henry R, Mathieu-Costello O, Richardson RS (2001) *Am J Physiol* 280:R441–R447.
21. Leone TC, Lehman JJ, Finck BN, Schaeffer PJ, Wende AR, Boudina S, Courtois M, Wozniak DF, Sambandam N, Bernal-Mizrachi C, *et al.* (2005) *PLoS Biol* 3:e101.
22. Puigserver P, Wu Z, Park CW, Graves R, Wright M, Spiegelman BM (1998) *Cell* 92:829–839.
23. Unger RH (2002) *Annu Rev Med* 53:319–336.
24. Voshol PJ, Haemmerle G, Ouwens DM, Zimmermann R, Zechner R, Teusink B, Maassen JA, Havekes LM, Romijn JA (2003) *Endocrinology* 144:3456–3462.
25. Um SH, Frigerio F, Watanabe M, Picard F, Joaquin M, Sticker M, Fumagalli S, Allegrini PR, Kozma SC, Auwerx J, Thomas, G (2004) *Nature* 431:200–205.
26. Zhou G, Myers R, Li Y, Chen Y, Shen X, Fenyk-Melody J, Wu M, Ventre J, Doebber T, Fujii N, *et al.* (2001) *J Clin Invest* 108:1167–1174.
27. Flowers MT, Miyazaki M, Liu X, Ntambi JM (2006) *J Clin Invest* 116:1478–1481.
28. Matsuzaka T, Shimano H, Yahagi N, Yoshikawa T, Amemiya-Kudo M, Hasty AH, Okazaki H, Tamura Y, Iizuka Y, Ohashi K, *et al.* (2002) *J Lipid Res* 43:911–920.
29. Schaffer JE (2002) *Am J Physiol* 282:E239–E246.
30. Matsusue K, Haluzik M, Lambert G, Yim SH, Gavrilova O, Ward JM, Brewer B, Jr, Reitman ML, Gonzalez FJ (2003) *J Clin Invest* 111:737–747.
31. Zhou J, Zhai Y, Mu Y, Gong H, Uppal H, Toma D, Ren S, Evans RM, Xie W (2006) *J Biol Chem* 281:15013–15020.
32. Goodwin B, Redinbo MR, Kliewer SA (2002) *Annu Rev Pharmacol Toxicol* 42:1–23.
33. Borter E, Niessen M, Zuellig R, Spinas GA, Spielmann P, Camenisch G, Wenger RH (2007) *Diabetes* 56:113–117.
34. Dobrzyn A, Ntambi JM (2005) *Obes Rev* 6:169–174.
35. Miyazaki M, Kim YC, Gray-Keller MP, Attie AD, Ntambi JM (2000) *J Biol Chem* 275:30132–30138.
36. Ntambi JM, Miyazaki M, Stoehr JP, Lan H, Kendziorski CM, Yandell BS, Song Y, Cohen P, Friedman JM, Attie AD (2002) *Proc Natl Acad Sci USA* 99:11482–11486.
37. Jakobsson A, Westerberg R, Jacobsson A (2006) *Prog Lipid Res* 45:237–249.
38. Tontonoz P, Nagy L, Alvarez JG, Thomazy VA, Evans RM (1998) *Cell* 93:241–252.
39. Memon RA, Tecott LH, Nonogaki K, Beigneux A, Moser AH, Grunfeld C, Feingold KR (2000) *Endocrinology* 141:4021–4031.
40. Cooksey RC, Jouihan HA, Ajioka RS, Hazel MW, Jones DL, Kushner JP, McClain DA (2004) *Endocrinology* 145:5305–5312.
41. Boudina S, Sena S, O'Neill BT, Tathireddy P, Young ME, Abel ED (2005) *Circulation* 112:2686–2695.
42. Norris AW, Chen L, Fisher SJ, Szanto I, Ristow M, Jozsi AC, Hirshman MF, Rosen ED, Goodyear LJ, Gonzalez FJ, *et al.* (2003) *J Clin Invest* 112:608–618.
43. Antinozzi PA, Segall L, Prentki M, McGarry JD, Newgard CB (1998) *J Biol Chem* 273:16146–16154.

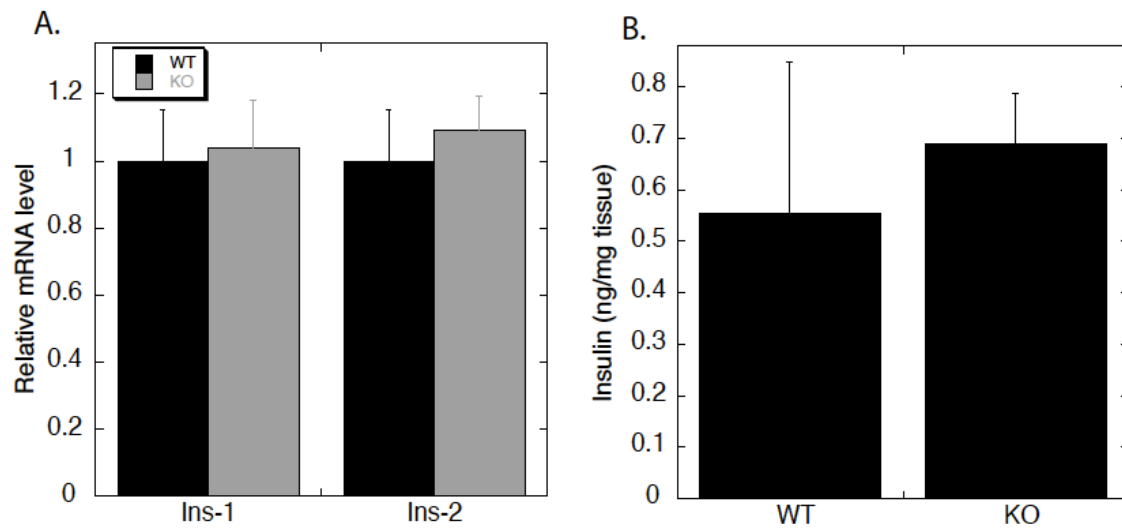**MEDICAL SCIENCES**

Supporting Information

Figure 3−S6). Analysis of insulin mRNA and protein levels. (A) Quantitative RT−PCR analysis of insulin transcript levels in WT and PASK$^{-/-}$ islets from 16−week−old male mice. Data represent the mean ± SD of six mice per genotype. RPL13A was used as normalizer. (B) Measurement of total insulin extracted from whole pancreas of 16−week−old male mice. Data represent the mean ± SD of four mice per genotype.
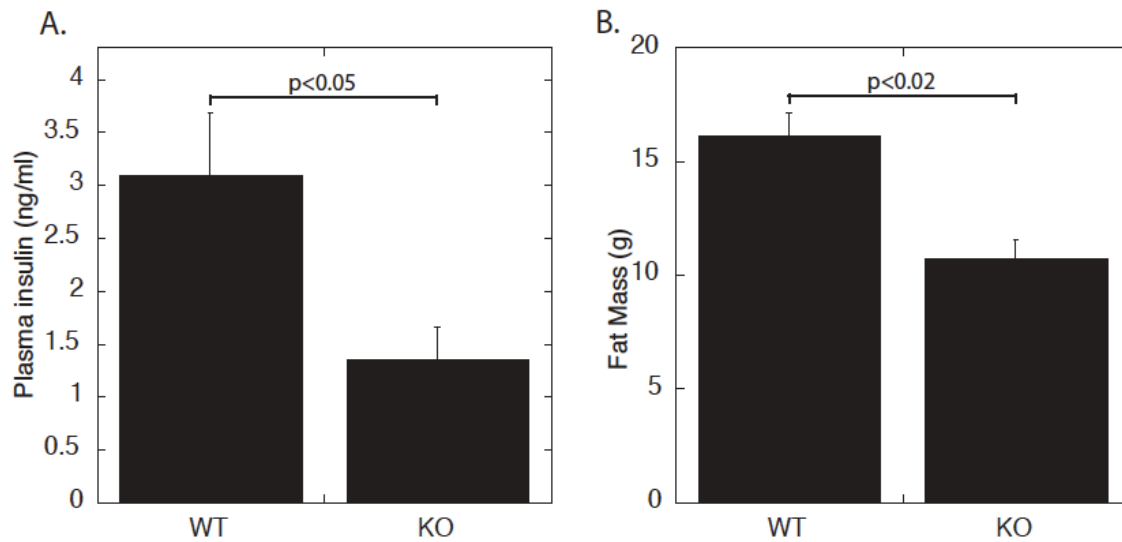
Figure 3–S7). PASK$^{-/-}$ mice on HFD exhibited reduced circulating insulin levels and adiposity. (A) Measurement of plasma insulin levels from 24–week–old HFD WT and PASK$^{-/-}$ male mice fasted for 8 h. Data represent the mean ± SD of 10 mice per genotype. (B) Body fat mass in 23–week–old WT and PASK$^{-/-}$ mice on HFD, measured by dual energy x–ray absorptiometry

Additional data not in

original manuscript

These data were not in the original manuscript however they strengthen the conclusions of the paper. PASK functions in a cell autonomous manner to regulate nutrient utilization. MEFs isolated from PASK-/- mice have increased glucose oxidation and increased ATP content (Fig 3-8). This supports the data found in shRNA knockdown of PASK in L6 cells. These data taken together indicate that in the absence of PASK cells become hypermetabolic.

It has been shown that PASK-/- mice and cells are hypermetabolic. In the absence of PASK mice are not able to normally regulate nutrient utilization. This failure to regulate nutrients in the mouse is due to a cell autonomous defect. These data indicate that PASK kinase is required for nutrient utilization however it does not indicate if PASK is sufficient to regulate nutrient utilization. We constructed L6 cell lines that over-express either PASK or PASK kinase dead (KD) which is suppressed by the addition of doxycycline. Over-expression of PASK causes a decrease in glucose oxidation, however PASK-KD over-expression does not induce the same decrease in glucose oxidation (Fig 3-9). These data indicate that PASK is sufficient to regulate nutrient utilization by a cell autonomous mechanism.
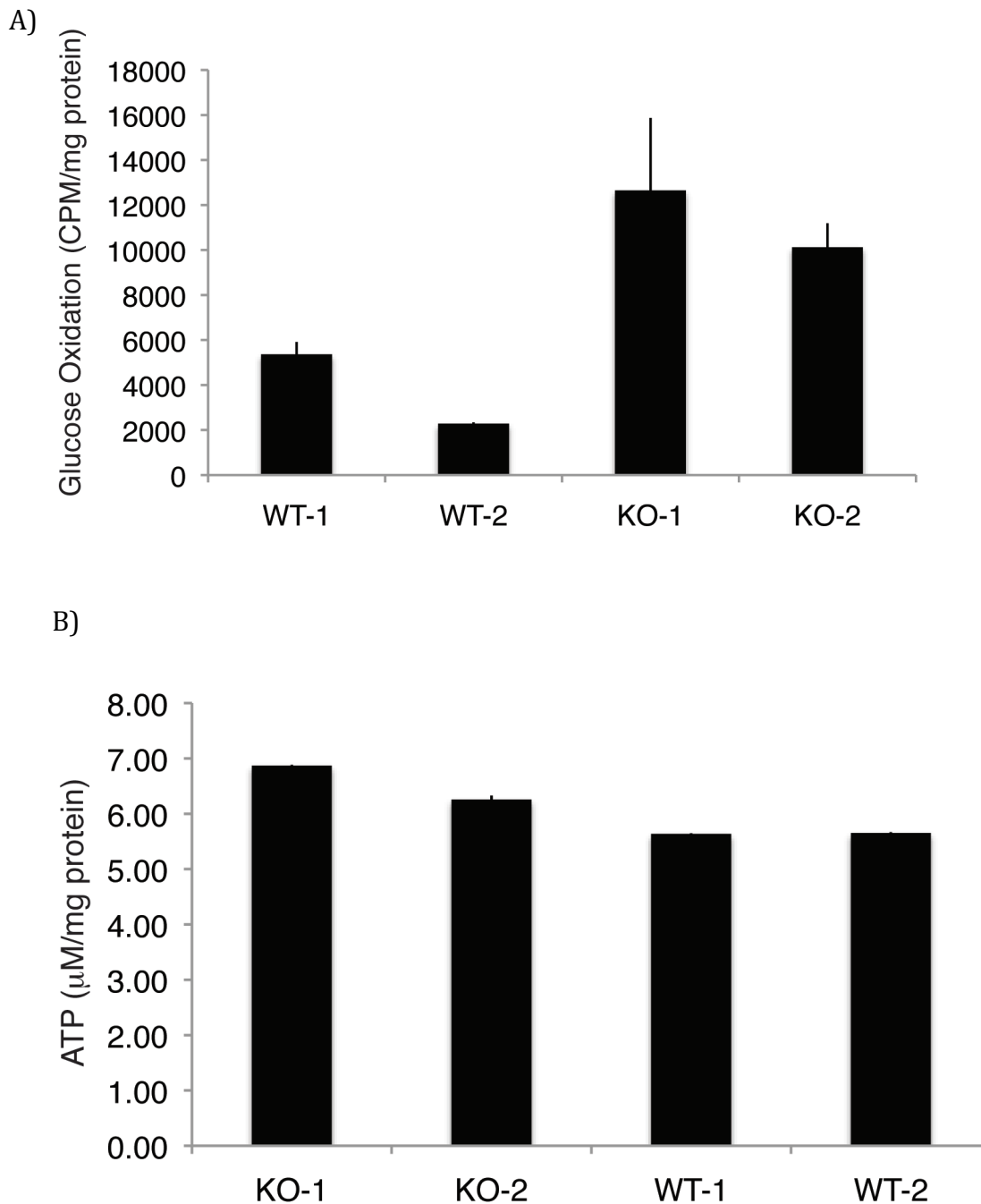
A)

B)

Figure 3-S8). PASK-/- mouse embryonic fibroblasts (MEF) have increased glucose oxidation and ATP content. MEFs were isolated from two littermates. Data represent mean+/- SD of triplicates per group. (A) Measurement of $^{14}CO_2$ release from indicated MEFs incubated in [^{14}C]glucose (B) Cellular ATP content measurement normalized to protein in extract.
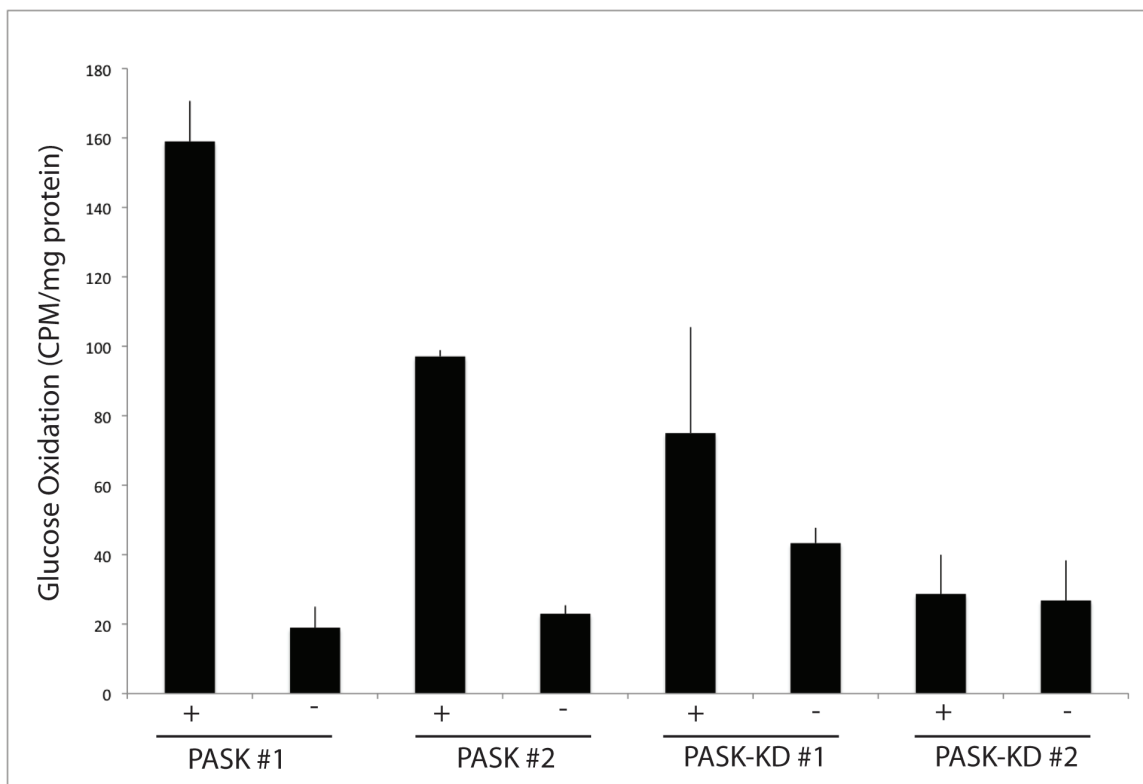
Figure 3-S9). PASK over-expression L6 cell lines show decreased glucose oxidation. Glucose oxidation rates in L6 clones over-expressing either wild-type PASK or PASK kinase dead in the absence of doxycycline. Data represent mean+/- SD of triplicates per group. (A) Measurement of $^{14}CO_2$ release from indicated L6 cell lines incubated in $[^{14}C]$glucose.

CHAPTER 4

CONCLUDING REMARKS

Conclusions

Every organism must strike a balance between energy consumption, for growth, and starvation. Growth requires the coordinated execution of biochemical processes, linked to nutrient availability and energy, by which organisms increase their size or cell number through the biosynthesis of new cellular components. Equally important is the ability to rapidly suppress these synthetic processes to conserve energy and survive in the presence of depleted nutrient conditions. Suppression of these pathways must be coordinated with mobilization of energy stores (glycogen and lipids), recycling of proteins and organelles through autophagy and inhibition of proliferation. Activation of these scavenging programs prevents death under conditions of fasting or starvation.

The ability to coordinately up-regulate biosynthetic cellular processes in response to available nutrients is largely dependent on activation of TOR signaling and inhibition of AMPK signaling. However when nutrients are depleted the cell must rapidly respond by activation of AMPK signaling via the AMP:ATP ratio and inhibition of anabolic TOR signaling. The capacity to respond rapidly can be the difference between reproduction or death. In order to integrate the myriad of signals from both within and without the cell there are many signaling pathways that impinge on both TOR and AMPK signaling. One such protein is PAS kinase, which in *S.cerevisiae* can regulate glucose partitioning and growth. In mammals, loss of PASK leads to a hypermetabolic state and resistance to diet-induced obesity.

Given the fundamental nature of coordinating growth decisions with available energy sources, the single celled eukaryote *S. cerevisiae* is a valuable tool for deciphering these signaling mechanisms. PAS kinase was originally characterized to be able to partition glucose in response to nonfermentative carbon sources or cell integrity stress. We have gone further to show that in the absence of TORC2 signaling that PAS kinase is necessary and sufficient for survival. Any mechanism that activates PAS kinase (over-expression, cell integrity stress, nonfermentative carbon sources) can suppress the lethality caused by an absence of TORC2 signaling. PAS kinase activation leads to phosphorylation of the metabolic enzyme Ugp1. PAS kinase-dependent phosphorylation of Ugp1 does not affect enzymatic activity. However it induces a translocation from the cytoplasm to the cell periphery. At the cell periphery P-Ugp1 nucleates the formation of a signaling complex that includes Rom2, a Rho1 GEF and Ssd1, an RNA binding protein. The complex is able to induce activation of Rho1, presumably through inclusion of Rom2 within the complex. Rho1 activation can act as a progrowth signal within the cell via polarization of the actin cytoskeleton and up-regulation of cell wall synthesis. Identification of this novel pathway increases our understanding of the integration of the signaling mechanisms of two nutrient responsive kinases, TOR and PAS kinase. This discovery also increases our understanding of the complex, integrated signaling that exists within the cell to coordinate nutrient availability to growth. Discovery of this novel pathway still leaves several major questions that remain unanswered.

Are there conditions in which TORC2 is inactivated and thereby PAS kinase is essential for growth? PAS kinase-dependent phosphorylation of Ugp1 is required for suppression of the Tor2 mutant. However it is not clear if the enzymatic activity of Ugp1 is required for suppression. P-Ugp1 nucleates the formation of a complex that includes Ssd1, an RNA binding protein, which brings up the possibility that RNA might be in the complex. If so, RNA might regulate some aspect of the complex activity or vice versa. Does formation of the complex and activation of Rho1 lead to activation of all of the pathways downstream of Rho1 or only a subset and if so, which pathways are activated?

PAS kinase has been shown to regulate nutrient partitioning and some aspects of polarized cell growth in *S. cerevisiae*. We have also shown that in mammals PAS kinase can regulate partitioning of nutrients. In particular, in the absence of PAS kinase mice are unable to properly regulate fat metabolism, which leads to a decrease in fat accumulation in the liver of mice on a high fat diet. These data taken together suggest that PAS kinase might be able to couple nutrient availability to growth decisions similar to TOR and AMPK. The effect of PAS kinase on growth remains to be fully elucidated.